DEFINITION AND UPSCALING OF KEY HYDROLOGICAL PROCESSES FOR APPLICATION IN MODELS

Report to the
Water Research Commission

by

Simon Lorentz, Kevin Bursey, Olufemi Idowu, Cobus Pretorius & Kalala Ngeleka

School of Bioresources Engineering and Environmental Hydrology
University of Natal, Pietermaritzburg

Head of School: Professor J.C. Smithers
Project Leader: Assoc. Professor S.A. Lorentz

WRC Report No 1320/1/08
ISBN 978-1-77005-722-7

June 2008

The research in this report emanated from a project funded by the Water Research Commission entitled:

'*Definition and Upscaling of Key Hydrological Processes Affecting Critical Perturbations to Water Resources for Application in Models*'

The reference Group responsible for this project consisted of the following persons:

Mr. R Dube	:	WRC (Chairman)
Dr. C Everson	:	CSIR
Dr. D Le Maitre	:	CSIR, Stellenbosch
Ms N Snyman	:	University of Zululand
Mr. A van Zyl	:	ARC-ISCW
Dr. M McCartney	:	IWMI
Prof. J Annandale	:	University of Pretoria
Mr. M Nepfumbada	:	Department of Water Affairs and Forestry
Prof. Y Xu	:	University of Western Cape

The financing of the project by the Water Research Commission (WRC) and the guidance, advice and assistance of the Reference Group is gratefully acknowledged.

EXECUTIVE SUMMARY

The clear definition and quantification of the sources and pathways of components of discharge making up stream flow is becoming increasingly important. Indeed the implementation of the National Water Act (1998) requires an understanding and quantification of dominant hydrological processes in order to faithfully manage water resources. This understanding is particularly important in quantifying low flows and the sources thereof; in assessing the impacts of land use change; in quantifying the hydrological perturbations resulting from climate change and in assessing impacts of non-point source pollution, especially where the source of the impact is to be identified.

The aims of this project were therefore to:

- Define key hydrological processes at a range of scales by observation and experimentation at these scales in order to
- Improve deterministic, physically based simulation tools and in particular, the *ACRU* agrohydrological model to represent these processes at a range of scales, so that
- Land use changes, stream flow reduction activities (SFRAs), surface and groundwater interactions and topological runoff generating mechanisms are linked conceptually and spatially to the responses at each scale.

A fruitful study of the source areas, flow pathways and residence time of water in the Weatherley research catchment has been concluded. They key outcome of the research has been the application and combination of a number of different tools and observation techniques, applied to the same area, which has led to a better and more comprehensive understanding of the hydrological processes which underpin the water resource impacts. Hydrodynamics observations, geophysics surveys and tracer methods have been combined to yield a consistent understanding of the catchment water yield mechanisms, despite the limitation of each method used independently.

Specific response dynamics resulting from the combinations of techniques in the catchment are:

- ***Overland flow.*** Overland flow discharge which reaches a surface water carrying conduit (stream or seepage line) during rainfall events is restricted to areas adjacent to these conduits. This observation has been made through runoff plot analyses,

where, even in an intense event of 31.4 mm in 20 minutes, overland flow distances were estimated to be no more than 30 m. Simulations of the hillslope water balance using the HYDRUS-2D model result in very small contributions from overland flow. However, this analysis was aimed more at the low flow discharge from the soil catena than event based discharge. The contribution to event based runoff from overland flow is clearly dependant on the antecedent moisture content as demonstrated in the rainfall-runoff analyses. In addition, the tracer based, three component hydrograph separation, using EC and Si as tracers, suggests that the direct contribution to event based stream flow from the event rainfall ranges between 14% and 26% of the event discharge.

- ***Near surface soil water.*** Observations in shallow tensiometers and free water collection tubes have demonstrated the existence of a rapid response, near surface discharge during rainfall events. These zones of near surface, lateral flow have been identified by hydropedological investigations and have been estimated by tracer aided separation techniques to yield up to 16% of event discharge.

- ***Hillslope groundwater water.*** Soil water accumulation on the interface of the soil and bedrock has been observed through groundwater observations holes and tensiometer responses. These accumulations generally occur on the hillslopes upslope of parent rock outcrops. During a series of event flows, this source of water has been estimated to yield 70% of the total discharge (EC and Si tracer based hydrograph separation). Using lumped isotope sample end member mixing analysis, this hillslope contribution to flows is estimated at 60% of the stream discharge during the wet season. During the dry season, the soil profile continues to generate stream flow well into the middle of the winter. Discharges estimated from the HYDRUS-2D analyses of measured soil water potentials ranges from 10% to 4% of total flow, slowing down to negligible flows by the end of June. Stream flow discharge during the low flow periods also emanates from the emergence of fractured bedrock flows re-entering the hillslope profiles as is evident from Electrical Resistivity Tomography surveys.

- ***Fractured rock groundwater.*** The existence of groundwater in the bedrock underlying the hillslopes and valley is evident through deep borehole observations as well as Electrical Resistivity Tomography surveys. It is clear that some proportion of this deep aquifer water contributes to the event flows, but, without tracer samples from these deep sources, the proportion cannot be estimated. It is also evident that, during the dry season, water percolating through the fractured rock contributes to low flow via two mechanisms. First, bedrock groundwater emerges at parent material outcrops on the hillslopes and contributes to hillslope soil water in the downslope profiles. Second, water enters the valley soil profiles from the bedrock below in response to upslope gradients. During the dry season the seepage water, spilling over the outcrops is estimated to contribute 32% and the subsurface seepage 68% of the winter flows as late as August.

A model algorithm, comprising threshold based subsurface responses and catena based linking has been proposed as a direct emulation of observed stream flow generation dynamics. Future hydrological model performance would be enhanced by including functions which represent the travel times of the different components of flow which could be observed by continuous observations of the combination of techniques applied in this study.

The implications of properly simulating the different components of stream flow should not be overlooked in assessing land use change, climate change, low flow and water quality impacts. Future investigations, using the combination of techniques introduced in this study can be usefully applied in other geologies, soil catenas and climate zones to begin a classification system of typical response dynamics of these hydrological zones.

TABLE OF CONTENTS

LIST OF FIGURES

List of Figures (contd)

List of Figures (contd)

LIST OF TABLES

CHAPTER 1
INTRODUCTION

In order to assess water resources faithfully and particularly to estimate the impacts of land use change, low flow generation and water quality impacts in catchments, it is necessary for hydrological models to represent the dominant features of runoff generation. Indeed, the implementation of the National Water Act (1998) requires a clear understanding and quantification of key hydrological processes. This can be accomplished by focusing on two endeavours:

- Conducting observations of hydrological processes at the scale of the problem being investigated and
- Improving the ability of deterministic, physically based simulation tools to represent the key hydrological processes realistically for a range of landscape and land use conditions.

Aims

This project, therefore, aims to:

- Define key hydrological processes at a range of scales by observation and experimentation at these scales in order to
- Improve deterministic, physically based simulation tools and in particular, the ACRU model to represent these processes at a range of scales, so that
- Land use changes, stream flow reduction activities (SFRAs), surface and groundwater interactions and topological runoff generating mechanisms are linked conceptually and spatially to the responses at each scale.

Key Objectives

The key objectives of this project are to:

- Assemble historic data from selected catchments where new techniques of hillslope flow generation models can be applied.

- Observe hydrological processes at the local, hillslope and nested small catchment (less than 10 sq. km), medium (10 to 100 sq. km) and large catchment (10 to 1000 sq. km) scales and to evaluate the responses at these scales in order to develop appropriate process descriptions and parameter sets for each scale;

- To include in these observations, the study of specific hydrological processes at specific scales to improve simulation at these scales and to provide algorithms for upscaling. These studies will include:
  - Hillslope runoff generating processes;
  - Surface, vadose zone and groundwater interfaces and responses, including hillslope, riparian and wetland interactions;
  - Local scale soil water dynamics in critical land uses, including forested hillslopes, and mining/industry related water use.

To continuously improve the modeling of the medium and large scale by iterative adjustment to process descriptions and parameter sets until the two objectives have been achieved.

While this study is focused on the integration of the dynamics of the different sources and pathways of stream flow into an improved catchment scale hydrological model, it is, nevertheless, important to describe these behaviours at different scales so that the dominant features of their behaviour can be successfully integrated into the model. Since it is impossible to measure each component of flow directly some of the behaviours which need to be included in the models can only be described in general terms from the outcome of the observations made. However, these descriptions can still lead to valuable partitioning of the components of stream flow in the models.

Observations and corresponding hydrological dynamics are described in this study at the local, hillslope and catchment scales in the Weatherley research catchment. This catchment has been monitored as a grassland catchment for 6 years before being afforested in 2002. Subsequent monitoring has not currently been analysed for impacts of the afforestation, but the monitoring program continues, uninterrupted. In addition to the hydrological processes study at the Weatherley catchment, a mining application of the ACRUSalinity model has been concluded in the Mpumalanga coal fields. Here, runoff and subsurface processes have been integrated with salinity dynamics for a coal mine in the upper Olifants catchment.

A review of the use of hillslope hydrological dynamics to inform catchment scale hydrological modelling is presented in Chapter 2. This is followed by a description of the head water, Weatherley research catchment and the 137 km^2, Mooi river basin in which it is located (Chapter 3). In Chapter 4 the results of observations at local, hillslope and catchment scale are presented using various observation, monitoring and survey techniques. These observations are integrated into proposed model algorithms in Chapter 5. Application of these in the Weatherley research catchment is demonstrated.

The final chapter concludes the study and highlights the unique value of using a combination of techniques to define surface and subsurface responses to rainfall events and dry season flows. The extension of the simulation algorithms to the larger Mooi river catchment was not concluded in this study and remains the topic of current research.

CHAPTER 2
UPSCALING HILLSLOPE PROCESSES OBSERVATIONS

Hydrological modelling at the catchment scale is generally either performed in a lumped or distributed mode. In the lumped mode, models may often yield accurate predictions of the runoff, but they may fail to represent the driving processes of the linked hillslope and stream network. In the distributed mode, the basins are broken down into small enough elements that are deemed sufficiently uniform for homogeneous principles to work, (Sivapalan, 2003). However it is most often impossible to simulate large basins by subdividing into homogeneous areas due to the large multiscale heterogeneities that nature exhibits. It is therefore proposed that the dominant units of hydrological response, the hillslope and the stream network, be preserved in the models and that these features be categorised according to their unique behaviour.

'Rivers carve the landscape into beautiful shapes called river networks, which seem to embody a deep sense of symmetry, and some general principles such as minimum energy are said to be at work. Geological facies tend to be discrete units associated with specific formational processes, sometimes organized in certain sequences. Soils tend to develop in response to state controls such as topography, with different parts of basin being formed by different processes and having different functions. The resulting soil patterns (soil catena) exhibit a common form of organization and symmetry, with water movement clearly being an active agent in their formation. The interactions between climate, soils, vegetation and topography thus contribute to the most amazing patterns that we see in natural basins, which must contain valuable information about the way they function. A fundamental aim of theoretical hydrology must be to identify such patterns, decipher the underlying order or symmetry occurring over a wide range of scales and the rules that govern them, and explore the mechanisms that generate them.' Sivapalan, 2003.

Three endeavours are proposed by Sivapalan, 2003:

- Field experiments in nested river basins: process studies, perceptual models and generalizations. This will include using deterministic models to simulate the rainfall-runoff processes without the direction of field measurements and using the differences between field observations and model outcomes to inform the model development,

- Derivation of new balance equations for nested river basins. Models must respect the stream network and component hillslopes,

- Learning from patterns: data-based approaches to making inferences about basin responses.

It is this search for patterns of behavior which is the subject of the following chapters. These behaviors are examined at the local, hillslope and catchment scales. It has been demonstrated by the measurements and observations at various scales that the contributions to the stream from differing sources in the hillslope prevail over long periods of time. These response times have been demonstrated in many studies and a selection of results are summarised in Table 2.1. Typically soil derived contributions have travel times of months to a few years whereas groundwater sources have travel times between 5 and 20 years.

These slow responses are not typically included in hydrological models. However, appropriately dimensioned transfer functions could be easily included in the models to represent specific combinations of geology, topography and soils.

Table 2.1 Summary of response times for soil, shallow perched groundwater and groundwater for selected catchments.

Catchment	Soil response (years)	Shallow response (years)	Groundwater or baseflow response (years)	Reference
River Fuegh, north Scotland	0.4 – 0.8	2	5	Rodgers *et al.,* 2005
Brugge, south Germany		2 - 3	5 - 20	Uhlenbrook *et al.,* 2002
Zastler, south west Germany		2 - 3	6 - 9	Hoeg *et al.*, 2000.
Takanami, Japan	0 - 0.07	0.06 – 0.18	>1	Asano, *et al.*, 2002
Cascade Mtns, OR, USA			0.8 – 3.3	McGuire *et al.*, 2005
Weatherley, NECF, South Africa	0 - 0.01	0.3		Lorentz 2003

The models would only require parameterisation of the hillslope and stream network as these behaviours have been shown to be scale independent (Siebert *et al.,* 2003; McGuire *et al.,* 2005). Figure 2.1 shows the relationship between hillslope mean residence time and various properties of their associated catchments, which ranged in size from 0.085 to 62.4 km^2. There is no apparent relationship between mean residence time and catchment size, despite the large variation in areas. However there are strong relationships between mean residence time and hillslope length and slope.

Hence the pursuit of typical hillslope behaviours would seem fruitful to enhance hydrological modelling efforts. Particularly in scaling up the behaviours observed in the Weatherley catchment to those in the Mooi river basin.

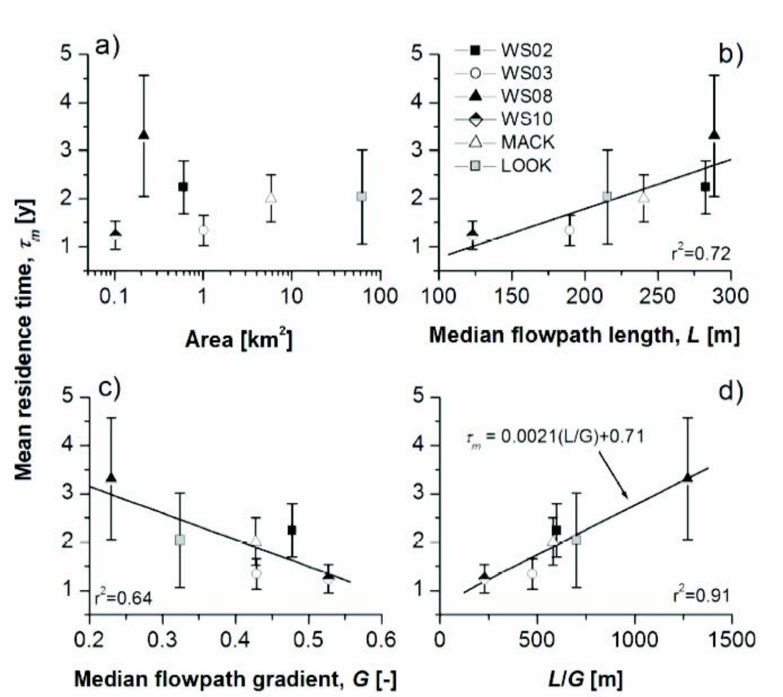

Figure 2.1 Shows the relationship between mean residence time of hillslope discharge and catchment area (a), median flow path length (b), median flow path gradient (c) and ratio of median flow path length and gradient (d), (McGuire *et al.*, 2005).

In this study the dominant hillslope mechanisms are examined using hydrometric observations of climate variables, soil water capillary pressure head (or tension), hillslope and deep groundwater levels and stream discharge. In addition, geophysical observations are made to define the distribution of subsurface water, both in the soil and in groundwater. Finally, various components of discharge are sampled and analysed for the stable isotopes of water, H^2 and O^{18}. The combination of these observations leads to the estimation of the contributing fluxes of the stream runoff. The dominant mechanisms that regulate the different components of flow are included in the development of the ACRU agrohydrological modelling system for future testing.

CHAPTER 3

WEATHERLEY RESEARCH CATCHMENT AND MOOI BASIN

A research catchment of some 1.5 km^2, Weatherley, was established in 1995 in a grassland zone prior to the introduction of trees in 2002. The catchment was instrumented with two met stations, soil moisture and tension sensors, groundwater level sensors, surface runoff plots and two stream gauging weirs, dividing the catchment into upper and lower subcatchments.

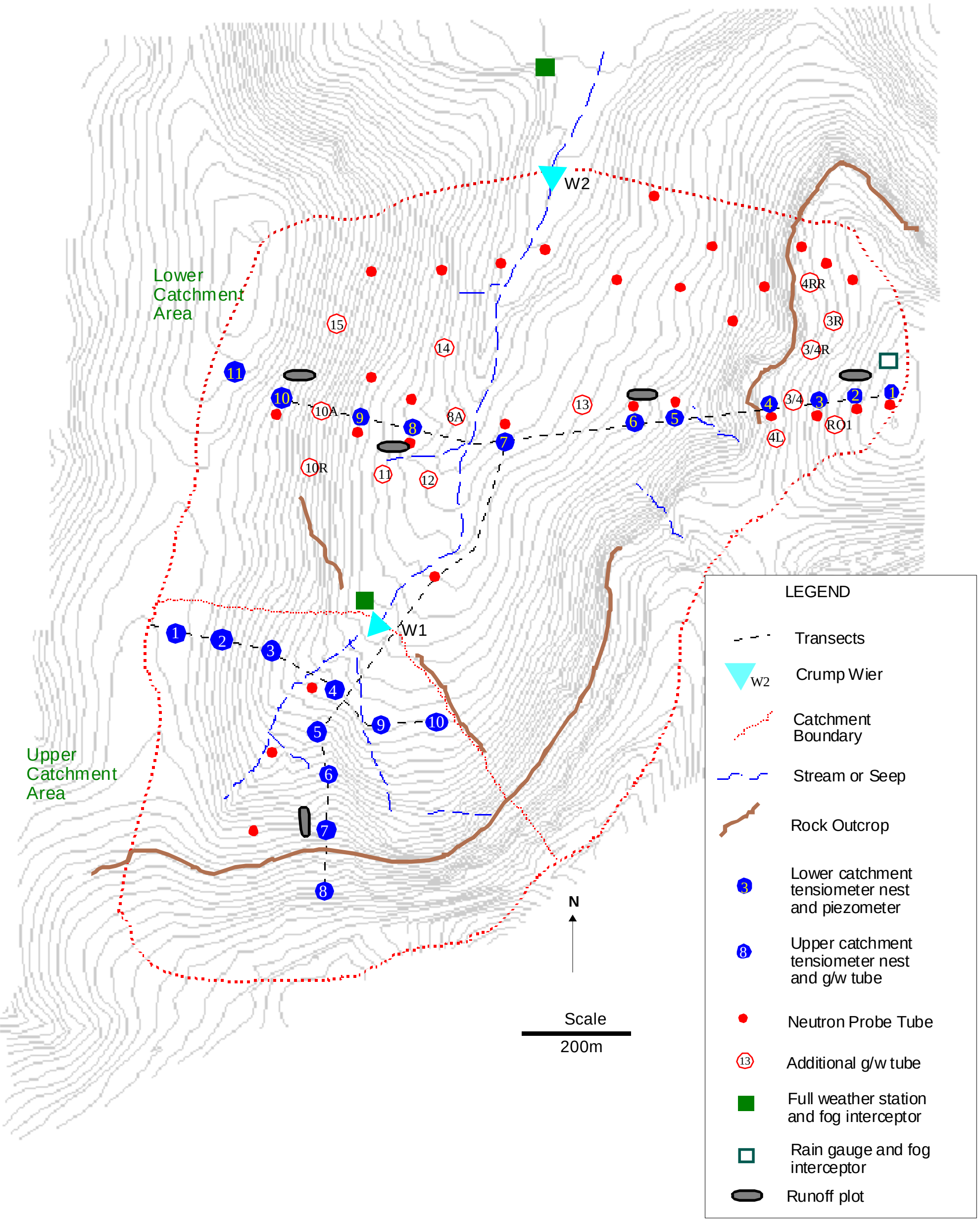

Figure 3.1 Layout of instrumentation at the Weatherley research catchment, northern Eastern Cape province.

The land cover at Weatherley is predominantly Highlands Sourveld grassland, which is generally in a moderate hydrological condition with a basal cover of 50-75% on the hillslopes, (Esprey, 1997). Wetland conditions exist along the entire reach of the stream and range in width from 100 to 400 m, being widest where marshy conditions are associated with lines of seepage from the contributing hillslopes. The Mean Annual Precipitation (MAP) is 740 mm and the Mean Annual A-pan Evaporation (MAE) is 1488 mm (Esprey, 1997). Average daily temperatures range from 11°C in the winter to 20°C in the summer, with frosts and snow falls at higher altitudes in winter. A monthly summary of rainfall, evaporation and daily temperatures is presented in Figure 3.2.

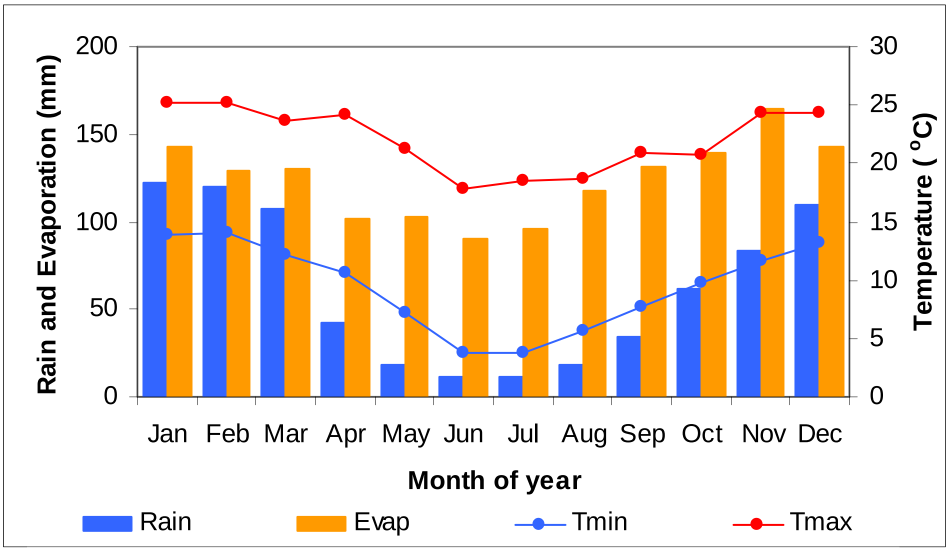

Figure 3.2 Summary of climate variables for the Weatherley research catchment (Lorentz et al., 2003).

The soils comprise a network with large spatial variation. An initial detailed soil survey, carried out by the Institute for Soil, Climate and Water (ISCW) identified 16 different soil forms (Roberts *et al.,* 1996). These soils display a varying degree of wetness and colour and include red and yellow apedal mesotrophic soils as well as neocutanic and hydromorphic soils (Lorentz *et al.,* 2003). Subsequent surveys have been conducted by the Soil Science department of the University of the Free State. In these most recent endeavours the soils have been defined in terms of their hydraulic performance on catenas.

The geology of the catchment is typical of the local flat bedded Molteno structures, comprising reddish-green mudstone-siltstone with intercalated sandstone. The harder sandstone layers form the typical breaks in the hillslopes and seepage areas are generally noted below these sandstone lenses where they contact with the low permeability mudstone-siltstone (van Wyk, 2006).

From the observations made since 2002, certain dominant mechanisms of flow from the hillslopes have been defined (Figure 3.3 and Table 3.1). These consist of surface, near surface, soil-bedrock interface and deep groundwater fluxes which exhibit characteristic functions during certain events and during low flows.

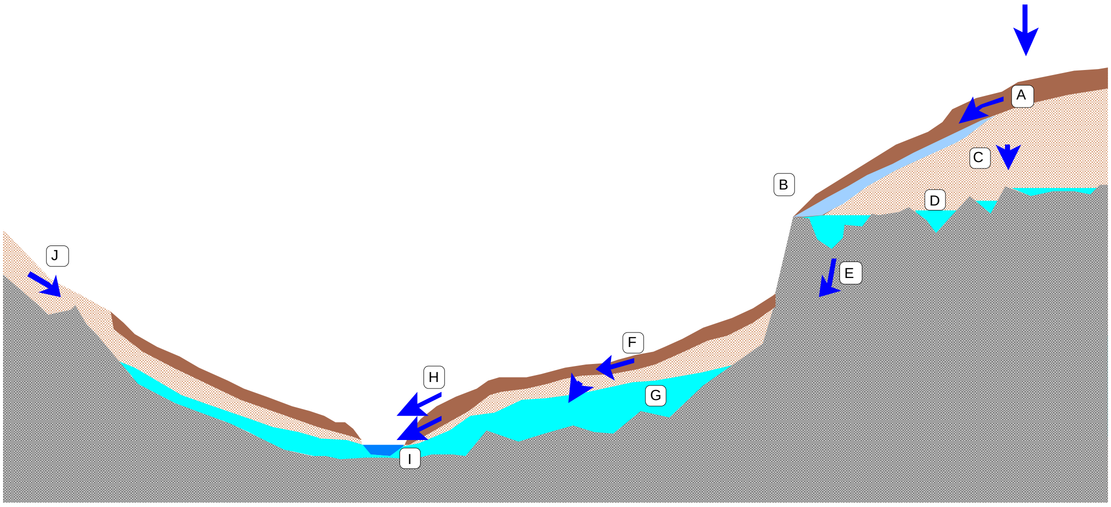

Figure 3.3 Dominant mechanisms of discharge from the hillslopes at the Weatherley research catchment (Lorentz *et al.,* 2003).

Table 3.1 Summary of streamflow generation mechanisms and their occurrence, Weatherley research catchment (after Lorentz *et al.,* 2003).

CODE	DESCRIPTION	OCCURRENCE
A	Rapid lateral flow near the surface due to macro-pore conductance. Local perched water table of short duration. Matric pressure head discontinuity with deeper perched water table, D.	In upper slope segments in downstream catchment during high intensity events and some low intensity events with large volumes (>30 mm).
B	Accumulation at the toe of the slope segment with emergence and flow over bedrock.	In upper slope segments in the downstream sub-catchment.
C	Slow percolation to water tables perched on bedrock.	In all slope segments for most events except low intensity and volume.
D	Water tables perched on bedrock and in bedrock hollows.	Disconnected from soil water in upper slopes of eastern side of downstream catchment, but connected in lower slopes and in upstream catchment during moderate to intense events.
E	Seepage of groundwater through fractured bedrock.	Assumed to occur in all slope segments.
F	Rapid macro-pore, lateral flow in flatter marsh slopes and infiltration to marsh ground water.	Vertical recharge is more rapid than lateral movement in lower slopes of downstream catchment and in upstream catchment, except when groundwater rises into macro-pore layers.
G	Marsh ground water level fluctuation	Rapid for most events in lower downstream catchment. Slower, but connected in upper catchment.
H	Exfiltration, surface runoff and macro-pore discharge to stream	In downstream catchment. Exfiltration not observed in upstream catchment.
I	Groundwater discharge into stream	Occurs in upstream and downstream catchments. Some near stream groundwater ridging during intense events.

J	Unsaturated redistribution of soil water to bedrock. No groundwater on soil/bedrock interface.	In upper parts of western slope. Generates slowly to soil/bedrock water table downslope.

It is these mechanisms that this current study is aimed at quantifying and integrating into a simple catchment model which could be used at a larger scale. It is hypothesised that the hillslope mechanisms in the Mooi river basin (Figure 3.4), will be similar to those observed in the Weatherley research catchment and so dominant modes of behaviour, defined and quantified at the research catchment scale can be applied at the larger scale. Clearly the detailed processes observed in the research catchment need to be simplified in a way which captures their dominant responses, before they can be applied at the large catchment size.

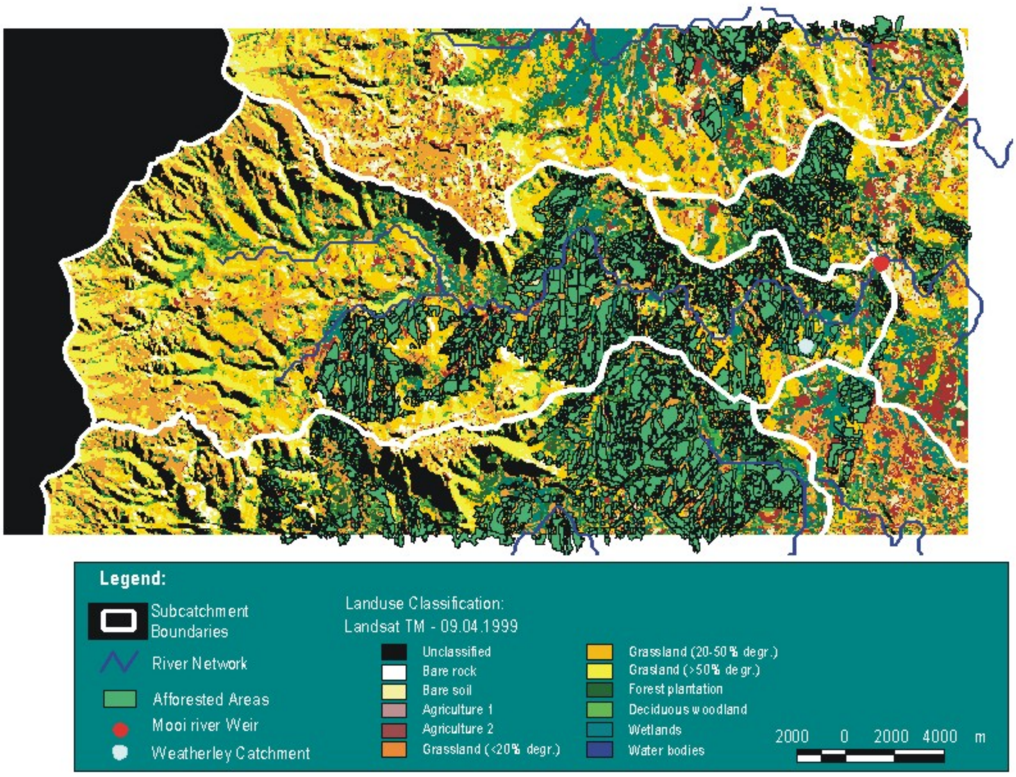

Figure 3.4 Land use in the Mooi river catchment, showing the location of the DWAF weir in Maclear and the Weatherley subcatchment.

CHAPTER 4
LOCAL TO CATCHMENT SCALE PROCESSES

The study of hydrological processes in the Weatherley research catchment has been divided into local, hillslope and catchment scales. The processes at the local and hillslope scales clearly impact on catchment scale behaviour, but it is prudent, first, to consider these separately.

4.1 Local Scale processes

4.1.1 Midslope responses and simulation

Local scale behaviour has been analysed in the Weatherley catchment in previous works (Lorentz and Esprey, 1998; Lorentz, 2001; Lorentz *et al.,* 2003). Dominant mechanisms, defined in these previous studies have been summarised in Figure 3.3 and Table 3.1. In this study the local scale soil water dynamics is simulated with the HYDRUS2D model in order to estimate the rate of accumulation of water in the soil-bedrock interface. The study aims, particularly, to define the discharge from the soil matrix during the dry season. The model was initially set up to represent sections of the hillslope in order to compare the model performance against soil water potentials at soil moisture monitoring stations.

The HYDRUS-2D model allows for a 2 dimensional representation of a hillslope section by defining a finite element grid in the shape of the hillslope or portion of hillslope to be modelled. Richards equation is solved for the unsaturated movement of water between the nodes of the finite element grid. Spatial distribution of soils can be defined by selecting appropriate hydraulic characteristics over defined zones. Plant uptake and soil water evaporation are defined by selecting rooting patterns and by identifying an atmospheric boundary at the soil surface.

In the initial, local scale simulation, a section of hillslope in the vicinity of the monitored profile, LC2 was represented by the finite element grid shown in Figure 4.1. With rainfall and potential evapotranspiration inputs, the water balance of the hillslope segment is simulated. Observation nodes are defined in the model at locations corresponding to the tensiometers. The observed tensiometer response is then compared to the simulated soil water potential at the location of the observation. The simulated and observed dynamics of the soil water potential or matric pressure head are shown for LC2 at the depths of 400 mm, 700 mm and 1900 mm in Figure 4.2.

The model required some adjusting for plant evapotranspiration characteristics, but fits the observed data remarkably well at all locations in the profile. The model parameters were preserved for use at the hillslope scale in order to predict the release of water from the toe of the slopes, during wet and dry periods.

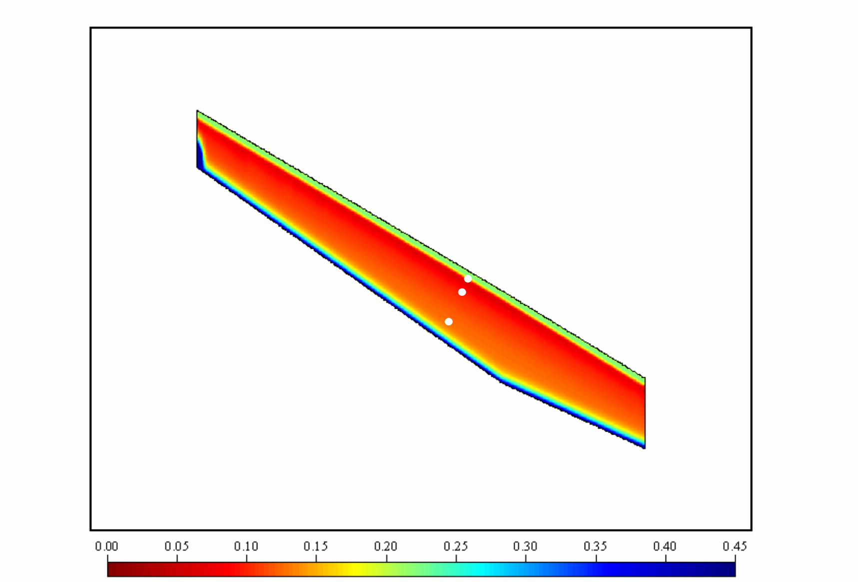

Figure 4.1 HYDRUS-2D finite element representation of the hillslope section at station LC2 in the lower catchment, showing the water content distribution in the finite element mesh.

In the local scale simulation, the observed and simulated responses agree favourably, particularly since the simulation matches each of the depth's behaviours in a single realisation of the section simulation. The near surface (400 mm) behaviour of the matric pressure head is rapid and dynamic, while at the lower depths the response is dampened. Soil water capillary pressure heads reduce rapidly after May at the 400 mm and 700 mm depths, but the response at the 1900 mm depth, on the soil-bedrock interface does not show this reduction over the winter. This reflects the moist conditions at this interface.

The simulated volumetric soil water contents can also be compared to neutron meter measurements as shown in Figure 4.3. Here the water contents do not compare favourably, particularly in the deeper part of the profile. This could be due to the discharge of soil water to the deeper part of the profile through preferential flow mechanisms, which the model does not simulate. Certain of the measured neutron probe measurements are clearly in error as they show a continuously saturated state during what are obviously drying periods.

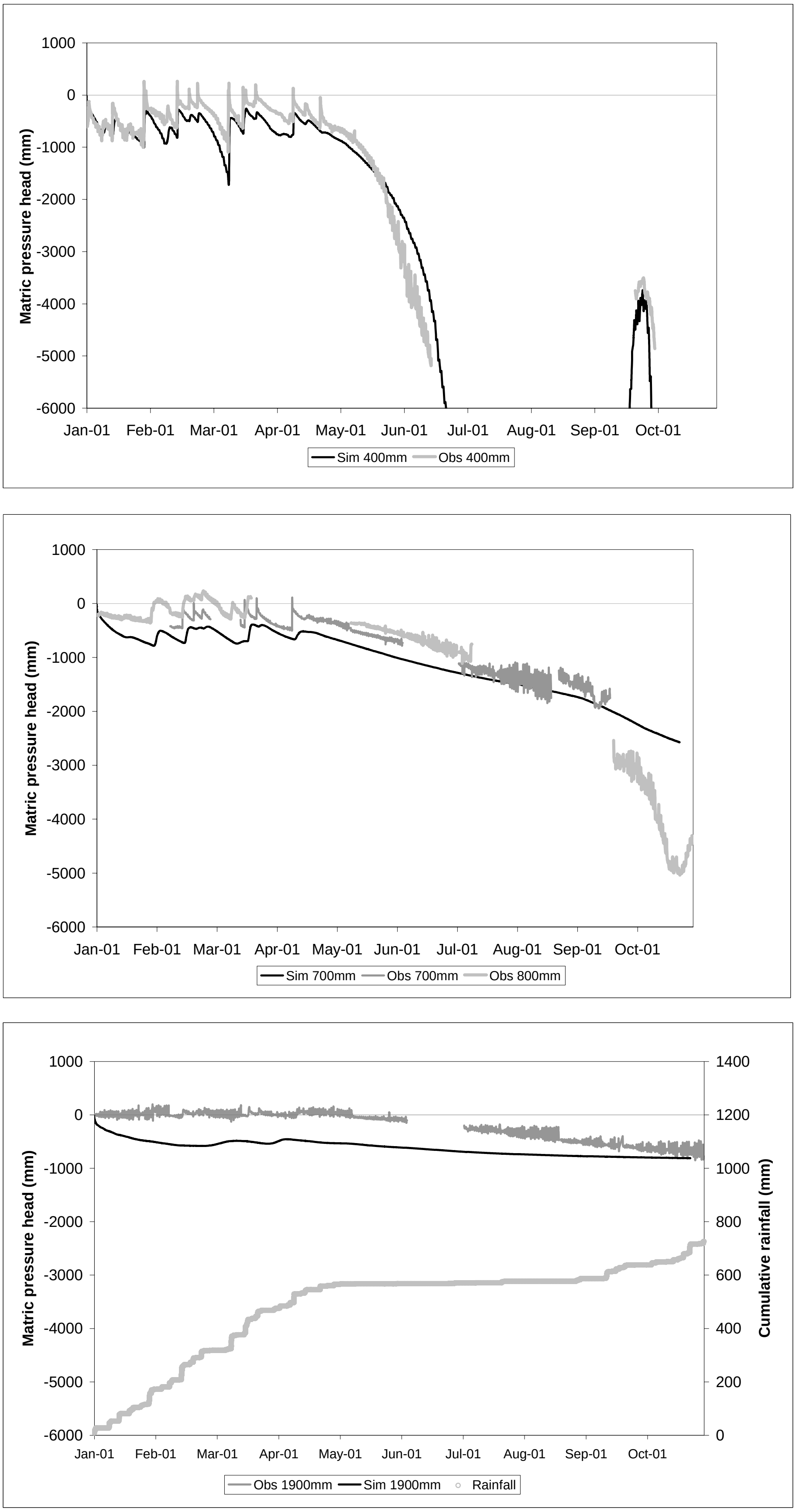

Figure 4.2 Comparison of the HYDRUS-2D simulation with observed tensiometer measurements at station 2 on the upper slopes of the lower catchment.

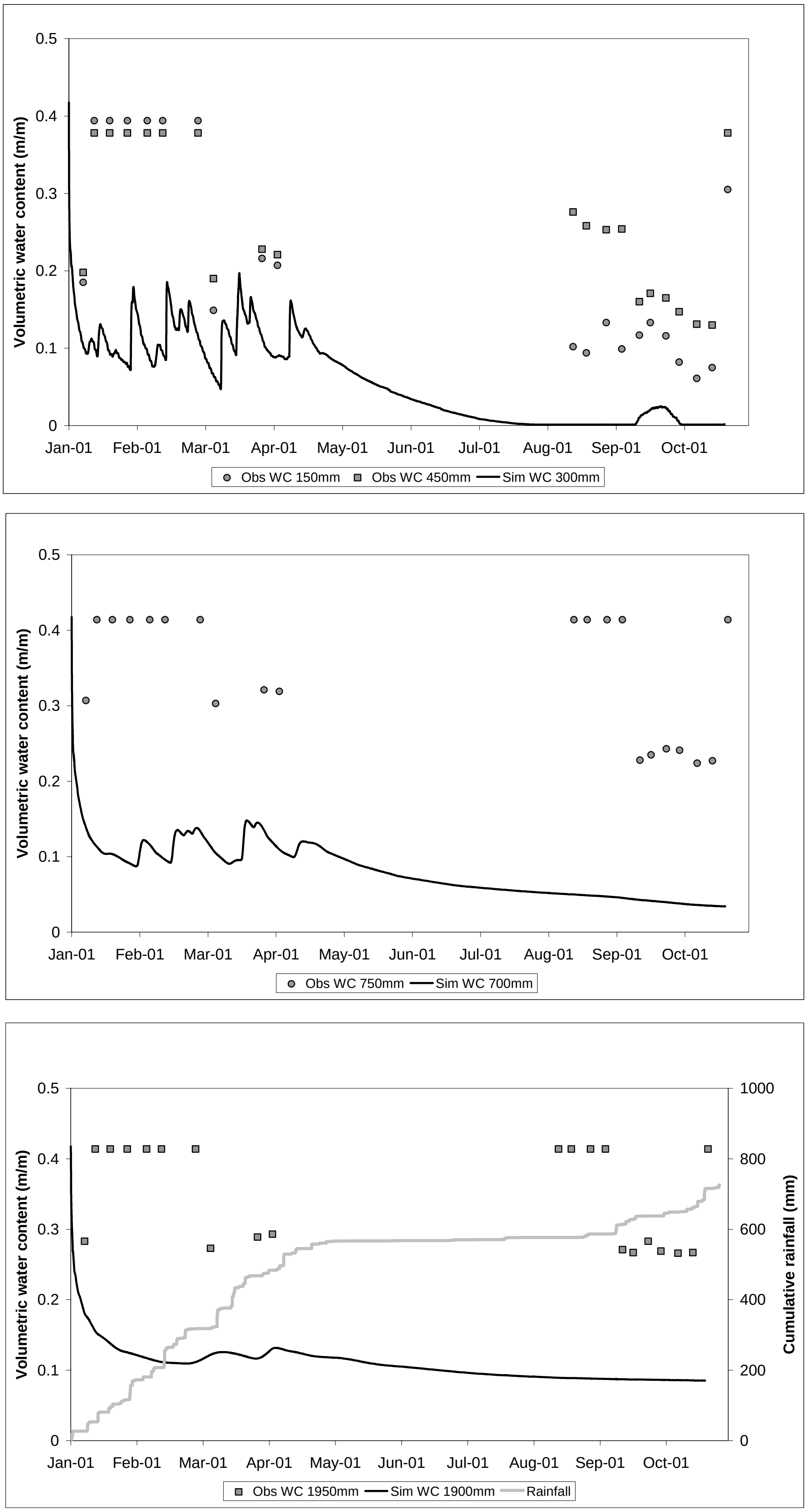

Figure 4.3 Comparison of the HYDRUS-2D simulation with observed neutron water meter measurements at station 2 on the upper slopes of the lower catchment.

4.1.2 Preferential flow

A dominant mechanism discerned through local scale tensiometer analyses was the rapid accumulation of water in the shallow (less than 500 mm) part of the soil profile. This was evident by the manifestation of positive pressures, discerned through the tensiometer response at the near surface sensor (0.45 m in Figure 4.4). Deeper sensors did not exhibit this response, indicating that the accumulation occurred only in the highly conductive near surface layer. Slower accumulations of water were observed in the tensiometer and groundwater observation holes, located at the interface between soil and bedrock or saprolite (Figure 4.4).

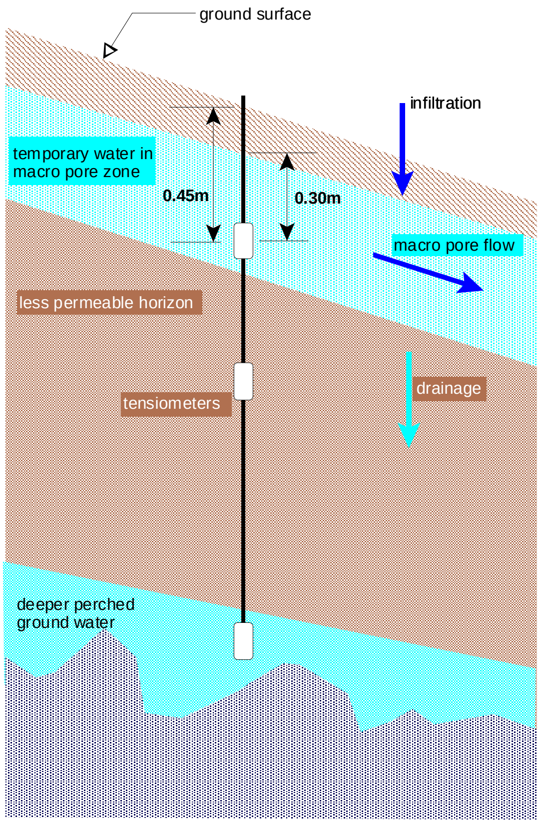

Figure 4.4 Schematic representation of the accumulation of soil water in the near surface as reflected in the near surface tensiometer responses, while slower accumulations are observed at the soil-bedrock interface.

4.1.3 Response at the toe of the slope section

The response at the toe of the hillslope section LC1 to LC4 (Figure 3.1) was examined to determine the seepage flux rate from this section of hillslope. The response at the toe of this upper slope segment in the lower catchment is shown in Figure 4.5. Here the tensiometer response reveals a slow build up to a positive head, indicating a water table or phreatic surface in the profile, in response to rainfall prior to May 2001 (Figure 4.5). The positive pressure during the period March to May 2001 at the 1200 mm depth is 1000 mm, indicating that the water table is some 200 mm below the surface during this period. After the beginning of May 2001 and the cessation of rain, the water table drops rapidly. The water drains from the profile until the deepest tensiometer at 1200 mm reveals a suction pressure in July 2001. At this time the seepage from the toe would likely cease. Simulation of this profile yields the soil water runoff component response shown in Figure 4.6. Flux estimates yield a soil water component contribution to the total runoff of 10% during the wet period. This drops off rapidly between May and July, in response to the declining water table.

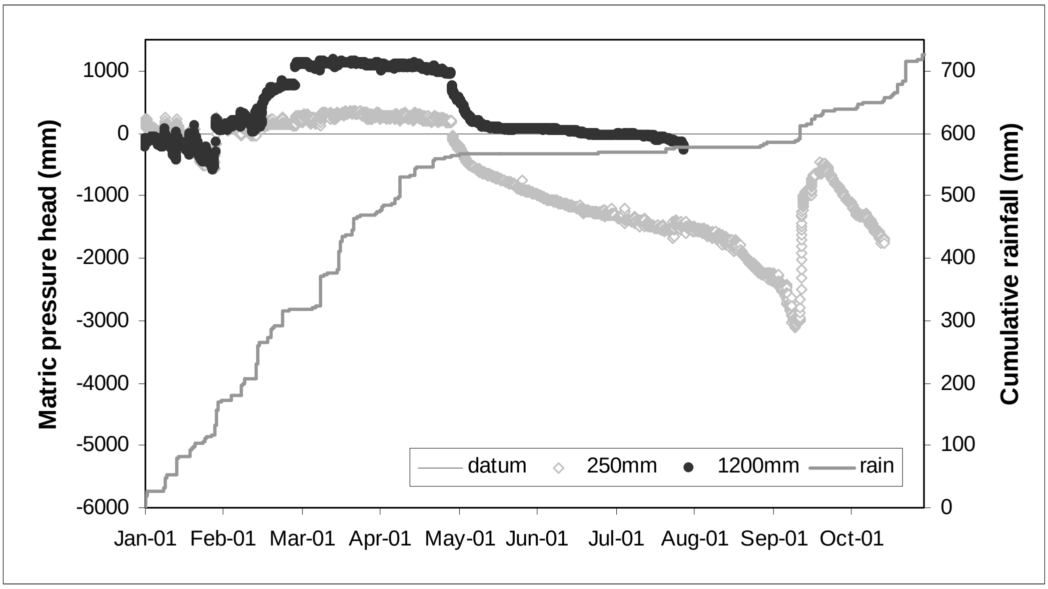

Figure 4.5 Tensiometer response (250 mm and 1200 mm below surface) at station LC4 during the end of the wet season and through the dry season of 2001.

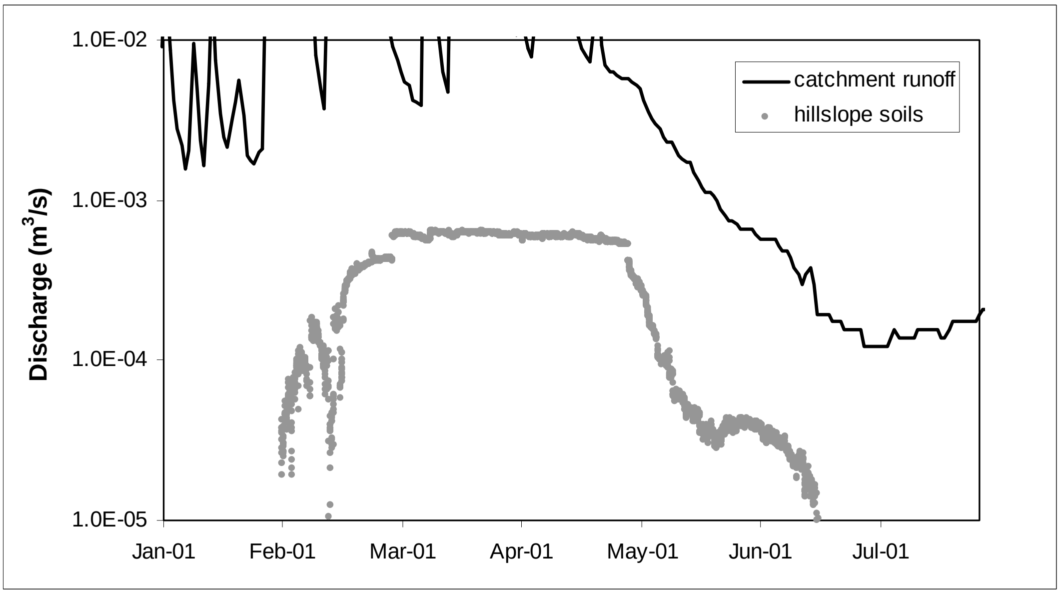

Figure 4.6 Low flow discharge in the downstream Weatherley weir (solid line) with the estimated contribution from the soil profile (circles).

While these analyses of selected locations along the hillslope sections reveal dominant mechanisms, the simulation of entire hillslope catenas will yield the soil water flux behaviour of the whole transect. The simultaneous match of simulated and observed soil matric potential as well as volumetric water content over all the profiles comprising the catena was held as a priority. These simulations are discussed in section 4.2.

4.2 Hillslope Scale Processes

4.2.1 Hillslope 2D simulation

The hydrodynamics of the vertical and lateral movement of subsurface water in three hillslope segments were simulated using the HYDRUS 2D model (Simünek *et al*., 1994).

4.2.1.1 Hillslope segments

Three hillslope segments were identified and simulated in this study. These segments comprised the upper slope in the lower catchment comprising profiles LC1 to LC4 (Figure 3.1). Immediately below LC4 the sandstone outcrop terminates the soil layer of this hillslope segment and water seeps from the soil profile over the outcrop into the second hillslope segment, a gentler sloping transect, comprising stations LC5 to LC7. Beyond LC7, soil water discharges into the stream (Figure 3.1). On the opposite bank, the third hillslope segment comprises profiles LC8 to LC10.

Each of these hillslope segments comprised at least 3 profiles and each profile comprised 2 to 3 depths at which the soil water matric pressure head was observed. In simulating the hillslope segments with the HYDRUS-2D model, the objective was to match the observed history of soil water potentials as well as volumetric water contents at each profile on the segment and at each depth in the profile. Table 4.1 summarises the profiles and the depths of observed record used in the simulation for each of the three hillslope transects. A finite element mesh was generated for each hillslope segment and observation nodes were specified at the position of the tensiometers. The finite element mesh for the hillslope segment LC1 to LC4 is shown in Figure 4.7. The top boundary of the mesh was specified as an atmospheric boundary condition, which permitted rainfall influx and soil water evaporation loss out of the boundary. Grass vegetation was simulated by specifying a root zone that varied in depth from 500 mm to 1000 mm below the surface. The bottom boundary condition was specified as a no-flow boundary and a seepage zone was specified at the toe of slopes where seepage has been observed. The seepage faces will yield water out of the hillslope segment when positive soil water pressures occur due to accumulation of upslope water at these boundaries.

Table 4.1 Summary of profiles in simulated transects.

Transect	Nest	Depths (mm)
LC1-4	LC1	550 1000
	LC2	450 840 2040
	LC3	440 990
	LC4	440 890
LC5-7	LC5	750 1280
	LC6	320
	LC7	460 880 1100
LC8-9	LC8	490 820 1450
	LC9	440 850
	LC10	530 830 1390

While it is clearly evident from tensiometer responses and field observations that preferential flows occur in the hillslope segments, these are not simulated in the HYDRUS-2D model, since the objective is to quantify the soil water yield during the low flow periods, when there is very little rainfall and no preferential flow mechanisms are likely to operate in the subsurface.

In addition, a single material type is used to represent the whole hillslope segment. The hydraulic characteristics of the material which yielded the best match to observed soil water matric pressure heads and volumetric water contents was assigned to the entire finite element mesh representing the hillslope segment.

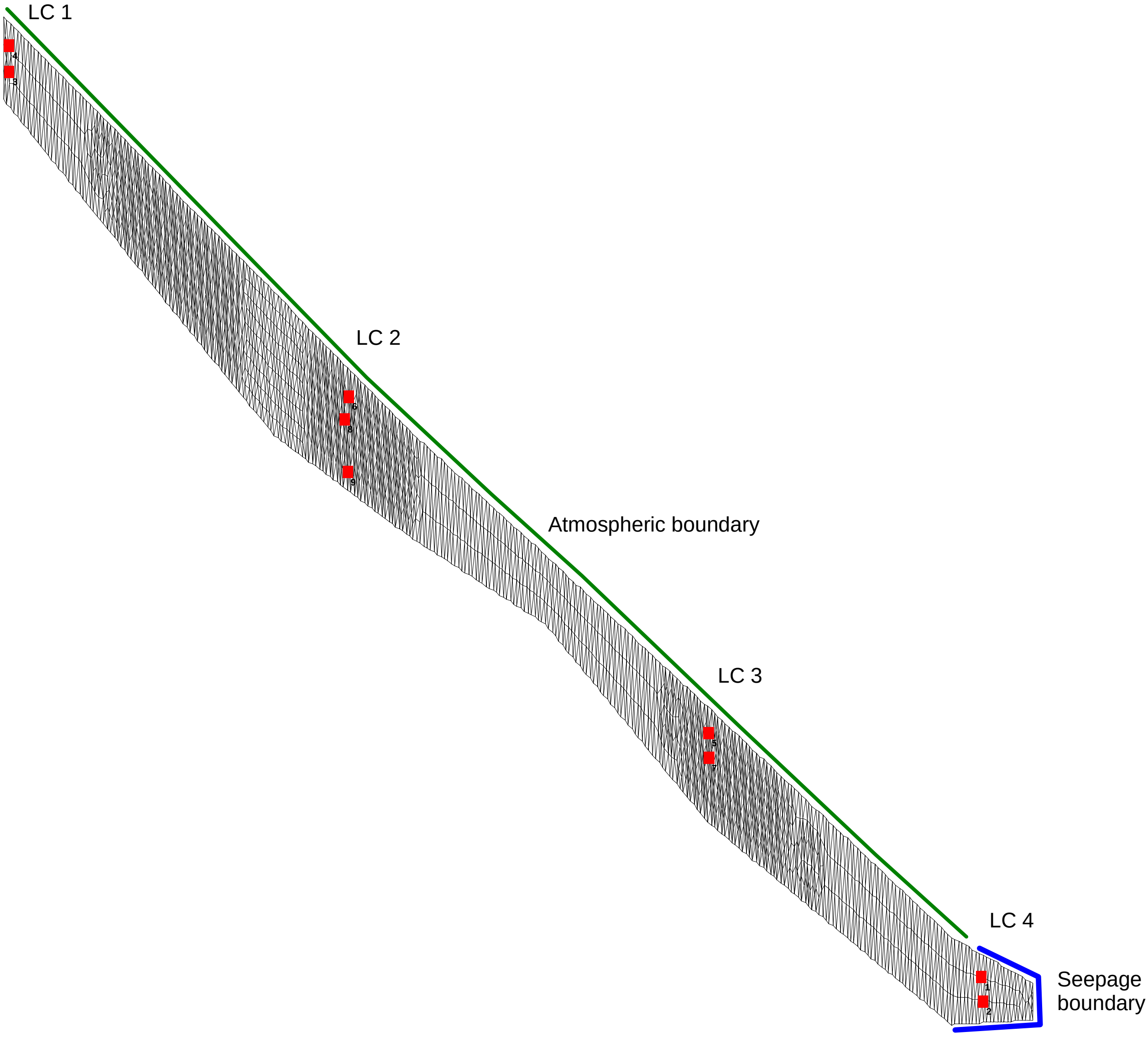

Figure 4.7 The finite element mesh of transect LC1 to LC4 showing the position of observation nodes, corresponding to tensiometer positions in the hillslope segment. (The vertical exaggeration is 10x).

4.2.1.2 Hydraulic characteristics of materials

A typical water retention characteristic, measured in a controlled outflow cell, (Lorentz *et al.,* 2003), is shown in Figure 4.8. Superimposed on these measured data is the retention characteristic which best represented the observed tensiometer behaviour in the HYDRUS-2D simulations. A full set of these characteristics for the transect LC1 to LC4 is included in

Appendix B. The theoretical characteristic has a larger porosity or saturated water content at all profile depths. The theoretic curves match the remainder of the measured values well in the case of LC2 at the 400 mm, 600 mm and 900 mm depths and at LC3 at the 1400 mm depth. In all other locations the measured values are drier than the theoretical characteristic, with the exception of LC2 at 1400 mm. The large saturated water content required for the simulation characteristic is indicative of the macropore structure of the material, which may not have been captured in the small laboratory samples.

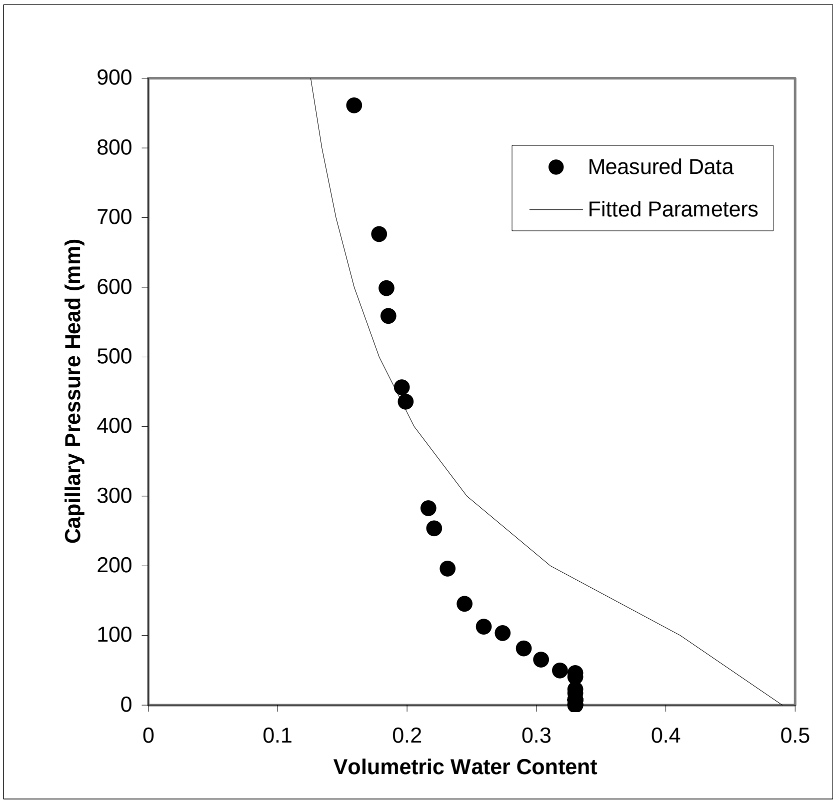

Figure 4.8 The water retention characteristic for station LC2 at 600 mm, showing the laboratory measured characteristic (dots) as well as the theoretical characteristic used in the HYDRUS-2D model (line).

Achet *et al.* (2006), also used the HYDRUS-2D model to simulate hillslopes and noted a discrepancy of several orders of magnitude in soil hydraulic properties between reported laboratory and the best parameters for the simulated results. Thus the parameters that were measured from field samples do not necessarily correspond to the optimum parameter sets utilised in the model. The measured values did, however, prove valuable for starting conditions and were used as a guide to constrain the theoretical curves adopted in the modelling.

4.2.1.3 Cumulative fluxes

The modelled soil water matric potential and volumetric water contents are compared with the observed values in Appendix C1 to C3 for the three hillslope segments. In general there is a far better fit to the matric pressure head data, measured by tensiometers, than to the volumetric water content data, measured with the neutron probe. This may be due to the small range of water contents observed with the neutron probe.

Hillslope segment LC1 to LC4

The matric pressure head simulations compare well to the observed data in the near surface for this transect, with rainfall and drying responses displaying the correct amplitudes. The observed water contents are also well represented in the simulation. In the deeper part of the material in this transect, the matric pressure heads are simulated well during the summer months and during the winter recession. However, the recovery during the early spring rains of 2001 is not effectively mimicked. This is likely due to the poor representation of vertical and lateral preferential flow, which results in accumulations in the deeper part of the profile at the onset of rainfall. The volumetric water contents reflect this inadequacy in the modelling, with no simulated increase in soil water content at depth after the onset of the spring rainfall at LC3 at 990 mm. However, the response to winter drying and the subsequent wetting up in spring at station LC4 is simulated well. This demonstrates the model's ability to simulate flow accumulations resulting from lateral discharge along the soil/bedrock interface, but its inadequacy in representing preferential lateral and vertical fluxes within the soil profile.

Hillslope segment LC5 to LC7

The soil matric pressure heads in the near surface sensors (300 to 500 mm below surface) are simulated well throughout the hillslope segment. Again, the water contents at this depth are poorly represented in the model. The introduction of a variable head boundary condition at the upper end of this hillslope segment improved the simulation form initial attempts. This variable head boundary condition represented the water input from the upslope segment, LC1 to LC4, into this lower segment. In the deeper part of the profile the matric pressure heads are reasonably simulated, reflecting the winter drying out, but the rebound at the onset of spring rains in September 2001 is missing from the simulated response. Hence the deep lateral accumulations are not well represented in the model. The simulated volumetric water contents in the deep part of the profile are generally dryer than those observed, again, reflecting the poor simulation of preferential movement of water in the vertical and lateral direction.

Hillslope segment LC8 to LC10

This hillslope segment is characterised by slower accumulation of water at depth in the profiles than is the case in the first two segments, due primarily to the lack of preferential flow responses. Matric pressure heads and volumetric water contents are adequately simulated except for locations near the crest of the hillslope segment at LC10, where the rebound in matric pressure head and volumetric water content at the 830 mm and 1390 mm depth during spring rainfall in September 2001 is poorly simulated. This is likely that upslope accumulation of vertical and lateral flow at LC10 is not represented in the model.

The resultant fluxes and changes in soil water content from the modelling of the three transects is shown in Figures 4.9 to 4.11. In the LC1 to LC4 transect, the seepage from the toe continues throughout the simulation period (Figure 4.9). A total of 160 mm of the 720 mm rainfall seeps from the toe of the hillslope segment during the simulation period. The cessation of seepage from this hillslope segment during the winter observed on site is not simulated. However, some seepage may continue at the toe into the fractured sandstone. In the LC5 to LC7 segment, the seepage tails off in midwinter after an increase in the seepage rate between March and June, resulting from the accumulated water from the summer rains (Figure 4.10). The seepage flux during the winter period at segment LC8 to LC10 (Figure 4.11) does not tail off as it does in the segment LC5 to LC7. The seepage flux also responds early to rainfall and is a maximum during the period January to March. The seepage fluxes in both LC5 to LC7 and LC8 to LC10 are similar to the segment LC1 to LC4, although slightly higher. In all three segments the change in volumetric water content in the segment reduces by some 100 mm during the simulation.

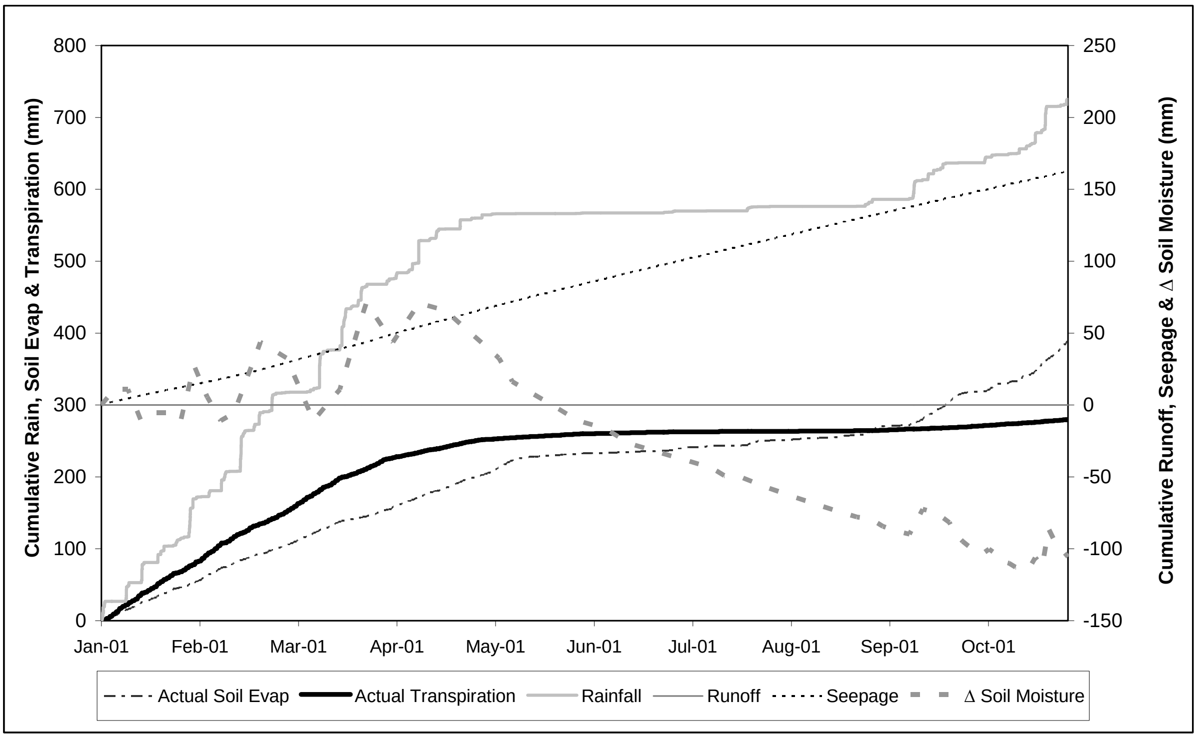

Figure 4.9 Soil water fluxes and changes in water contents in the hillslope segment LC1-LC4.

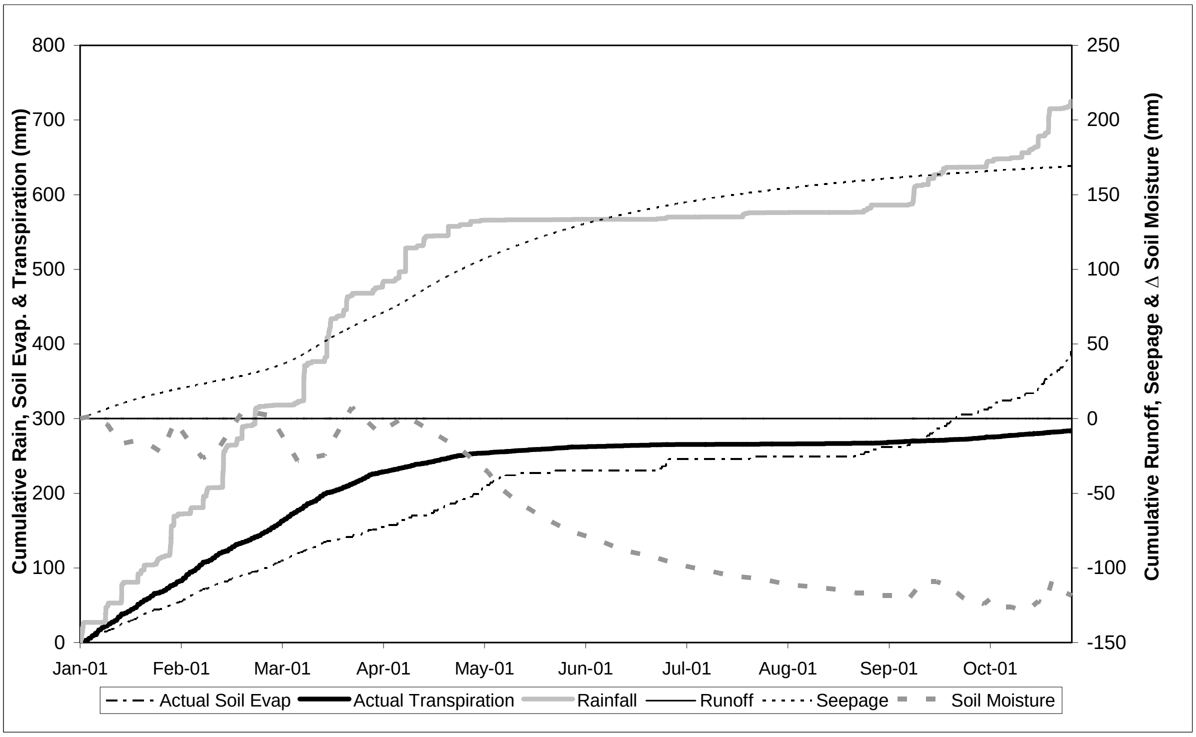

Figure 4.10 Soil water fluxes and changes in water volume in the hillslope segment LC5-LC7.

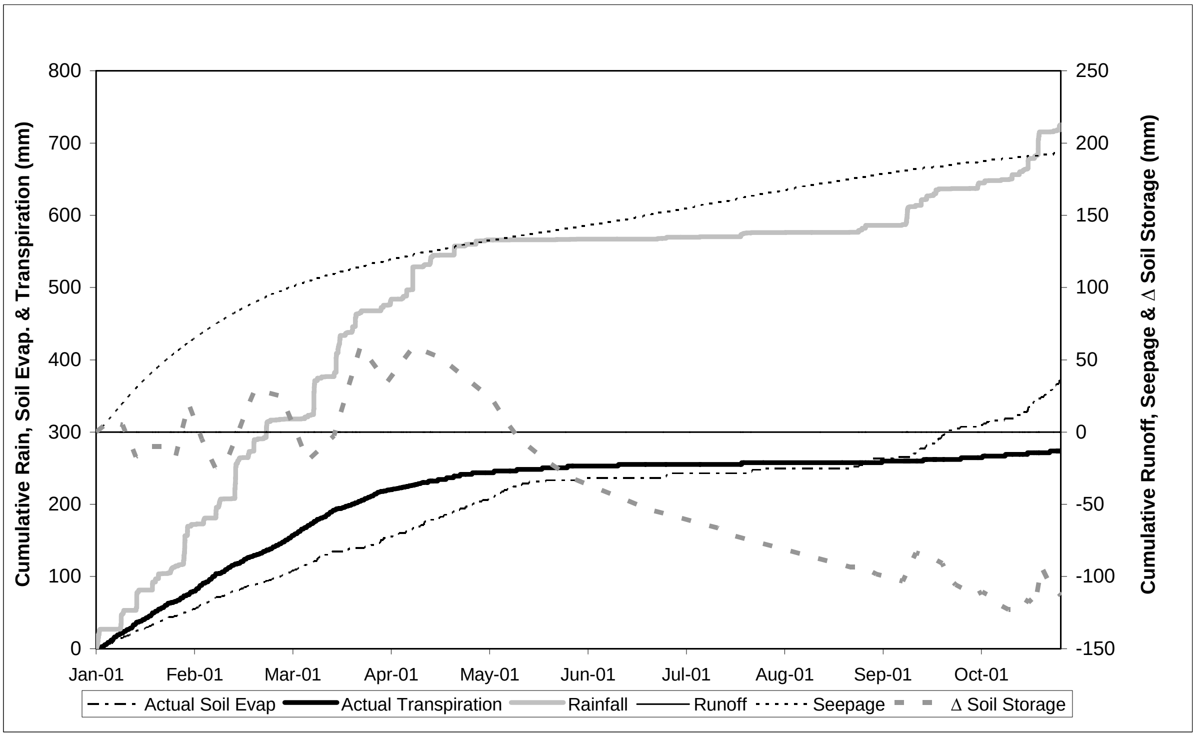

Figure 4.11 Soil water fluxes and changes in water volume in the hillslope segment LC8-LC10.

4.2.2 Geophysical observations

Since the flow in the Weatherley stream persists throughout the dry period, the source of water during this time must come from sources in addition to the soil profile. 2D electrical resistivity surveys were performed in February 2004 to determine the distribution of the source of water within the fractured sandstone in the hillslopes.

The subsurface resistivity is related to various geological and hydrological parameters: the lithology (rock and grain sizes, porosity, mineralogy), the fluid content (solutes) and the degree of water saturation. The resistivity surveys were carried out using the Syscal Junior Switch System with 24 electrodes and two multi-core cables (maximal spacing between two electrodes 5 m). The electrodes were set along hillslope transects, and a roll along procedure (installing half of the electrodes at the end of the transect as soon as the first half of the electrodes are free) enable one to investigate transects of several hundred meters with a spacing between the electrodes of only 2 m. This provided results in an appropriate spatial resolution to a depth of 5-7 m. At an electrode spacing of 5 m the penetration depth is some 20 m, but the resolution of features is lower than for the 2 m spacing. In a 2-D survey the different pairs of the 24 electrodes that serve either as current or potential electrodes are used, and the distance between the electrodes is varied systematically. The 2-D Wenner configuration was used as the electrical array. The measured pseudosections (apparent resistivity) were processed with a 2-D inverse numerical modelling technique (RES2DINV) to give the estimated true resistivities of the subsurface.

Resistivities less than 60 ohm.m in the sandstone indicate the presence of water, as is evident in the transect from station 1 to 4 in the upper slope of the lower subcatchment shown in Figure 4.12. Deeper surveys, using a wider spacing of resistivity probes, reveal the distribution of water in the fractured material (Figure 4.13). Water from this fractured sandstone clearly contributes to the hillslope response, even emerging in the upper slope prior to station 4.

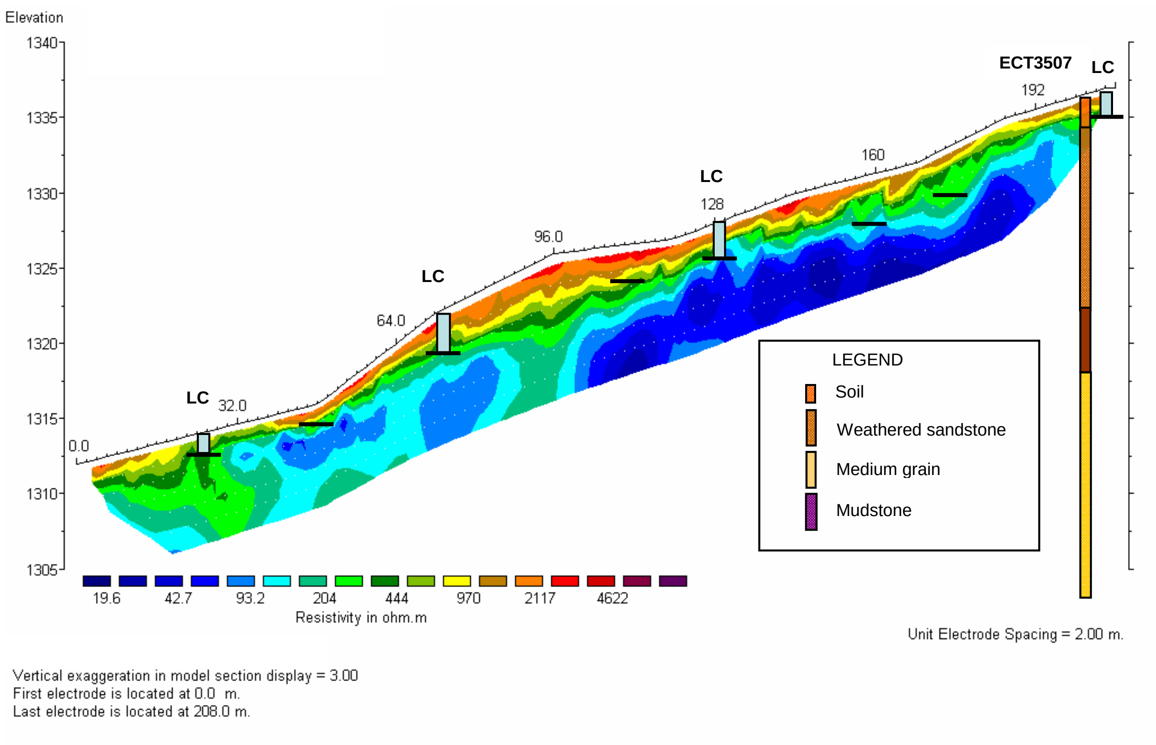

Figure 4.12 2D resistivity transect (2 m spacing) through stations 1-4 in the lower catchment (February 2004) showing the borehole log and water levels for November 2004.

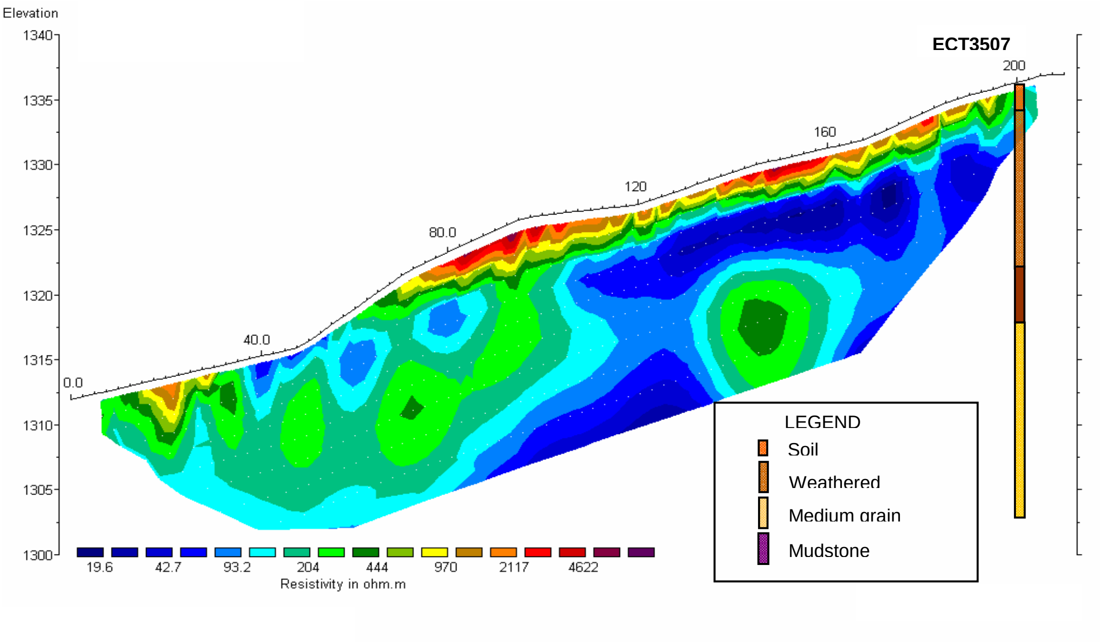

Figure 4.13 2D resistivity transect (5 m spacing) through stations 1-4 in the lower catchment (February 2004) showing the borehole log and water levels for November 2004.

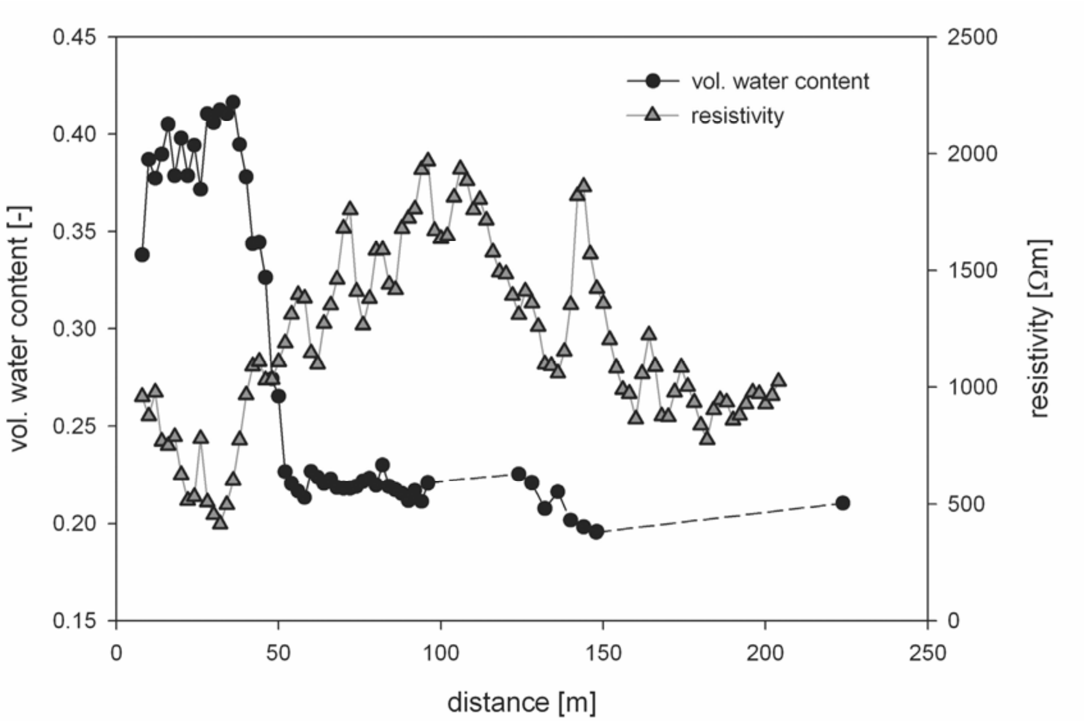

Figure 4.14 Comparison of resistivity and volumetric water content, measured with the TDR in the upper 300 mm along transect LC1 to LC4, shown against distance from the toe of the slope segment near LC4.

A further survey was performed between the west slope stations 7 to 11, (Figure 4.15). Here it is clear, again, that hillslope water contributes to the stream via the fractured rock underlying the soils. In addition, it is evident, that the stream does not intersect a permanent aquifer since the material below the stream appears dry to a depth of some 20 m below the stream. This is confirmed by the near stream borehole observations. Hence, the stream discharge during the later part of the low flow period is sustained predominantly by contributions through the hillslope bedrock.

The value of Electrical Resistivity Tomography (ERT) is enhanced by comparison with borehole logs and water table observations. In addition calibration against observed soil water contents could extend the value of the surveys. To this end, the water content in the top 300 mm in hillslope segment LC1 to LC4 was determined by inserting a 300 mm TDR probe and reading the average water content over this depth with a Campbell Scientific TDR100 apparatus. The electrical resistivity over the 300 mm depth was extracted from the shallow ERT survey represented in Figure 4.12. The resultant comparison is shown in Figure 4.14. It is clear that there is an inverse relationship between the water content and the effective electrical resistivity over the 300 mm depth. An increase in water content near the toe of the hillslope segment is paralleled by a decrease in the resistivity. Upslope of LC4 (at distance 30 m from the toe of the slope), the water content decreases rapidly, to a minimum at some 50 m from the toe (Figure 4.14). This decrease in water content is matched by an increase in electrical resistivity. The low value of water content of approximately 0.22, between 50 m and the crest of the slope at 220 m is reflected in a resistivities ranging between 1000 and 2000 ohm.m.

This simple study is an introduction to what could be a valuable correlation in future surveys, particularly in examining the variability of soil water content near the surface.

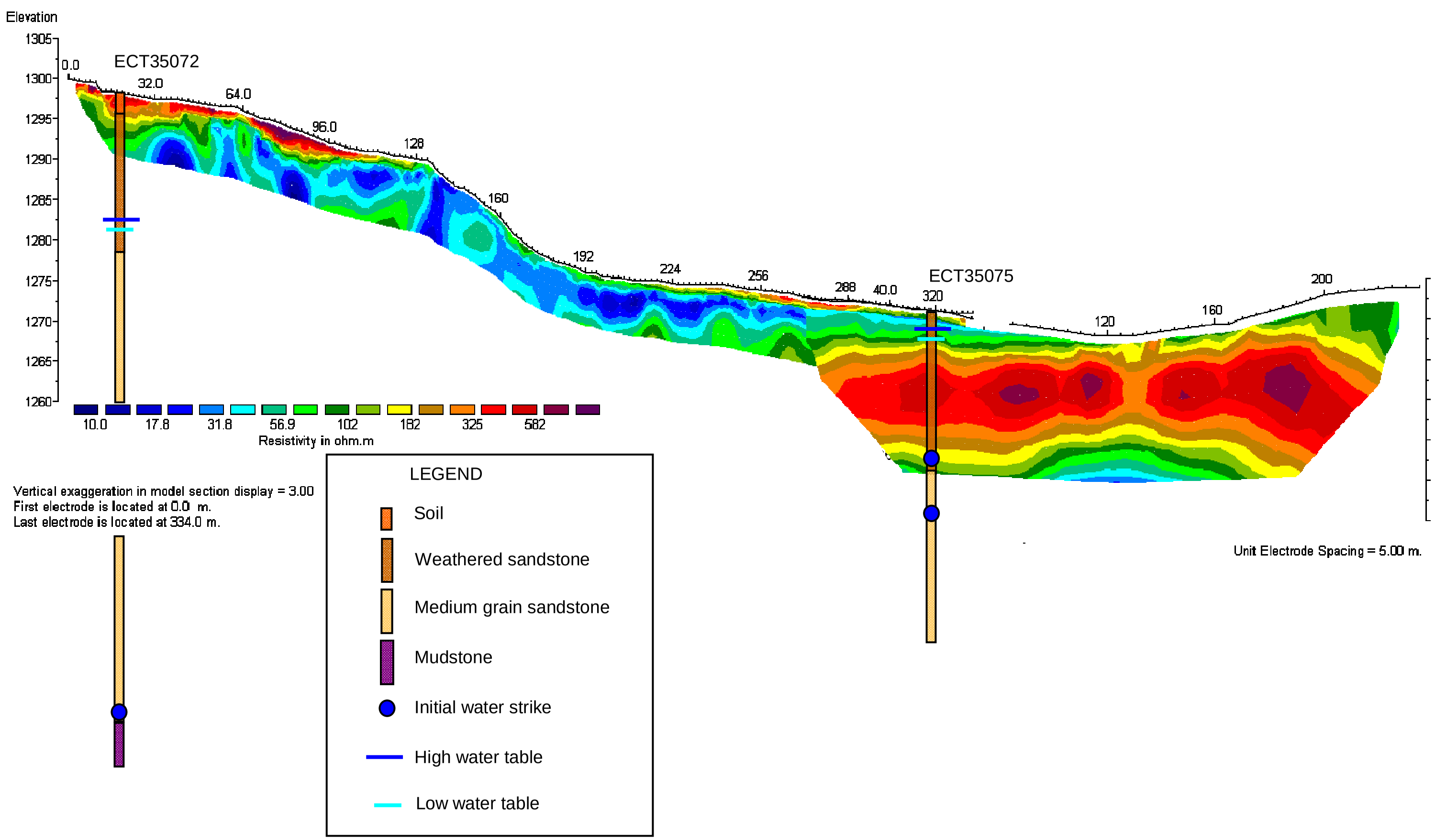

Figure 4.15 2D resistivity transect (5 m spacing) through stations 1-4 in the lower catchment (February 2004) showing the borehole log and water levels for November 2004.

4.3 Integrating Hillslope and Catchment Scales

While the observations, simulations and surveys at the local and hillslope scale are valuable in describing the dominant mechanisms in the catchment response, the distribution of groundwater and the sampling of isotopes yield information of general catchment response which the smaller scale observations supplement.

4.3.1 Rainfall-runoff analysis

In order to develop a general understanding of the rainfall-runoff dynamics, a simple time series analysis was performed by dividing the precipitation into separate events for the hydrological year 2004 (Wenninger 2007). An individual rainfall event was assumed to be one in which there was no cessation of precipitation for more than 4 hours. For each rainfall event (P), a 7-day antecedent precipitation index, API_{-7} was calculated as:

$$API_{-7} = \sum_{i=1}^{7} P_{(-8+i)} \cdot (0.1 \cdot i) \qquad \text{(mm).}$$

Runoff events were defined as those exceeding the mean daily discharge (MQ) for the year 2004. In order to statistically assess the rainfall-runoff relationships only those events which exceeded five times the annual mean of daily discharge were considered. This peak runoff threshold was defined as $Q_{threshold}$.

The results of the statistical analysis are shown in Table 4.2. A total of 16 events were included in a Pearson's product moment correlation coefficient, r with level of significance, p analysis for the year 2004. As can be expected, long-duration precipitation events cause slow rising times between the beginning of runoff and peak discharge (r=0.766; p=0.001), whereas events with high rainfall intensities produce short rise times, (r=-0.574; p=0.02) and high peak discharge (r=0.552; p=0.027). Large volume rainfall events produce peak runoff, (r=0.671; p=0.004) and high runoff volume (r=0.717; p=0.002).

There is a moderate dependency on the antecedent precipitation index of runoff rising times (r=-0.520; p=0.039), which demonstrates the importance of the antecedent soil water content on the generation of runoff.

Table 4.2 Pearson's product moment correlation coefficient (r) and level of significance (p) for rainfall and runoff characteristics of 16 events during the hydrological year 2004. (After Wenninger *et al*., 2007).

	Precip. duration	**Precip. amount**	**Precip. mean intensity**	**Precip. max intensity**	**Precip. API_{-7}**	**Runoff delay time**	**Runoff rising time**	**Runoff peak discharge**
Precip. amount	.116 (.669)							
Precip. mean intensity	***-.696** (.003)***	.282 (.289)						
Precip. max intensity	-.200 (.458)	*.533* (.033)*	.364 (.165)					
Precip. API_{-7}	-.242 (.367)	-.048 (.861)	.192 (.477)	.119 (.660)				
Runoff delay time	.483 (.058)	-.322 (.224)	-.472 (.065)	-.371 (.157)	-.432 (.094)			
Runoff rising time	***.766** (.001)***	-.029 (.915)	*-.574* (.020)*	-.304 (.253)	*-.520* (.039)*	*.572* (.021)*		
Runoff peak discharge	-.303 (.254)	***.671** (.004)***	*.552* (.027)*	.424 (.102)	.007 (.978)	-.330 (.212)	-.453 (.078)	
Runoff total volume	-.156 (.565)	***.717** (.002)***	.467 (.069)	.468 (.067)	.164 (.544)	-.419 (.106)	-.397 (.128)	***.908** (.000)***

***** significant at the 0.01 level***
** significant at the 0.05 level*

4.3.2 Groundwater distribution

A great deal can be learned about the catchment response by observing the groundwater levels. Two groundwater systems have been observed in the catchment, a deep bedrock aquifer and saturated water bodies perched on the interface between soil and saprolite or bedrock. These two systems have been observed respectively, through deep boreholes, drilled into bedrock and through observation holes manually augured though the soil profile to the underlying dense saprolite or bedrock. Six deep boreholes were successfully installed by the DWAF in August 2004 in the Weatherley research catchment (Figure 4.16). The results of the borehole logs and of the geophysical logging reported in February 2006 are presented in Appendix A. Two of the boreholes are positioned near the stream, one at the lower weir site (ECT35075) and one at the upper weir site (ECT35076). Four deep boreholes are located on the upper hillslopes, two in the northern part of the lower subcatchment (ECT35070 on the east slope and ECT35072 on the west slope) and two in the southern part of the lower subcatchment (ECT35069 in the east and ECT35071 in the west).

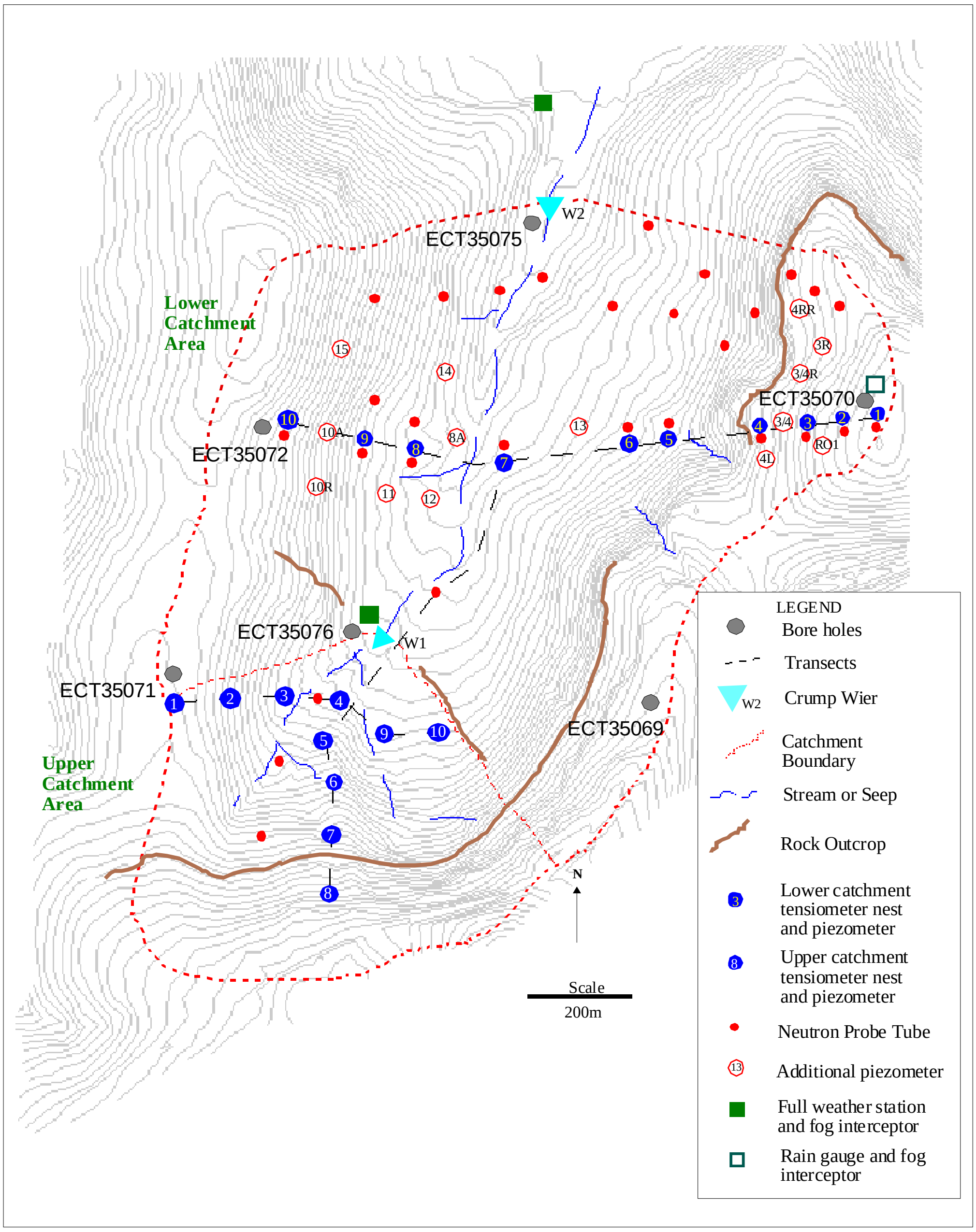

Figure 4.16 Location of the boreholes in the Weatherley research catchment.

Groundwater levels in these deep boreholes are monitored on a monthly basis. The study of responses in these deep boreholes (Figures 17 to 20) together with the observations of water perched on the soil/bedrock interface (Figures 21 to 23), builds on the hillslope descriptions of the subsurface processes in the catchment. Both the deep and perched groundwater levels are examined for the period July 2005 to April 2007.

Deep boreholes near the stream

The groundwater levels are the shallowest in the boreholes ECT3075 and ECT3076 adjacent to the stream (Figure 4.17). Water levels in the borehole in the lower catchment ECT35075 have a smaller range (3.1 m – 5.3 m), than the borehole in the upper catchment, ECT35076 (3.4 m – 4.3 m). This is possibly due to the steeper gradient in the upper catchment. It is evident, though, that in both instances, the groundwater lies within the bedrock material as the soils in the riparian zone do not exceed 2 m. On drilling the boreholes, the first strike was significantly lower than the groundwater levels observed subsequently, as is shown in the transect sections in Figures 4.19 and 4.20. Strikes occurred at 18 m below surface in the downstream borehole, ECT35075, and at 33 m below surface in the upstream borehole, ECT35076 (Appendix A). The groundwater aquifer apparently lies on a mudstone layer which occurs at approximately 50 m below surface. It is assumed that, subsequent to drilling, the hillslope subsurface water is intercepted by the riparian boreholes. The deep strikes also indicate that the supply of water to the riparian rock is slow. Indeed, the response of the groundwater levels lag the high rainfall during January 2006 (300 mm) by 1 month in the upper catchment borehole and by 2.5 months in the lower catchment (Figure 4.17).

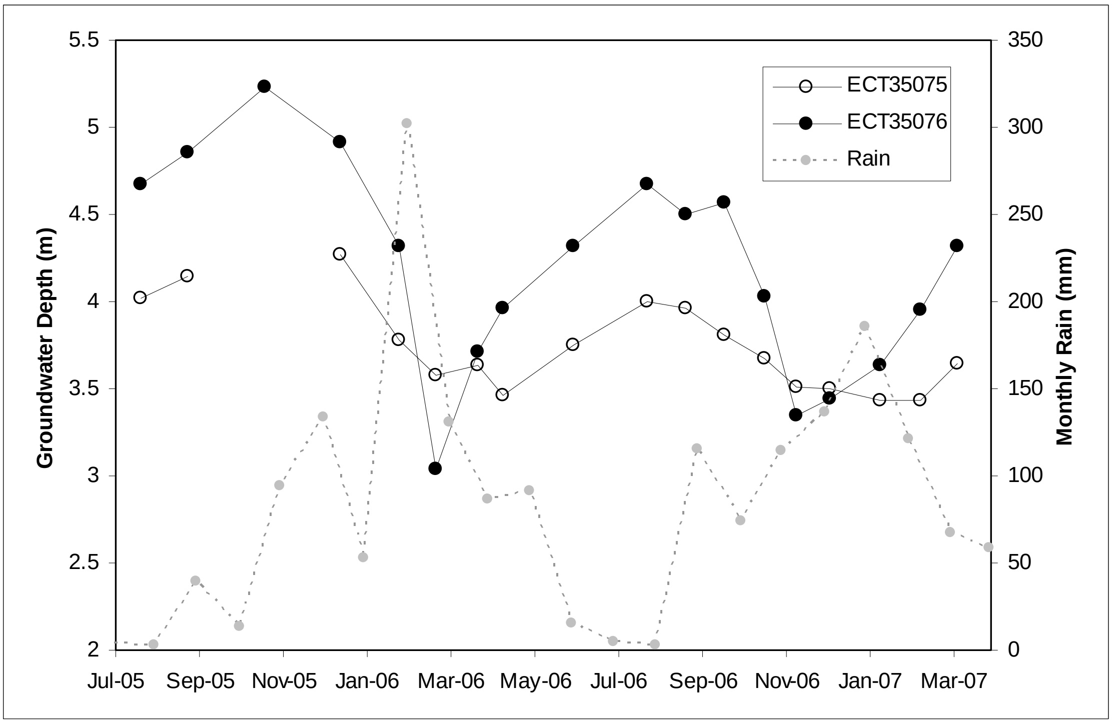

Figure 4.17 Time series of groundwater depth below surface in the riparian boreholes for the period July 2005 to April 2007.

Deep boreholes on hillslopes

The groundwater is significantly deeper on the hillslopes than in the riparian zone, occurring between 13 m and 17 m below the surface (Figure 4.18). The groundwater level in the borehole on the north, eastern hillslope, ECT35070, has consistently measured between 45 and 50 m below surface and is considered blocked. The amplitude of response, between dry and wet season is slightly less than 4 m, although the deepest measurements, taken in mid October 2005, after a prolonged dry season, have not been repeated in 2006, when significant rain occurred in August, September and October. The maximum rise in borehole water level response occurs one month after the month of maximum rainfall.

The responses of both the hillslope and riparian borehole water levels confirm the observation of lateral water movement in the fractured rock from hillslope to geological outcrops and the riparian zone, as deduced from the ERT observations. Effective gradients of the fractured rock groundwater are 1:8.1 in the lower catchment (Figure 4.19) and 1:6.6 in the upper catchment (Figure 4.20). The groundwater hydraulic potential gradients are sufficient to permit upward emergence of water from the fractured rock into the soil profile in lower hillslope positions.

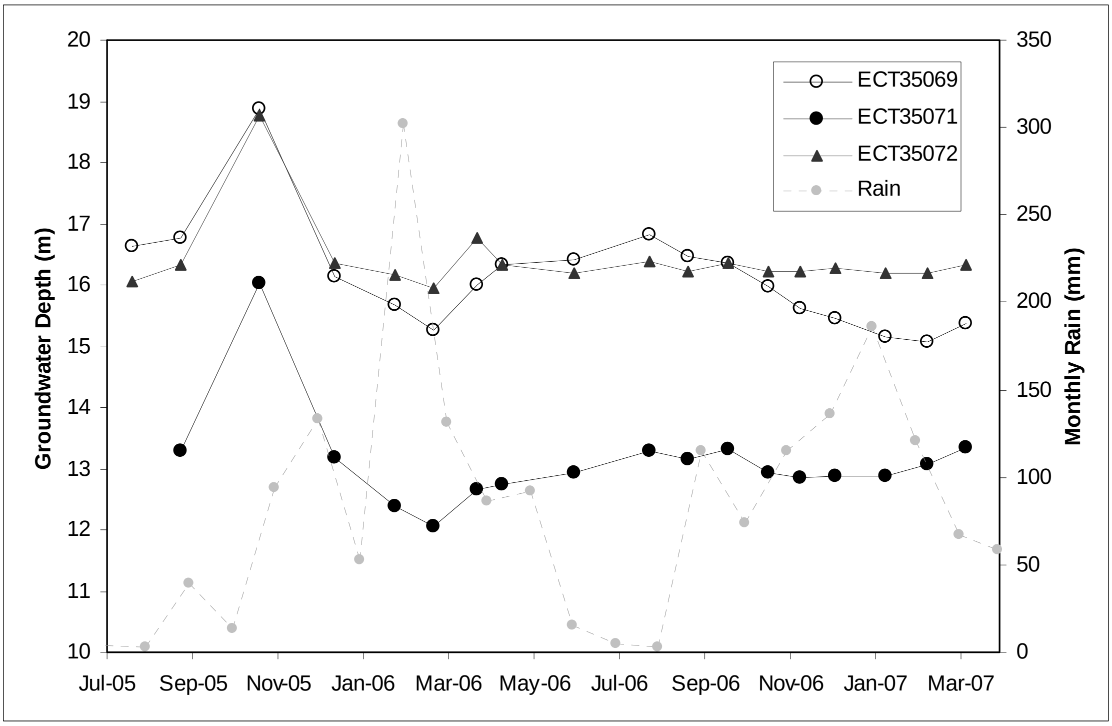

Figure 4.18 Time series of groundwater depth below surface in the hillslope boreholes for the period July 2005 to April 2007.

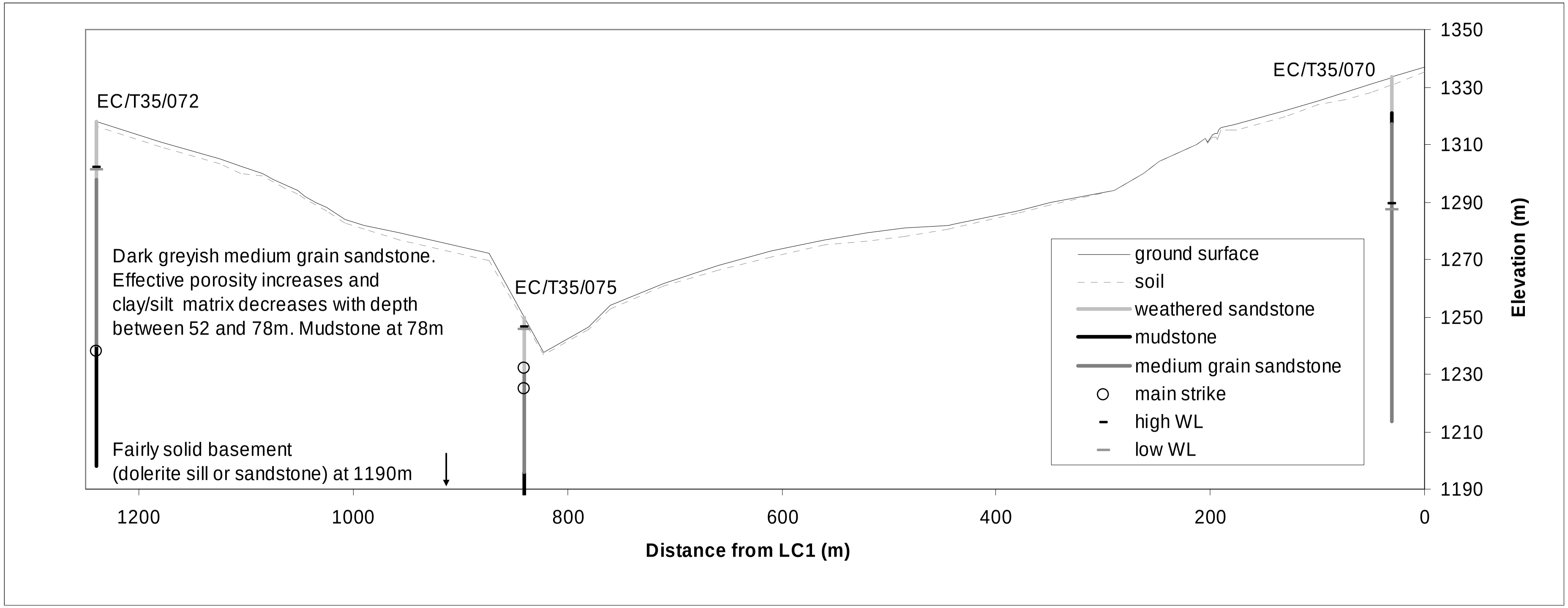

Figure 4.19 West-East cross section of the geology and groundwater through the lower catchment.

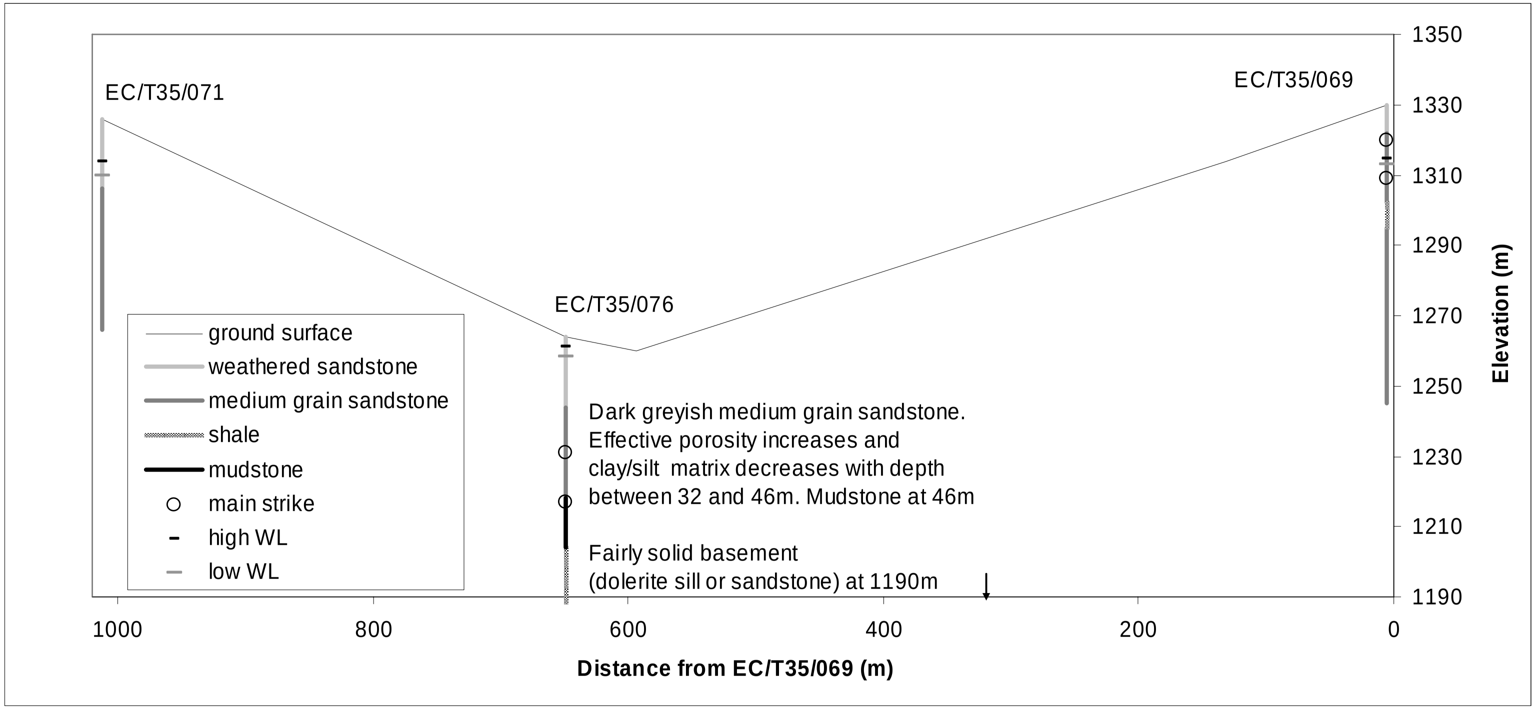

Figure 4.20 West-East cross section of the geology and groundwater through the upper catchment.

The hand augured groundwater observation holes were fitted with plastic tubes which were slotted from the bottom, where they contacted the saprolite or bedrock, over their full length to the soil surface. Although care was taken to seal these above ground, so that no overland flow would enter the tubes, these observation holes do intersect water discharging laterally in the near surface soils, a phenomenon observed in tensiometer data and shallow soil water collector pipes. Nevertheless, the delayed response to high rainfall periods and the long duration of groundwater ponding is indicative of the presence of perched groundwater.

Perched water table LC1-LC4

On the eastern slope segment in the lower catchment four observation holes were constructed adjacent to the tensiometer stations LC1 to LC4 (Figure 4.16). Here it is clear that LC1 and LC4 are perched on a rock outcrop since the groundwater is shallow (less than 1 m) and the water accumulations from upslope endure at least three months after high rainfall (Figure 4.21). The perched water table at the toe of this slope segment is present until July and responds immediately to early rain in August. The continued discharge of this perched groundwater source, well into the dry season confirms the earlier observations of the tensiometers at this location (Section 4.1.3).

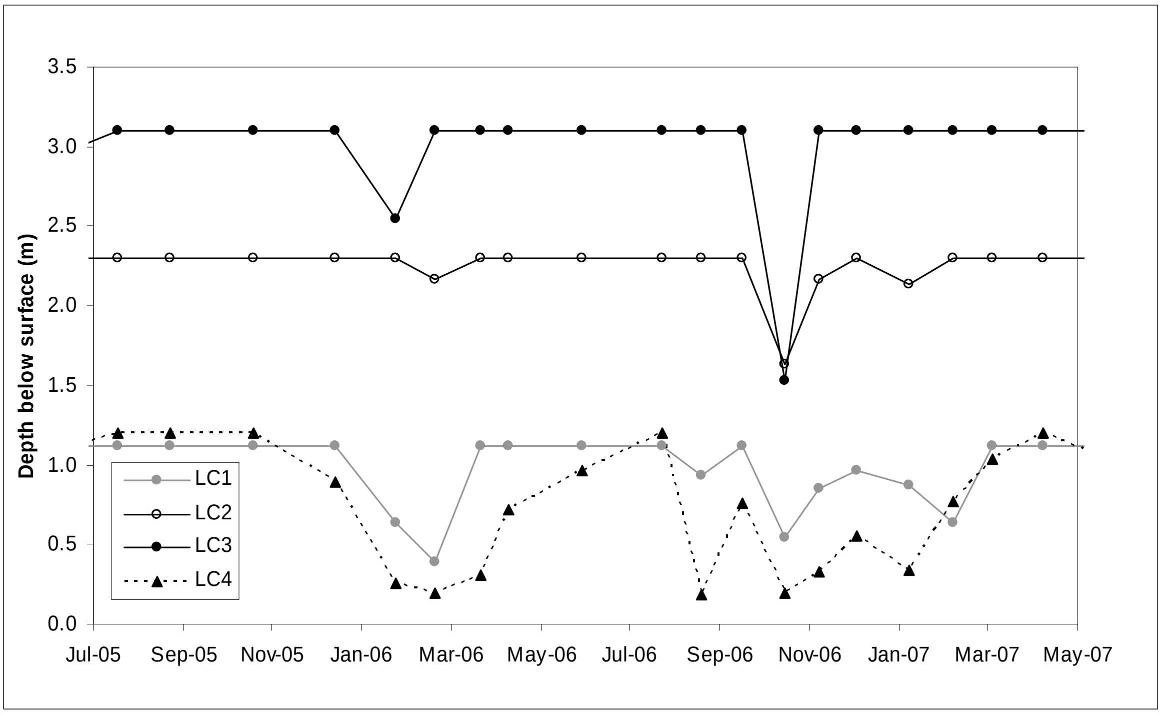

Figure 4.21 Time series of the perched groundwater depths in transect LC1 to LC4 for the period July 2005 to May 2007.

The deeper profiles at LC2 and LC3 only respond to high rainfall events and do not appear to receive lateral discharge from upslope. The water reaching the soil/bedrock interface is clearly subject to lateral, downslope accumulation as well as percolation into the bedrock fractures.

Perched water table LC5-LC7

The water level at LC4 is within 0.6 m of the surface throughout the year. This location receives water from the upper hillslope segment, LC1-LC4 via seepage over the outcrop and possibly from the bedrock below in response to the driving hydraulic gradient. During high rainfall events (300 mm in a month or events of more than 60 mm), the water levels rise to within 0.1 m of the surface (Figure 4.22). The groundwater levels at LC6, in a similar location, but not as close to the seepage line as LC5, are also close to the surface most of the year. At LC7, near the stream, the response to the high rainfall input of 300 mm during January 2006 peaks in late February and contributions from upslope are observed until August, well into the dry season (Figure 4.22).

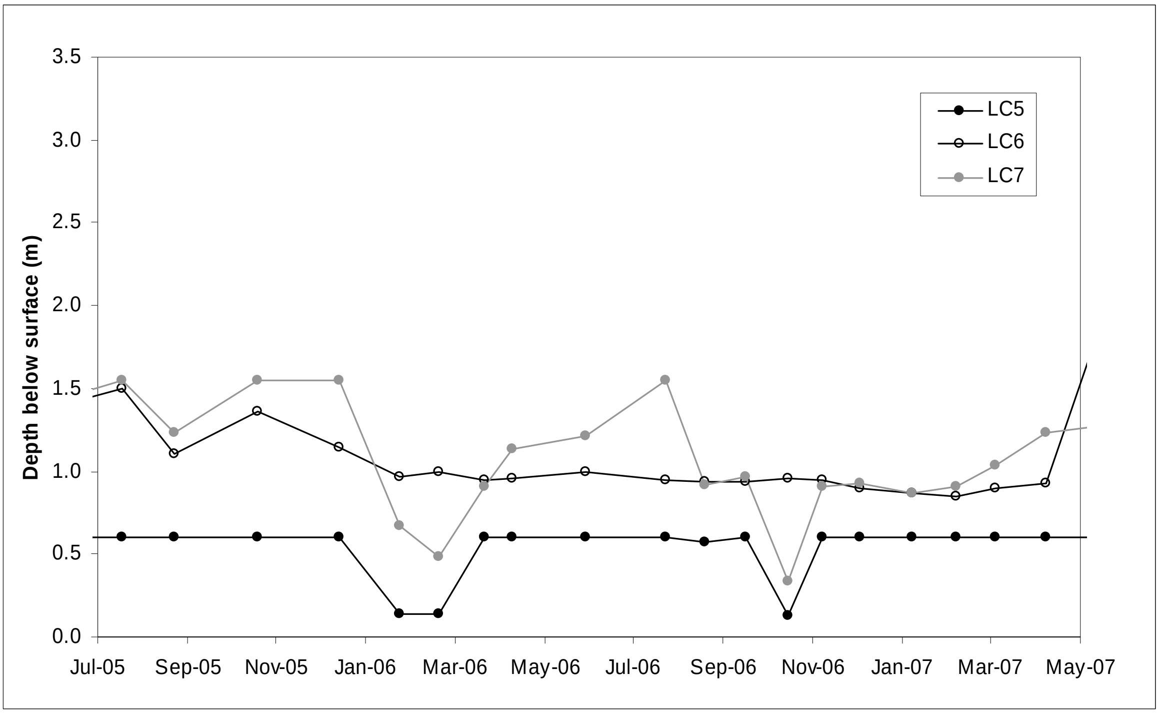

Figure 4.22 Time series of the perched groundwater depths in transect LC5 to LC7 for the period July 2005 to May 2007.

Perched Water table LC7 to LC11

On the opposite slope, the entire hillslope responds to perched groundwater indicating a continuous lateral connection on the soil/bedrock interface (Figure 4.23). The range of groundwater depths is large, with groundwater levels typically varying from 0.1 m below surface in the wet summer to 1.5 m below surface in the dry winter. Again, the lag between high rainfall input and maximum groundwater response is approximately one month. The entire hillslope contributes water until August in the dry season. Based on the ERT results, contributions from this perched water source are likely to be not only lateral along the interface, but also vertical into the fractured rock. Groundwater that enters into the fractured rock is likely to contribute to the observations in the deep riparian boreholes. Indeed the response times of the perched water table match those in the deep riparian aquifer so travel time through the fractured bedrock is probably minimal, with travel time delay being mostly attributed to the lateral accumulation in the soil profile.

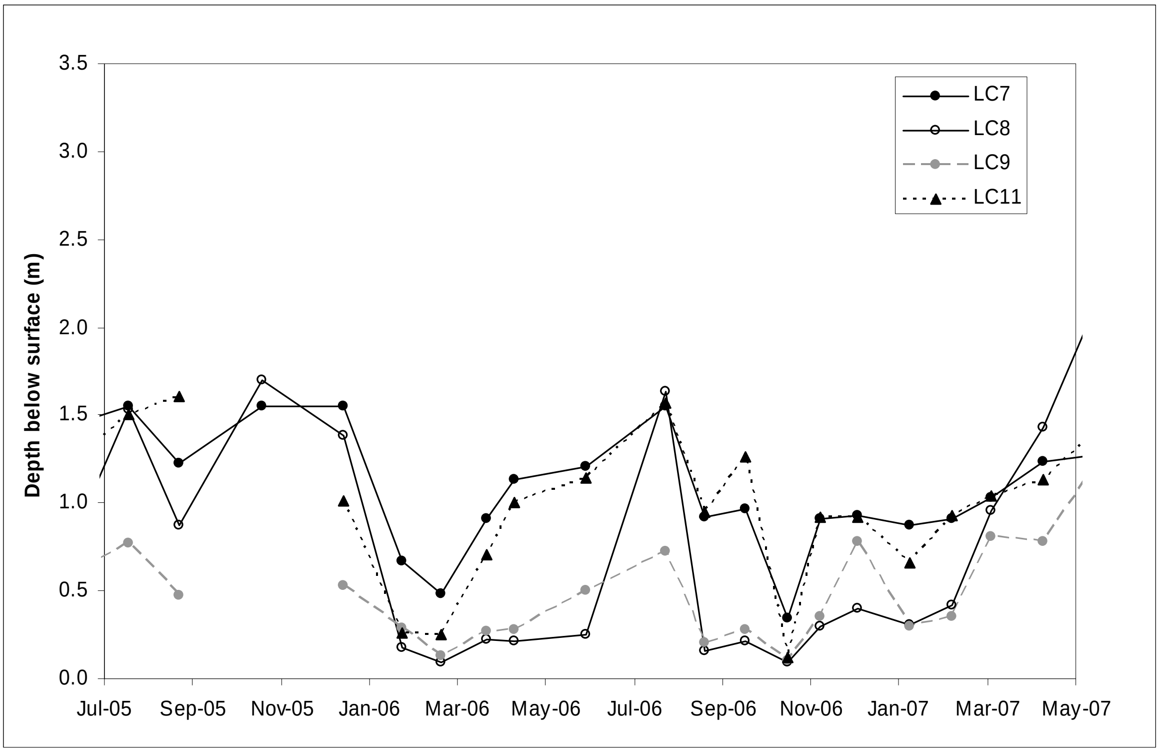

Figure 4.23 Time series of the perched groundwater depths in transect LC5 to LC7 for the period July 2005 to May 2007.

4.3.3 Isotope observations

The integrated mix of the sources of discharge to a stream can be usefully distinguished by observing the natural isotope concentrations in the various streamflow sources as well as in the stream and the rainfall. Natural isotope samples were collected in the Weatherley and Mooi catchments during the wet period between December 2002 and January 2003 and again during the dry period in August 2004. The natural isotope data are plotted as differences (δ value) between the measured value and a standard (VSMOW Vienna Standard Mean Ocean Water) and are expressed as a part per thousand (‰). Analytical errors are normally ±0.2‰ for δO^{18} and ±0.1‰ for δH^2. Generally δH^2 is plotted against δO^{18}, as shown in the schematic diagram, Figure 4.24. Natural isotopes from ocean water typically fall on the global meteoric water line, (a), but local rainfall may occur above or below this line as shown in line b. isotope concentrations may occur at the lower end of this line due to rain out of the heavier isotopes. Rainfalls with these concentrations are typical of higher elevations, cooler zones and inland locations. Isotope concentrations occurring at the higher end of line b occur in lower altitudes, warmer areas and nearer the ocean. Rainfall which experiences evaporation prior to falling may exhibit concentrations along line c. The components of runoff may exhibit the current event's rainfall signature (c), prior rainfall signatures (c) or may have experienced some enrichment due to evaporation from the soil or during flow over rock outcrops. Such a sample may have an isotope concentration such as that shown at point e.

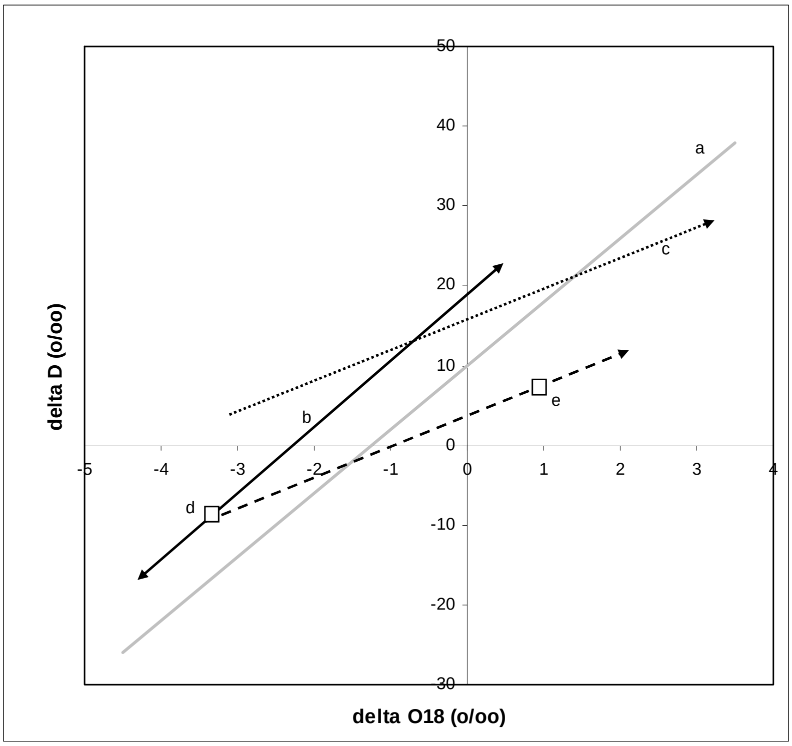

Figure 4.24 Conceptual primary forcings on isotope compositions of rainfall and runoff, (after Aggarwal *et al.*, 2002).

The rainfall isotopes collected in the Weatherley research catchment during the wet season of December 2002 to January 2003 are shown in Figure 4.25. There is a wide range of isotope concentration, but two typical patterns seem to describe the type of rainfall occurring at the site. An attempt at determining what sort of weather may contribute to these isotope signatures was made by obtaining descriptions of the rainfall from the S.A. weather services (Table 4.3). Knowledge of what sort of weather behaviour results in the two isotope patterns would be useful in evaluating responses of the different components of streamflow. The steeper isotope rainfall pattern appears to originate from rainfall drawn in from the ocean, whereas the flatter pattern is developed from frontal rainfall events. Examination of the intensities associated with these events did not reveal a definite correlation with the isotopes' relationship.

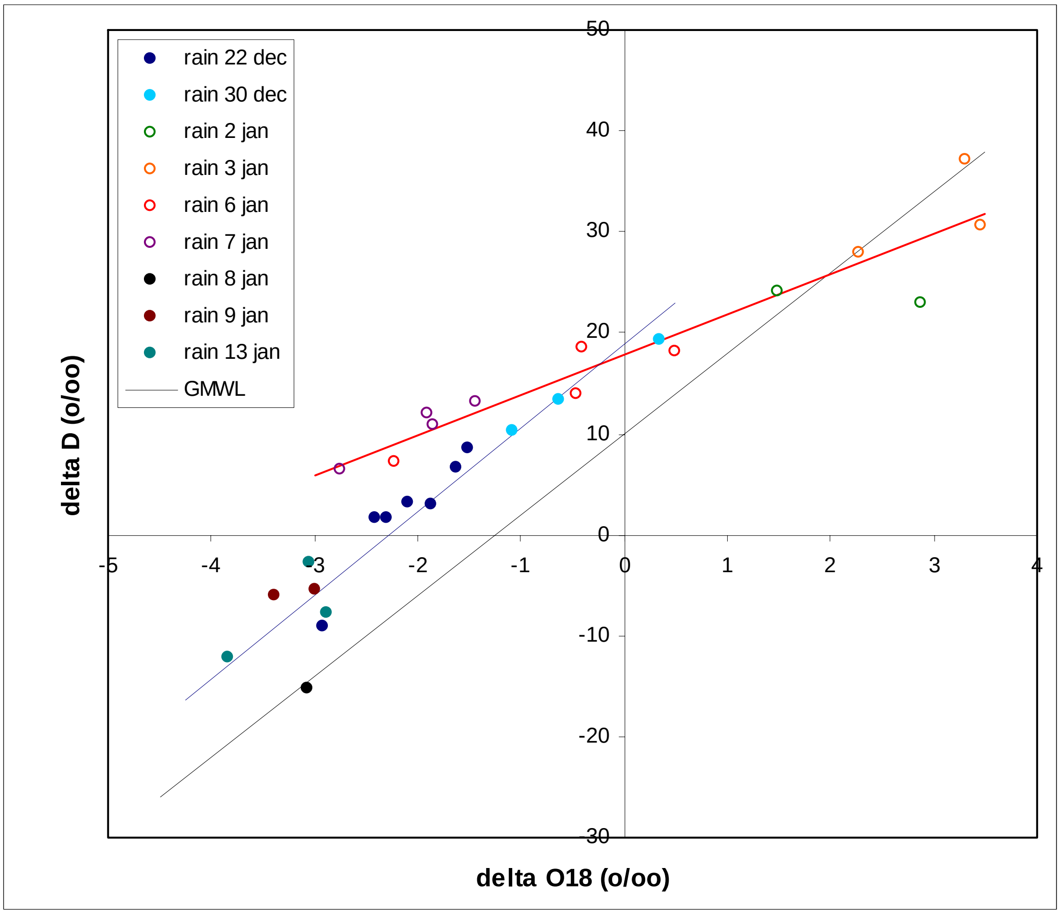

Figure 4.25 Rainfall isotopes collected from the Weatherley catchment during December 2002 and January 2003.

Table 4.3 Summary of rainfall patterns during the isotope monitoring period, December 2002 and January 2003 at Weatherley.

Rainfall date	Description	Category
22-Dec-2002	8.2 mm of rain fell between 22:00 and 24:00. The rainfall was likely from a thunderstorm which developed east of the surface trough which was lying over the interior of the country. There was a cut-off low pressure in the upper atmosphere, indicating quite a strong weather system. The rainfall that fell at Elliot was associated with south-easterly surface air flow.	SE Frontal
30-Dec-2002	Rainfall at Elliot started falling around 22:00 and ended at about 24:00. Once again there was thunderstorm activity east of the surface trough lying across the country, resulting in a surface airflow from a south-easterly to easterly direction.	SE-E Frontal
2-Jan-2003	The automatic weather station at Elliot experienced communication problems on this day and so it is not possible to determine the timing of the rainfall. A cold front was approaching the country from the west. In advance of this front, there was quite a strong onshore flow and so it is likely that whatever rain did fall, originated from maritime air that was fed inland from the south-east.	SE Maritime
3-Jan-2003	Rain fell at Elliot from 14:30 to 20:00. The cold front passed south of the country and there was a well established surface trough lying over the central parts of the country. Convergence ahead of this trough resulted in thunderstorm activity. The surface flow was easterly to south-easterly.	E-SE Frontal
6-Jan-2003	Rain fell from 19:30 to 24:00. There was a deep surface low pressure lying off the west coast. In addition there was a weak coastal low pressure lying off Port Elizabeth. The interaction of these two systems allowed for convergence to the north-west of Elliot. The rainfall thus originated to the north-west of Elliot.	NW Frontal
7-Jan-2003	No rainfall was recorded at the Elliot station. The trough that had been lying off the west coast the day before had now moved further eastwards and was lying across the western interior of the country. The South Atlantic Anticyclone had started to ridge around the country and was feeding moist maritime air in over the southern parts of the country. There was a south-easterly airflow at the surface, but throughout the upper air, the flow was north-westerly. The surface system was thus not very well developed and this is possibly why few thunderstorms occurred ahead of the trough.	SE Maritime
8-Jan-2003	Rain fell at Elliot throughout the day from 09:00 to 22:00. The surface trough had strengthened overnight and now extended into the upper air. There were widespread thunderstorms ahead of the trough and most of the surface airflow at Elliot was from the south-east.	SE Frontal
9-Jan-2003	Rain fell throughout the day at Elliot. There was interaction between the persistent strong surface and upper air troughs as well as a cold front which was passing south of the country. This resulted in widespread rain over large parts of the country. The surface flow at Elliot was south-easterly for most of the day.	SE Frontal
13-Jan-2003	No rain fell at Elliot on 13 January 2003, but there was rainfall on 12 January 2003. Rain fell from 14:00 to 15:30 on 12 January 2003. Surface airflow on 12 January was westerly to north-westerly. This flow direction persisted for most of the morning of 13 January, but hanged to a south-easterly flow in the afternoon.	W-NW Frontal

(The South African Weather Service only operates an automatic weather station at Elliot. This is the closest automatic weather station to Maclear. The five-minute data from the Elliot station was analysed in conjunction with the synoptic and upper air data for the relevant days).

Components of the flow as well as the stream discharge itself were sampled to discern what proportions of each component made up the stream discharge. The samples were analysed for isotopes O^{18} and H^2 in the iThemba Labs, Johannesburg by mass spectrometry. A complete set of these data are presented in Figure 4.26. The stream flow isotope values during this wet season period are typically lined up on the rainfall pattern and show contributions from a mix of sources. The isotopes of the near surface water, collected in tubes inserted within the top 0.5 m of the profile, the shallow groundwater samples collected from the groundwater perched in the soil/bedrock interface and the deep groundwater samples fall primarily below the stream samples, whereas the rainfall isotope values are above those of the streamflow. The streamflow concentrations fall in between the preceding rainfall concentrations and that of the near surface and shallow groundwater concentrations, revealing a mix of these two sources of discharge. Some of the shallow groundwater samples in the upper catchment have concentrations close to that of the rainfall, indicating the rapid response of the subsurface. While the sampling campaign was simply aimed at assessing the value of isotope sampling in distinguishing source components contributions to discharge, some estimates have been made of these contributions by lumping the samples from each source into typical end member values.

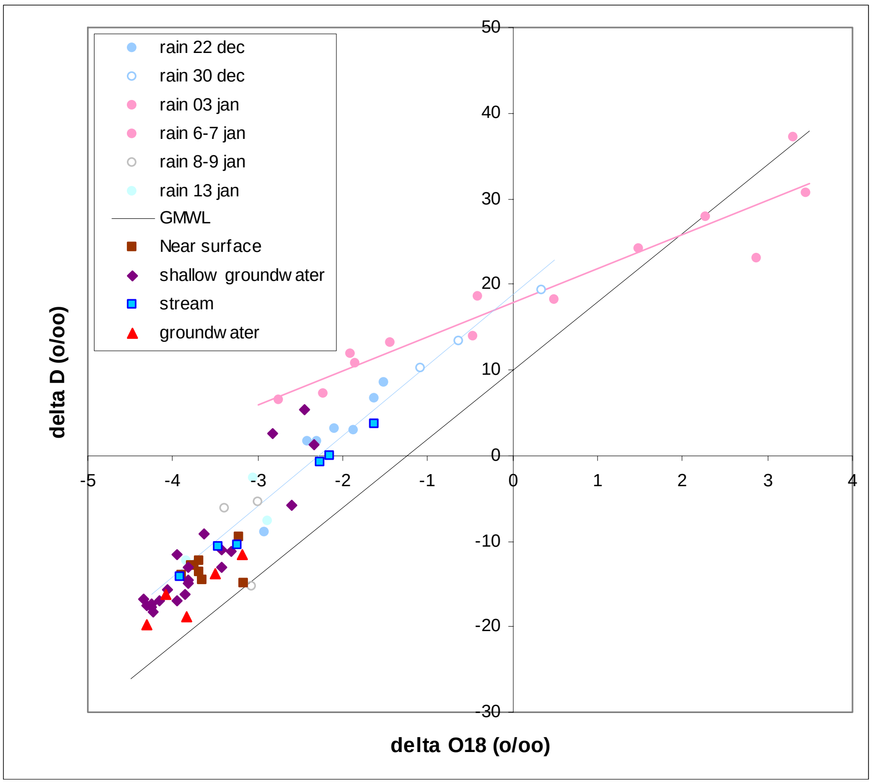

Figure 4.26 Natural isotope concentrations for different components of runoff in the Weatherley catchment during December 2002 and January 2003. (The rainfall data are shown in light shades).

Wet season isotope samples

The isotope values for samples collected during a typical series of events between the 2nd and 8th of January, 2003 is shown in Figure 4.27. A two end-member analysis was performed by estimating the end members for hillslope contributing water and rainfall or event water contribution to streamflow. The end members (EM) were estimated by calculating volume averaged the values for the rainfall and the streamflow samples and averaging the values of the hillslope source. This simple end member analysis indicates that the streamflow average lies closer to the hillslope groundwater end member than it does to the rainfall end member (EM). A linear interpolation between the end members reveals that the hillslope source contributes 60% of the total surface flow, while event water (rainfall) contributes 40%. Hence the contribution of overland flow and near surface rapid response runoff would comprise 40% and the remainder would emanate from the hillslope groundwater, whether from the soil/bedrock interface or from the fractured rock aquifer.

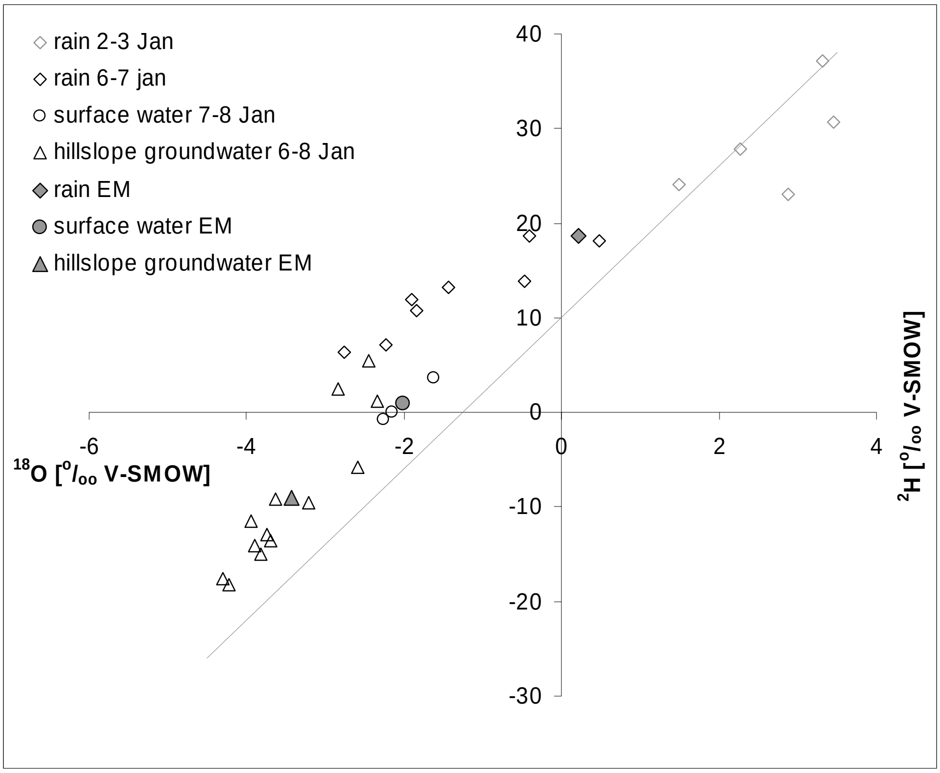

Figure 4.27 Isotope data during a wet period (January 2003) in the Weatherley catchment.

Another summer campaign took place in February of 2004 (Wenninger *et al.,* 2007). Although detailed sampling of rainfall isotopes was not possible, an evaporated component was evident during low flows between events. This would likely be due to the slow progression of water down the catena. End members could not be distinguished from this set of data (Figure 4.28).

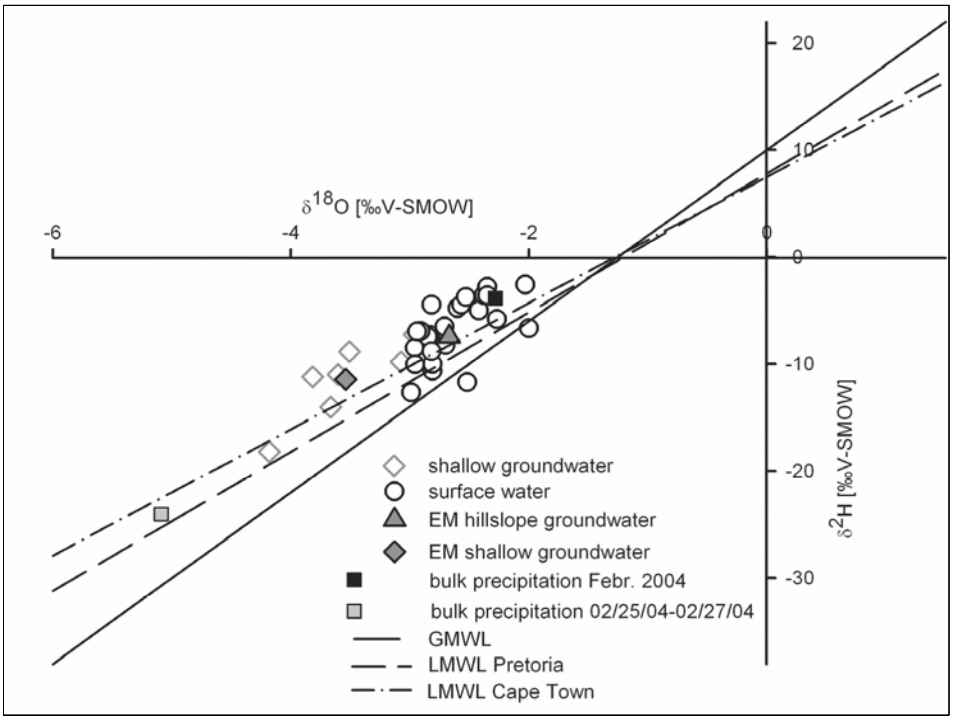

Figure 4.28 Isotope samples taken in a wet period (February 2004) in the Weatherley catchment (Wenninger *et al.,* 2007).

Dry season isotope samples

Isotope samples collected during the dry season (August 2004) showed the stream discharge biased towards the isotope concentrations of seepage samples which were collected from rock outcrops, where they had been subject to evaporation and this exhibited the enriched concentrations Figure (4.29). A line drawn between these sample values and the hillslope groundwater sample values, intersects the streamflow sample values. This indicates that a mixture of near surface water, seeping from outcrops in the upper hillslopes, and hillslope groundwater in the seepage zones and wetlands contributes to the low flow discharges. Additional sampling of the recently installed deep groundwater wells may reveal the quantities and travel times of this apparently important source of water.

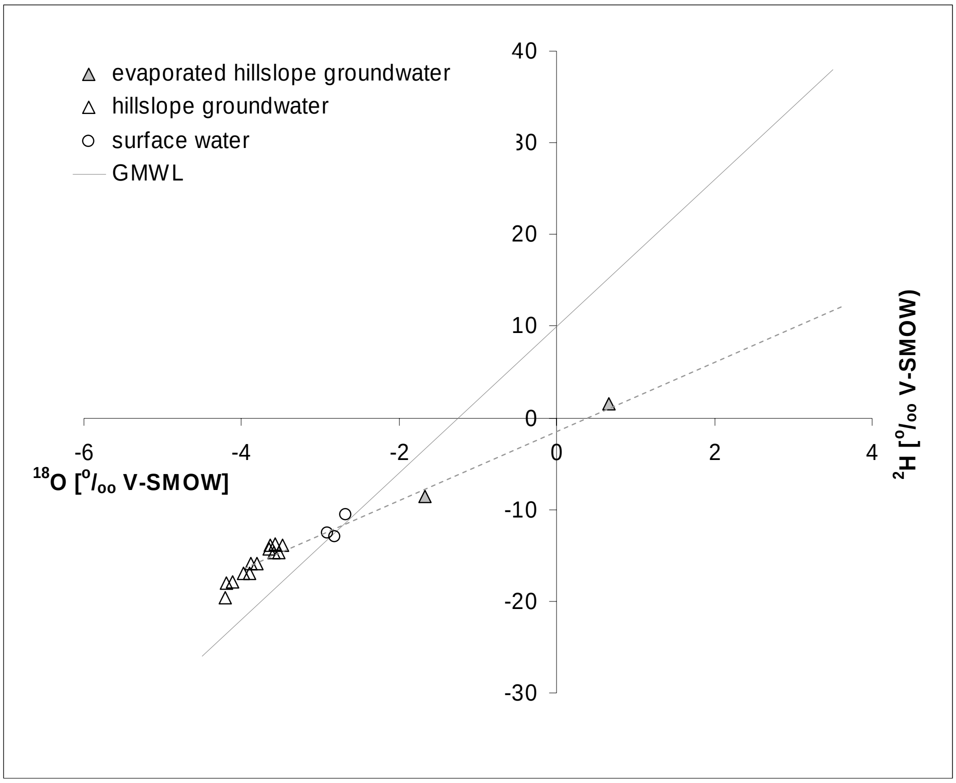

Figure 4.29 Isotope data during a dry period in the Weatherley catchment (August 2004).

4.3.4 Other tracer observations

In February 2004, temporally distributed samples were taken at the lower catchment weir and analysed for electrical conductivity (EC) and dissolved silica (Si) as shown in Figure 4.30 (Wenninger *et al*., 2007). The dissolved silica concentrations were measured by photometry, using heteropoly acids produced by the reaction of ammonium molybdate with silica, according to DIN38405 part 21(DIN 1981). Previous studies had proved successful in using Si to distinguish components of stream discharge (Laudon and Slaymaker, 1997; Uhlenbrook *et al*., 2002) and was used in the Weatherley catchment to distinguish between event water (rainfall), near surface groundwater and perched groundwater. A 3-component hydrograph separation technique was used in which specific end member concentrations were assigned to the three components. The concentrations for rainfall were taken as 0.1 mg l^{-1} for Si and 5 $\mu S\ cm^{-1}$ for EC. The concentrations for the near surface groundwater were estimated from soil water and shallow groundwater samples and set at 5.81 mg l^{-1} for Si and 20 $\mu S\ cm^{-1}$ for EC. The concentrations for the groundwater were estimated using the baseflow values of the surface water samples during dry periods between events and set as 6.05 mg l^{-1} for Si and 42.6 $\mu S\ cm^{-1}$ for EC.

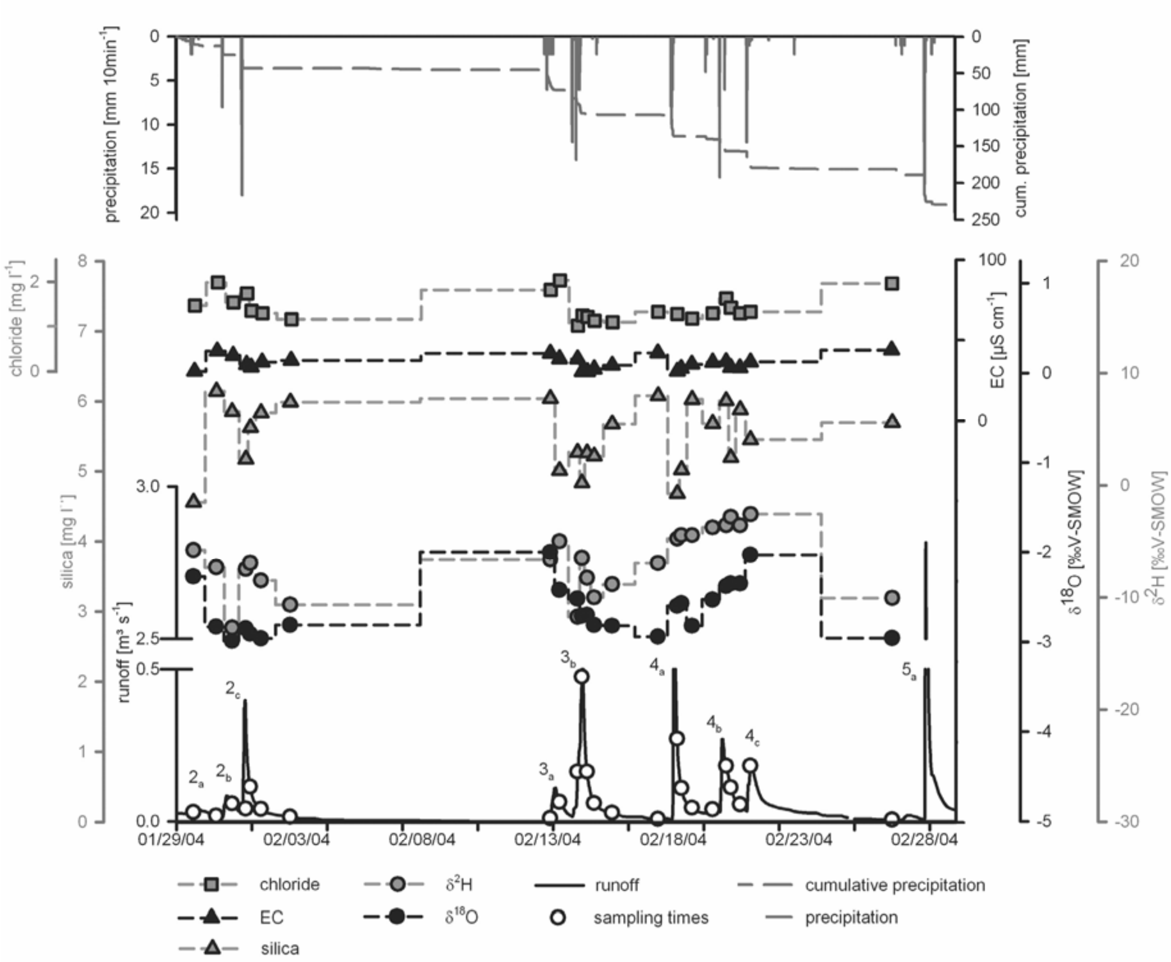

Figure 4.30 Isotope, Silica, chloride and EC of samples collected during February 2000, (Wenninger *et al.,* 2007).

The hydrograph separation technique is based on the mass balance of water and tracer, (Sklash and Farvolden 1979; Uhlenbrook and Hoeg, 2003) and can be expressed simply as:

$Q_{SF} = Q_R + Q_{NSW} + Q_{GW}$ and

$c_{SF}Q_{SF} = c_RQ_R + c_{NSW}\,Q_{NSW} + c_{GW}Q_{GW}$ where:

Q_{SF}, Q_R, Q_{NSW} and Q_{GW} are the stream flow, event rainfall, near surface water and groundwater discharges respectively and c_{SF}, c_R, c_{NSW}, and c_{GW} are the concentrations of those components.

The results of this three component separation revealed again, that hillslope groundwater contributed significantly, estimated at 70% of the discharge. Near surface groundwater contributed some 16% in most events other than two low discharge events where near surface groundwater was estimated to contribute between 1 and 4%.

4.4 Summary of Component Contributions to Stream flow

Based on the local, hillslope and catchment scale observations, surveys and analyses, the following generalisations can be made for the various contributing sources of stream flow (refer to Figure 3.3).

- ***Overland flow*** *(H in Figure 3.3)*

Overland flow discharge which reaches a surface water carrying conduit (stream or seepage line) during rainfall events is restricted to areas adjacent to these conduits. This observation has been made through runoff plot analyses, where, even in an intense event of 31.4 mm in 20 minutes, overland flow distances were estimated to be no more than 30 m (Lorentz *et al*., 2003).

Simulations of the hillslope water balance using the HYDRUS-2D model result in very small contributions from overland flow. However, this analysis was aimed more at the low flow discharge from the soil catena than event based discharge.

The contribution to event based runoff from overland flow is clearly dependant on the antecedent moisture content as demonstrated in the rainfall-runoff analyses. In addition, the tracer based, three component hydrograph separation, using EC and Si as tracers, suggests that the direct contribution to event based stream flow from the event rainfall ranges between 14% and 26% of the event discharge.

- ***Near surface soil water*** *(A, F and I in Figure 3.3)*

Observations in shallow tensiometers and free water collection tubes have demonstrated the existence of a rapid response, near surface discharge during rainfall events. These zones of near surface, lateral flow have been identified by hydropedological investigations (van Huysteen *et al*., 2007) and have been estimated by tracer aided separation techniques to yield up to 16% of event discharge.

- ***Hillslope groundwater water*** *(D and G in Figure 3.3)*

Soil water accumulation on the interface of the soil and bedrock has been observed through groundwater observations holes and tensiometer responses. These accumulations generally occur on the hillslopes upslope of parent rock outcrops. During a series of event flows, this source of water has been estimated to yield 70% of the total discharge (EC and Si tracer based hydrograph separation). Using lumped isotope sample end member mixing analysis, this hillslope contribution to flows is estimated at 60% of the stream discharge during the wet season.

During the dry season, the soil profile continues to generate stream flow well into the middle of the winter. Discharges estimated from the HYDRUS-2D analyses of measured soil water potentials ranges from 10% to 4% of total flow, slowing down to negligible flows by the end of June.

Stream flow discharge during the low flow periods also emanates from the emergence of fractured bedrock flows re-entering the hillslope profiles as is evident from Electrical Resistivity Tomography surveys.

- ***Fractured rock groundwater*** *(E in Figure 3.3)*

The existence of groundwater in the bedrock underlying the hillslopes and valley is evident through deep borehole observations as well as Electrical Resistivity Tomography surveys. It is clear that some proportion of the this deep aquifer water contributes to the event flows, but, without tracer samples from these deep sources, the proportion cannot be estimated.

It is also evident that, during the dry season, water percolating through the fractured rock contributes to low flow via two mechanisms. First, bedrock groundwater emerges at parent material outcrops on the hillslopes and contributes to hillslope soil water in the downslope profiles (B, G and I in Figure 3.3). Second, water enters the valley soil profiles from the bedrock below (G in Figure 3.3) in response to upslope gradients. During the dry season the seepage water, spilling over the outcrops is estimated to contribute 32% and the subsurface seepage 68% of the winter flows as late as August.

CHAPTER 5
MODEL ALGORITHM DEVELOPMENT

5.1 Historic Application of ACRU in Weatherley

Subsequent to much of the data analysis of the Weatherley research catchment in the northern Eastern Cape Forests, the "topmodel" approach of surface topology related flow accumulation was found to be inappropriate for application at the Weatherley catchment, since allowance was required for distinct flow generation zones, pathways and fluxes. A research version of the *ACRU* model was developed, which included the spatial distribution of water and sediment generation, particularly in terms of the topography of hillslopes (van Zyl and Lorentz, 2004). The approach, used in the van Zyl and Lorentz, 2004, study included:

- Flow generation based on hillslopes contributing areas instead of a grid basis,
- Near-surface discharge due to accumulation of macro-pore generated water above a hydraulic discontinuity in the profile and delivery of this discharge to the riparian zone B horizon, (Figure 5.1),
- Baseflow contributions from the macro-pore zone and grassland profiles to the riparian zone, (Figure 5.1), and
- Time distributed arrival of subsurface water based on hillslope criteria,

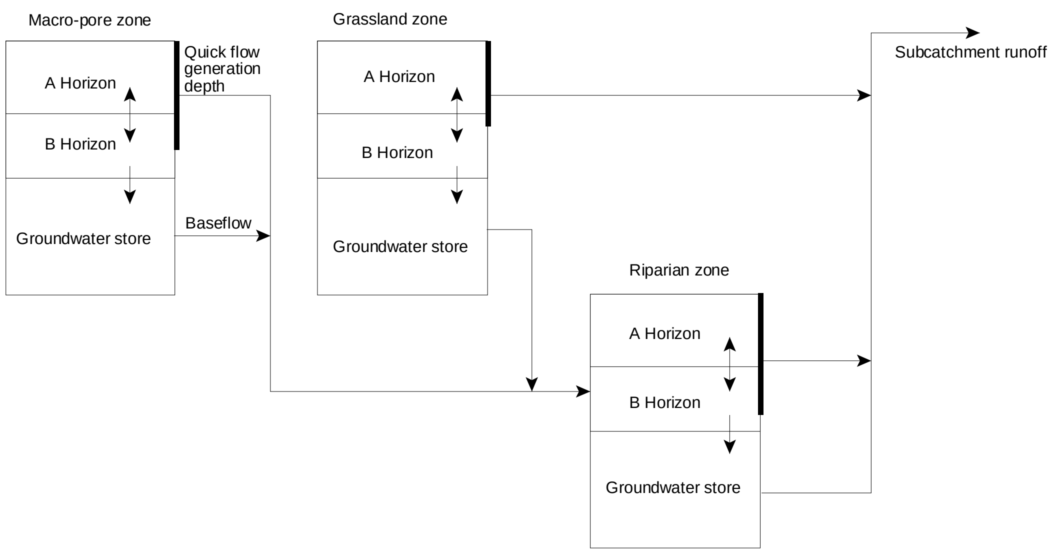

Figure 5.1 Schematic subcatchment streamflow generation zones and pathways simulated in the topological version of *ACRU*. (Van Zyl and Lorentz, 2004).

The different zones, identified by soil water response observations are presented in Figure 5.2 for the Weatherley catchment. The catchment configuration comprised grassland and macro-pore dominated grassland zones discharging into a wetland zone as shown in Figure 5.2. The upper catchment wetland zone discharges into the lower catchment wetland zone. The Zululand catchment was divided into subcatchment response units based on the occurrence of crest, midslope, footslope and riparian units.

Typical results of the soil water contents from the *ACRU* simulations of the Weatherley catchment are shown in Figure 5.3 for monitoring station LC1. The model proves accurate in simulating the soil water response. The runoff response is also accurately simulated at the lower weir as shown in Figure 5.4. However, this accuracy was not achieved without the model modifications and response unit delineation of subcatchments.

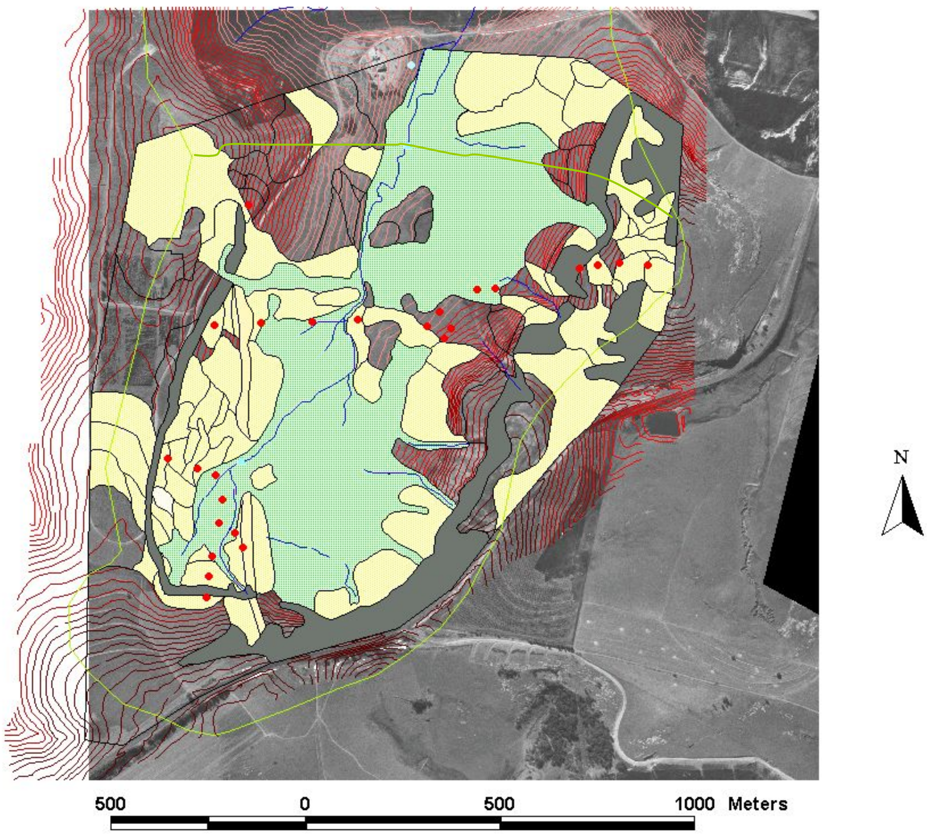

Figure 5.2. Topological ACRU, hydrological response units in the Weatherley subcatchment including rapid near surface lateral response zones (yellow), grassland (orthophoto grey), rock outcrop (grey) and wetland (green) (After van Zyl and Lorentz, 2004).

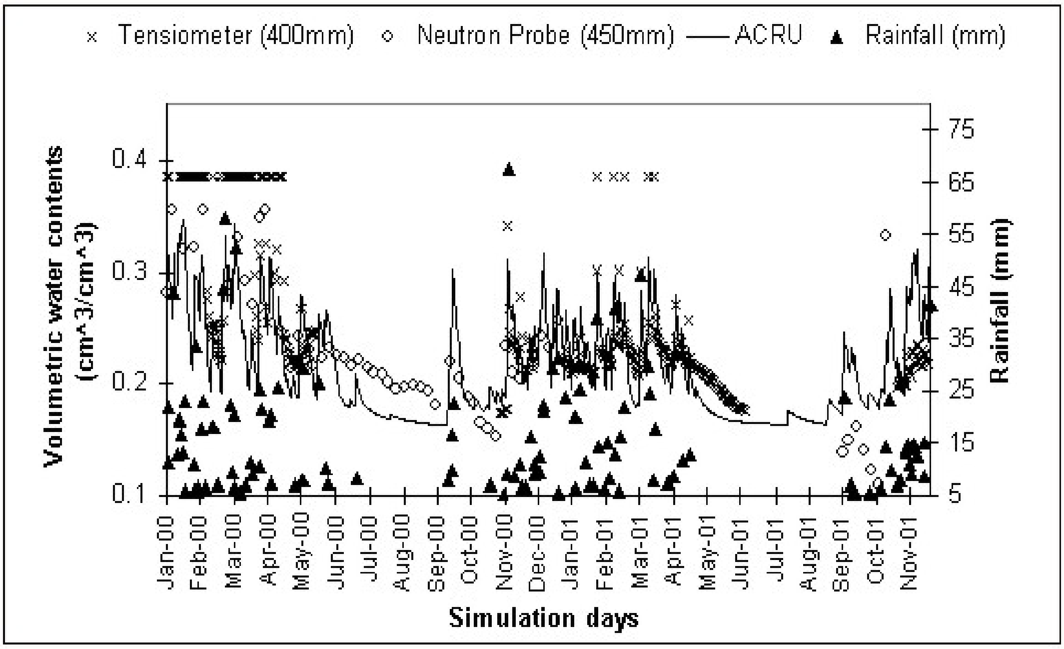

o

Figure 5.3. Results of the *ACRU* simulation at station 1 (400 mm) in the Weatherley catchment.

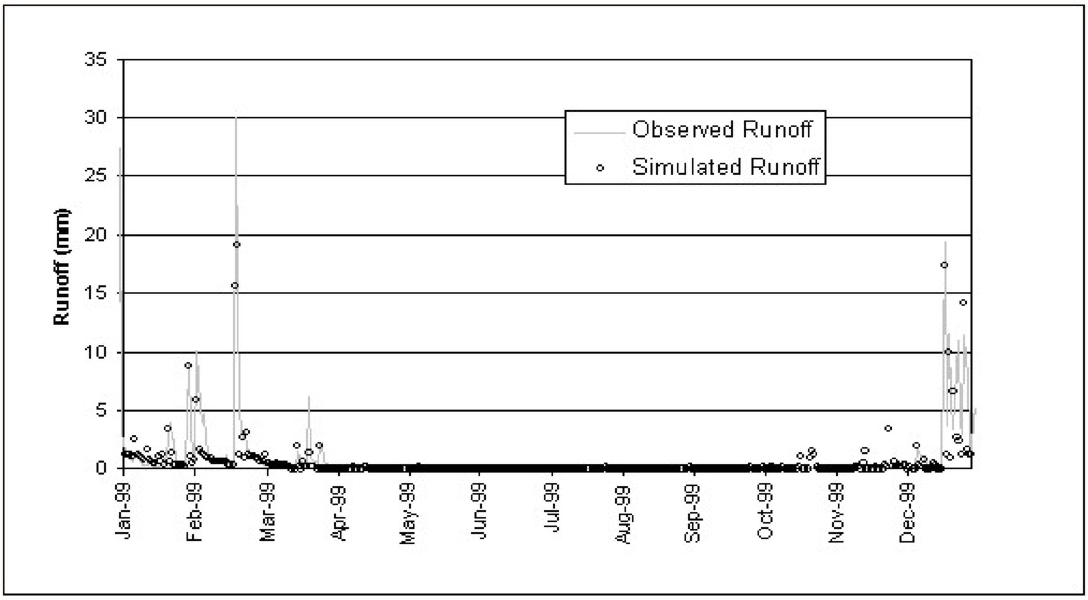

Figure 5.4. Results of the *ACRU* simulation of runoff at the lower weir in the Weatherley catchment.

5.2 Application of a Transfer Function Model (TFM) in Weatherley.

Paramount to the success of catchment scale hydrological simulation is the proper representation of the component sources of water making up the response and the rate at which these sources deliver water from hillslopes to the receiving stream. Inherent in most hydrological models, therefore, is a representation of the mechanisms through which different sources transfer water from hillslopes to the streams. This representation is difficult as there are often no direct measurements available to quantify how these mechanisms should be transferred. In fact there are those who subscribe to the view that "regardless of our understanding of hillslope processes, our ability to make predictions at watershed scale has advanced relatively little" (Sivapalan, 2001). Nevertheless, hydrological models have been developed which attempt to differentiate between sources and flow paths of water.

The *ACRU* model (Schulze, 1995) inherently, has linear transfer functions relating the storage state in a groundwater and slow stormflow reservoirs to the fluxes from these components. These simple functions can be expressed as:

$$Q_{igw} = k_{gw}S_{igw} \quad \text{and}$$
$$Q_{isf} = k_{sf}S_{isf} \quad \text{where}$$

Q_{igw} = flux from the groundwater store on day, i,
k_{gw} = groundwater release constant
S_{igw} = groundwater storage state on day, i and

similarly for the slow flow response with subscript sf. These fluxes are added to the quick flow response to effective rainfall, generated by a modified SCS method. Siebert and McDonnell, 2001, simulate the hydrology of the Maimai catchment in New Zealand with a three reservoir (or box) model, comprising Hillslope, Hollow and Riparian storage boxes. The Hillslope and Riparian boxes have linear release functions, while the Hollow box has an additional threshold-based release function, allowing for macro-pore response which only occurs during specific storage states.

Attempts to disaggregate the runoff hydrograph into component source responses have also been the subject of considerable research. These have taken the form of time dependant unit runoff response functions applied to different components of flow (McDonnell *et al*., 1991; Lorentz and Kienzle, 1994; Lorentz *et al*., 2003). The unit response functions are convoluted with an excitation function to yield the runoff response. This takes the form of the convolution integral:

$$q_{out} = \int_0^\infty g(t').\delta(t-t').dt'$$

where

$\delta(t)$ = the excitation function, (e.g. the time series of excess rainfall, i_e) dependant on time, t,
$g(t)$ = the unit response function and
q_{out} = the runoff response.

The advection-dispersion functions of solute transport are used by Weiler *et al.,* 1998, to develop unit response functions for various sources of discharge. These response functions represent the travel time distribution of the discharges from each source and a typical solution to the advection-dispersion process would be the exponential function given by:

$$g(t) = \left(\frac{4\pi Dt}{\tau}\right)^{-1/2} t^{-1} e^{\left(-1(1-t/\tau)^2\tau/(4Dt)\right)}$$

where

D = the dispersion coefficient, describing the spread of travel times and
τ = response time.

Moussa, 1997, applies a diffusive wave equation to route the combined responses through a catchment reach. A unit pulse response function is used by Yue and Hashino, 2000, to represent quick and slow flow components of runoff response. Exponential and piston flow type functions are used by Asano *et al*., 2002, to represent the time distribution of water from component sources while Denic-Jukic and Jukic, 2003, apply various relationships to develop unit hydrograph responses to quick and slow flow components which are combined to yield the composite runoff response. Attempts to identify parameters from catchment data have been made to develop transfer functions by Iorgulescu and Beven, 2003. Attempts to combine runoff and tracer data in developing runoff response units have been particularly successful. Weiler *et al.,* 2004 have developed the TRANSEP model by using discharge and chemical species concentration and constraining the unit hydrograph runoff response with tracer transport response functions.

The transfer function methods have been applied to components of flow in the Weatherley research catchment (Lorentz *et al.,* 2003) and found to represent the response of the catchment adequately for various events.

5.3 Proposed Model Algorithm

Besides the spatial distribution of antecedent water by topmodel algorithms, an attempt has been made to include the effects of threshold induced, event based, lateral discharge and groundwater recharge of subsurface water, (Howe and Lorentz, 1995; Howe 1999). Pertinent to that study was the inclusion of a soil layer below the B-horizon, which was bounded at the base by impermeable bedrock, semi permeable saprolite or clay layer as shown in Figure 5.5. This boundary could just as easily be the base of a preferential flow or macropore continuity. The processes are simplified in this layer in that the volume of water contained in it, is assumed to be distributed in an equilibrated water retention relationship from the base to the upper boundary of the layer (Figure 5.5). Additional volumes of water into this layer move the moisture status at the bottom boundary closer to saturation. Once saturation is obtained, additional water into this layer will ultimately result in a positive pore water pressure head condition at the interface. It is at this stage that lateral water is allowed to discharge at the rate of a specified horizontal hydraulic conductivity. This is obviously a simplification of the observations made in hydrological process studies, but it will be pursued in the development of simple algorithms for larger scale catchment modelling.

The major features included in that work were:

- The spatial distribution of land use and sediment source areas,
- Topmodel update of antecendent moisture at each location,
- Infiltration/runoff by Green-Ampt infiltration,
- Macro-pore feature for rapid arrival of water at the soil-bedrock interface and
- Accumulation of perched water table on the soil-bedrock interface prior to percolation into the bedrock aquifer store (Figure 5.5).

It is this threshold response, both in the near surface horizon and in an intermediate layer between the B horizon and bedrock or saprolite that is suggested for an improved dynamic of soil water, based on the responses observed in this study. A series of interlinked land segments made up of these profile components is proposed for simulating the dynamics of water transfer in a hillslope catena (Figure 5.6).

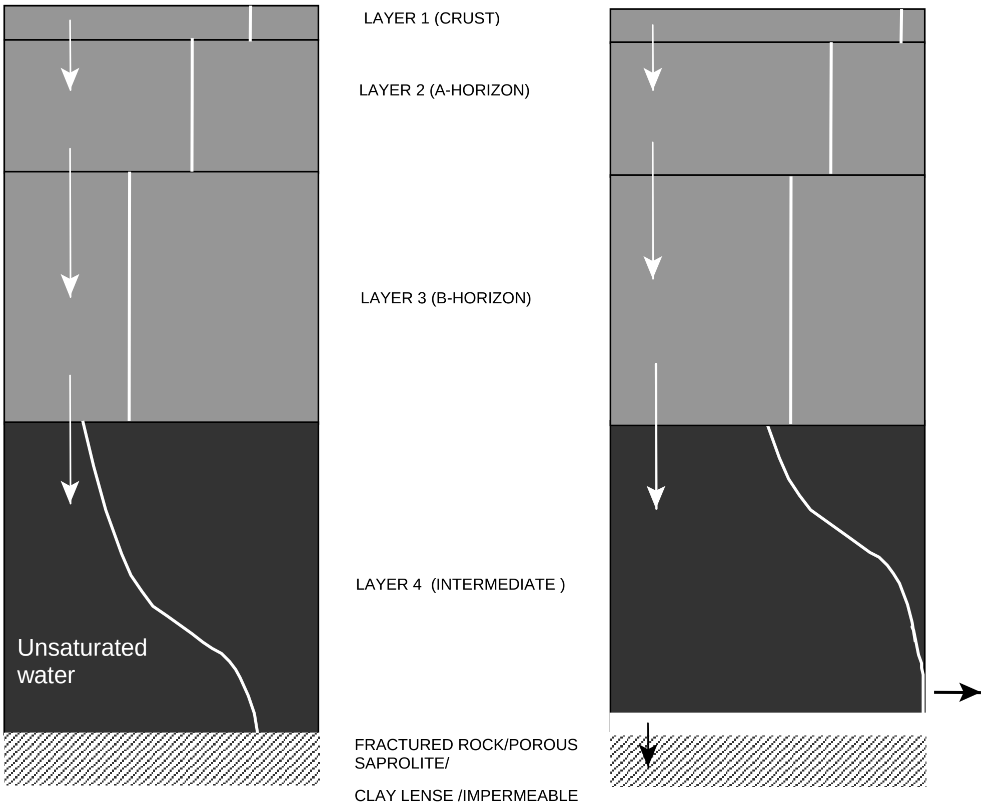

Figure 5.5 Schematic of soil/bedrock layered system showing increasing volume accumulation in the intermediate layer.

Each land segment includes a surface layer, soil A and B horizon, an intermediate layer and a groundwater store. Near surface water can be partitioned into rapid surface and subsurface response (via the near surface soil horizon) an infiltration component and a component which discharges the intermediate layer through preferential flow. The intermediate layer and groundwater store can be linked laterally to downslope land segments in a user specified network according to dominant soil and geologic controls. Lateral and vertical discharge from the intermediate layer is triggered when the water retention volume in the layer exceeds the equilibrium water retention and positive pressures are developed at the soil/bedrock interface. Responses from the intermediate layer and groundwater layer are controlled by a unit response function (either an exponential function, an advection-dispersion function (ADF) or dual source ADF) In the Weatherley example only two land segments are used, 1) a hillslope segment and 2) a wetland segment. The hillslope land segment discharges intermediate zone and deep groundwater into the A horizon of the common wetland land segment which discharges to the stream. Vertical and lateral preferential flow (shallow groundwater) is partitioned from the SCS generated event volume by exponential response functions.

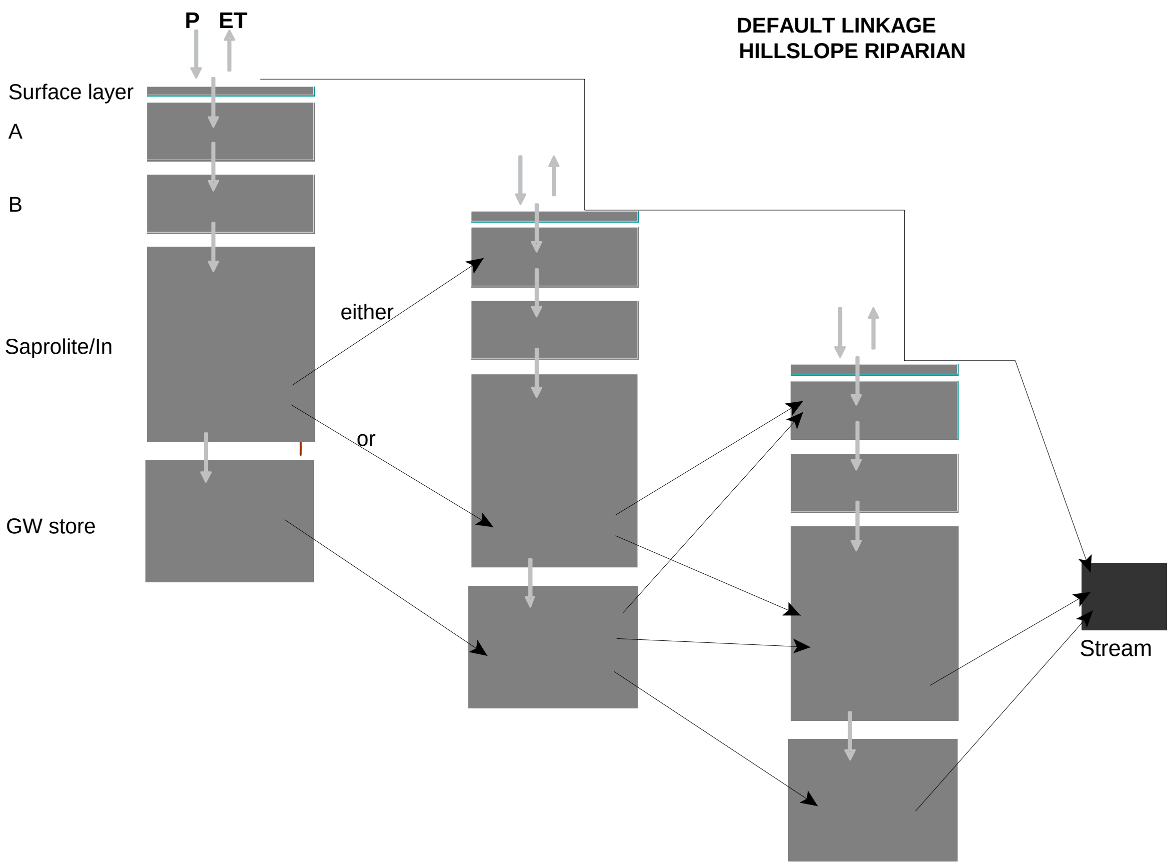

Figure 5.6 Schematic of the land segment linkage structure in the model.

CHAPTER 6
CONCLUSIONS AND RECOMMENDATIONS

A fruitful study of the source areas, flow pathways and residence time of water in the Weatherley catchment has been concluded. Such understanding is critical to properly characterise runoff dynamics, water resource perturbations due to land use changes, water quality responses and low flow determinations. The application and combination of a number of different tools and observation techniques, applied to the same area, has led to a better and more comprehensive understanding of the hydrological processes which underpin the water resource impacts. Hydrodynamics observations, geophysics surveys and tracer methods have been combined to yield a consistent understanding of the catchment water yield mechanisms, despite the limitation of each method used independently.

Significant findings include:

- Hillslope generation of water to stream flow during wet season events comprises some 60-70% of the total discharge and emanates primarily from subsurface water accumulated on the soil/bedrock interface. This has been demonstrated by 2D modelling of hillslope soil water dynamics as well as wet season isotope (δO^{18} and δH^2) and tracer (EC and Si) sampling.

- Rapid response, near surface lateral hillslope discharge has been shown to contribute between 1% and 26% of the total event discharge during wet season tracer sampling (EC and Si).

- Hydrodynamic observations, hillslope 2D modelling and isotope sampling have demonstrated that the contribution of the soil profile to low flows ranges between 10 and 4% and extends into July.

- However, Electrical Resistivity Tomography (ERT) and late winter isotope sampling demonstrate that significant contributions to low flow originate from the fractured sandstone in the hillslope and emerge overland at bedrock outcrops or emerge upwards into downslope soil profiles due to groundwater hydraulic gradients (ERT observations).

- These low flow contributions prevail for extended periods of time and travel time through this pathway could exceed several years.

- A model algorithm, comprising threshold based subsurface responses and catena based linking has been proposed as a direct emulation of observed dynamics.

The following recommendations are offered to continued research:

- The combination of ERT and hydrodynamic observations and tracer sampling provide a valuable set of techniques to properly quantify the dynamics of catchment responses. These should be used, together in a continuous mode, rather than in the trial campaigns of this study. Better time based resolution of these observations, together with evapotranspiration observations will serve to capture the full range of wet and dry season stream flow generation dynamics.

- The useful combination of these observation techniques should be used to supplement observations in other areas to being a set of typical response characteristics of different geologies, soil catenas, climates and vegetation. This will allow useful model development to capture the essential dynamics of various hydrological zones.

- Hydrological models performance would be enhanced by including the behaviour of the dominant components of discharge through the hillslopes. While these general hillslope responses are inherently included in many models, including the *ACRU* model, the specific behaviour of the components of flow in specific hillslopes is not.

- Hydrological model performance would be enhanced by including functions which represent the travel times of the different components of flow.

- The contribution of deep aquifer (particularly from those contributing from outside the surface water divide) should be quantified by appropriate isotope sampling or tracer methods.

7 REFERENCES

Achet, S. H., J. P. McNamara and D. Chandler. 2006. Insights Into the Unsaturated Subsurface Flow Mechanism in Streamflow Generation In Semiarid Environment: Applying HYDRUS2D Combined With Field Experiments in Dry Creek, Boise, ID. Water Resources Research. In Press. (http://earth.boisestate.edu/home/sachet/publications.doc)

Aggarwal P.K., Gibson, J.J. and Azuzena, O. 2002. Report of a Research Coordination Meeting on Design Criteria for a Network to Monitor Isotope Composition of Runoff in Large Rivers (2002-2006). IAEA, Headquarters, Vienna, Austria.

Asano, Y., Uchida, T. and Ohte, N. 2002. Residence times and flow paths of water in steep unchannelled catchments, Tanakami, Japan. J. Hydrol. 261:173-192.

Denić-Jukić, V. and Jukić D. 2003. Composite transfer functions for karst aquifers. J. Hydrol. 274:80-94.

DIN (1981) Deutsche Einheitsverfahren zur Wasser-, Abwasser- und Schlamm-Untersuchung Wiley-VCH: Weinheim.

Esprey, L.J. 1997. Hillslope experiments in the North Eastern Cape to measure and model subsurface flow processes. Unpublished MSc dissertation, Department of Agric. Eng. University of Natal.

Hoeg, S. Uhlenbrook, S. and Leibundgut, Ch. 2000. Hydrograph separation in a mountainous catchment combining hydrochemical and isotopic tracers. Hydrol. Process. 14:1199-1216.

Howe B.J. and Lorentz S.A., 1995. Modelling sediment yield in the Mzinduzi basin using contributing area techniques. Proc. 7th South African National Hydrology Symposium. IWR Grahamstown.

Howe, B.J. 1999. Development of New Techniques for Variable Source Area Sediment Yield Modelling. Unpublished MSc Dissertation, University of Natal, Pietermaritzburg.

Iorgulescu, I. and Beven, K.J. 2003. Data-based modelling of runoff and chemical tracer concentrations in the Haute-Mentue (Switzerland) research basin, EGS-AGU-EUG Joint Assembly, Nice, France.

Laudon, H. & Slaymaker, O. (1997) Hydrograph separation using isotopes, silica and electrical conductivity: an alpine example. J. Hydrol., 201, 82-101.

Lorentz S.A. and Kienzle S.W. 1994. The merits and limitations of GIS linked transfer function modelling of basin scale sediment yield. GIS Workshop Presentation: 50 Years of Water Engineering in South Africa, 14-15 July 1994. Water Engineering Division, South African Institution of Civil Engineers, University of the Witwatersrand.

Lorentz, S.A. and Esprey, L.J., 1998. Baseline hillslope study prior to afforestation in the Umzimvubu headwaters of the North East Cape Province, South Africa. In: Kovar, K., Tappeiner, U., Peters, N.E. and Craig, R.C. (eds.) Hydrology, Water Resources and Ecology in Headwaters (Proceedings of the Headwater '98 Conference held at Meran/Merano, Italy, April

1998) IAHS Publ. No. 248:267-273.

Lorentz, S. 2001. Hydrological Systems Modelling Research Programme: Hydrological Processes. Phase I: Processes Definition and Database. Report to the Water Research Commission on the project: A *Hydrological Systems Modelling Research Programme: Processes Research.* WRC Report 637/1/01, Water Research Commission, Pretoria, South Africa.

Lorentz, S., Thornton-Dibb, S., Pretorius, C. and Goba, P. 2003. Hydrological Systems Modelling
Research Programme: Hydrological Processes: Phase II Quantification of Hillslope, Riparian and Wetland Processes. Report to the Water Research Commission on the project: '*A Field Study of Two and Three Dimensional Processes in Hillslope Hydrology for Better Management of Wetlands and Riparian Zones*' and '*Experimental and Laboratory Measurements of Soil Hydraulic Properties*'. WRC Report No.: K5/1061 and K5/1086. November 2003.

McDonnell J., Stewart M. and Owens I. 1991. Effect of catchment scale subsurface mixing on stream isotopic response. *Water Resources Research*, 27(12):3065-3073.

McGuire, K., McDonnell, J.J., Weiler, M., Kendall, C., McGlynn, B.L., Welker, J.M. and Siebert, J. 2005. The role of topography on catchment residence time. Water Resour. Res. (*in press*).

Moussa, R. 1997. Geomorphological transfer function calculated from Digital Elevation Models or distributed hydrological modelling. Hydrological Processes, 11: 429 - 449.

Roberts, V., Hensley, M., Smith-Baillie, A. and Paterson, D. 1996. Detailed soil survey of the Weatherly catchment. Institute for Soil, Climate and Water. Report GW/A/93/36. S.A.

Rodgers, P., Soulsby, C., Waldron, S. and Tetzlaff, D. 2005. Using stable isotope tracers to identify hydrological flow paths, residence time and landscape controls in a mesoscale catchment. Hydrol. Earth Syst. Sci. Discuss. 2:1-35

Schulze, R.E. 1995. Hydrology and Agrohydrology: A text to accompany the ACRU 3.00 Agrohydrological Modelling System. Water Research Commission, Pretoria TT 69/95. pp AT23-1 to AT23-15.

Siebert, J. and McDonnell, J. 2001. Towards a better process representation of catchment hydrology in conceptual runoff modelling. *In*: Leibundgut, C., Uhlenbrook, S. and McDonnell, J. 2001. *Runoff generation and implications for river basin modeling*. Proceedings of the International Workshop on Runoff Generation and Implications for River Basin Modelling, October 2000. Freiburg, Germany. Freiburger Schriften zur Hydrologie: Band 13.

Siebert, J., Rodhe, A. and Bishop, K. 2003. Simulating interactions between saturated and unsaturated storage in a conceptual runoff model. Hydrol. Process. 17:379-390.

Simünek, J., Vogel, T. and Van Genuchten, M. Th. 1994. The SWMS-2D code for simulating water flow and solute transport in two-dimensional variably saturated flow. U.S. Soil Salinity Laboratory, USDA, Research Report No. 132: pp 196-197.

Sivapalan, M. 2001. Process complexity at hillslope scale, process simplicity at the watershed scale: Is there a connection? AGU Chapman Conference on State-of-the-Art in Hillslope

Hydrology. Sunriver, OR, Oct 8-12, 2001. Abstracts. p41.

Sivapalan, M. 2003. Prediction in ungauged basins: a grand challenge for theoretical hydrology. Hydrol. Process., 17:3163-3170.

Sklash, M.G. and Farvolden, R.N. 1979. The role of groundwater in storm runoff. J. Hydrol. 43:45-65.

Uhlenbrook, S. Frey, M. Leibundgut, C. And Maloszewski, P. 2002. Hydrolgraph separations in a mesoscale mountainous basin at event and seasonal timescales. Wat. Resour. Res., 38(6):1-14.

Uhlenbrook, S. and Hoeg, S. 2003. quantifying uncertainties in tracer-based hydrograph separations: a case study for two, three and five-component hydrograph separations in a mountainous catchment. Hydrol. Process. 17:431-453.

Van Huyssteen C.W., Le Roux, P.A.L., Hensley, M. and Lorentz, S. 2007. Relationship between soil water regime and soil profile morphology: A proposal for continued research. Water Research Commission: Report Number: KV 179/07, WRC, Pretoria.

Van Wyk, E. 2006. Geophysical logging at Weatherley, Maclear. DWAF Hydrological Services. Feb 2006.

Van Zyl, A.J. and Lorentz, S.A. 2004. Impact of Farming Systems on Sediment Yields in the Context of Integrated Catchment Management. Water Research Commission Report No: K5/1059. Pretoria.

Weiler, M., Naef, F. and Leibundgut, C. 1998. Study of runoff generation on hillslopes using tracer experiments and a physically based numerical hillslope model, IAHS, pp. 353 - 360.

Weiler, M., McGlynn, B.L., McGuire, K.J. and McDonnell, J.J. 2004. How does rainfall become runoff? A combined tracer and runoff transfer function approach. Water Resources Research 39(11):SWC4.1-4.13.

Wenninger, J., Uhlenbrook, S. and Lorentz, S. 2007. Identification of runoff generation processes using combined hydrometric, tracer and geophysical methods in a headwater catchment in South Africa. J of Hydrology. (In review).

Yan, J. and Smith, K. R. 1994. Simulation of integrated water and groundwater systems – model formulation. Water Resources Bulletin. Vol. 30, No 5. 879-890.

Yue, S. and Hashino, M. 2000. Unit hydrographs to model quick and slow runoff components of streamflow. Journal of Hydrology, 227: 195 – 206.

8 BIBLIOGRAPHY

Bouwer, H. and Maddock I, T. 1997. Making sense of the interactions between groundwater and streamflow: Lessons for water masters and adjudicators. Rivers, Vol. 6 No.1, 19-31.

Dooge, J.C.I. 2004. Bringing it all together. Hydrol. Earth Sys. Sci. Discuss. 1:41-73.

Hughes, D.A. 2004. Incorporating groundwater recharge and discharge functions into an already existing monthly rainfall-runoff model. Hydrol. Sci. Journal. 49(2):297-311.

Jakeman, A.J. and Hornberger, G.M. 1993. How much complexity is warranted in a rainfall-runoff model? Water Resour. Res. 29(8):2637-2649.

McDonnell, J.J., Bonell, M., Stewart, M.K. and Pierce, A.J. 1990. Deuterium variations in storm rainfall: Implications for stream hydrograph separation, Water Resour. Res. 26(3):455-458.

McDonnell, J.J. 2003. Where does water go when it rains? Moving beyond the variable source area concept of rainfall-runoff response. Hydrol. Process. 17:1869-1875.

McGlynn, B.L. and McDonnell, J.J. 2003. quantifying the relative contributions of riparian and hillslope zones to catchment runoff. Water Resour. Res. 39(11):1310SWC2.1-20.

Parsons, R. 2004. Surface Water: Groundwater Interaction in a South African Context – A Geohydrological Perspective. WRC Report TT 218/03, Water Research Commission, Pretoria, South Africa, pp 1.1-11.1.

Saayman, I.C., Scott, D.F., Prinsloo, F.W., Moses, G., Weaver, J.M.C. and Talma, S. 2003. Evaluation of the application of natural isotopes in the identification of the dominant streamflow generation mechanisms in TMG catchments. WRC Report 1234/1/03. Water Research Commission, Pretoria, South Africa pp 52.

Stewart, M. and McDonnell, J. 1991. Modeling base flow soil water residence times from deuterium concentrations. *Water Resour. Res.* 27(10):2681-2693.

Uchida, T., Tromp-van Meerveld, H.J. and McDonnell, J.J. 2003. Simplicity from complexity: How lateral soil pipes define clear threshold relations at the hillslope scale. AGU Fall Meeting, 2003. Abstract H42G-1156.

Von der Heyden, C.J. and New, M.G. 2003. The role of a dambo in the hydrology of a catchment and the river network downstream. Hydrol. Earth Syst. Sci., 7(3):339-357.

Wagener, T. 2003. Evaluation of catchment models. Hydrol. Process. 17:3375-3378.

APPENDIX A

Geophysical Logging and Borehole Information at Weatherley

Hydrological Services

E van Wyk
wca@dwaf.gov.za
Cell: 082-801-1740

REPORT TYPE: REVIEW REPORT (1)

PROJECT: Geophysical Logging at Weatherley – Mc Clear
REFERENCE: C. Moseki

Background:

This sub-directorate was commissioned to support an integrated monitoring programme in the Mc Clear area on a piece of land designated for forestry (Proposed new Mondi forest/plantation). A surface water monitoring network consisting of flow gauging structures and surface water sampling devices has been installed. Following this development, the groundwater component of the flow regime had to be incorporated into the total monitoring programme and subsequently a few bores were drilled in the catchment to capture the groundwater flow regime.

The site area is fairly well covered with fine grass land and very few outcrops have been observed on site; apart form the typical sandstone cliffs all around the sides of the drainage valley. The geology of the region is typical flat lying Molteno formation, consisting of reddish/green mudstone-siltstone with intercalated silty to course sandstone. This has been confirmed through borehole video logging.

What has been observed in the area is the presence of seeps below the sandstone lenses where the contact with the low permeable mudstone-siltstones.

Investigation method:

A group of 4 bores out of 6 were logged with the geophysical and video logging equipment during the week of 19 to 20 October 2005. The videos were recorded on VHS cassettes for future reference. The following geo-electrical and radiometric logging was performed:

- Natural Gamma and Neutron-neutron
- BRD & LSD Density
- Resistivity & SP
- Calliper; and
- Full Wave Sonic.

Results:

According to information six (6) exploratory boreholes were drilled during 2004 on the site area; depths varies from 85m to 120m. These boreholes cover a vertical depth of ±1351mamsl down to ±1174mamsl (177m of Karoo Sequence); thus an extreme thin portion of the local formation to deduce regional hydrogeological characteristics.

Video Logging: The geological package consists of extremely homogenic mudstones with sandstone horizon of various thicknesses. The sandstone horizons vary from thick homogenic sandstones to interlayer sandstone and probably a silty sandstone. What has been observed was the presence of a mud-pellet conglomerate developed at the base of these sandstone horizons; associated with a much courser basal sandstone.

The mudstone is typical massive and homogeneous in texture, with reddish to greyish green colouring.

Secondary structures (joints and fractures) are minute in size and intermittently transect the width of the borehole diameter. The effective porosity of the rock mass should therefore be low.

The main water strikes are probably in the upper weathered portion of the formation; no evidence of major brittle zone/fractures has been spotted. Unfortunately, the clarity of the borehole water deteriorates with depth to such a degree that video visibility completely closes down.

Radiometric (Natural Gamma and Neutron-Neutron[N≈N]) Logging: Confirms the presence of course sandstone and shales in a mudstone rock mass with thicknesses varying between 2 and 12m and <1 and 4m respectively. Bore EC/T35/070 penetrates a prominent sandstone horizon from 1333mamsl to 1321mamsl. This horizon could not be traced to surrounding bores (EC/T35/069 for example); thus indicating either lateral facies changes over short distances and/or the pattern in which these sandstone beds have been deposited (meandering fluvial systems).

BRD & LSD Density: Variation in BRD and LSD density logs do not show substantial changes. Apparent values vary between 2.5 and 2.75 g/cc, with values in the order of 2.25 g/cc above the saturated zone. (This data needs further interpretation!!!-2006).

Resistivity (Res#2) & SP: Not any particular anomalies; indicating a fairly homogenic rock mass in terms of resistive/conductive layering. Borehole EC/T35/072 and EC/T35/076 however gives an interesting correlation between Gamma-N≈N-Res#2 in terms of lithological composition. In EC/T35/072 (collar elevation=1318masl) from around 52m (1266mamsl) to 78m (1240mamsl) , the formation's resistance and effective porosity (higher N≈N cps) gradually increases, which might indicate downward coarsening into a sandstone (or upward fining from sandstone to mudstone), whilst a gradual decrease in the Natural Gamma indicates a downward decrease in a clayey/silty matrix. A very prominent "drop-off" occurs at about 78m to a typical mudstone material. This gradual change in silt/sand content is typical of fluvial/deltaic type sedimentation (? – under what geological environment was the Elliot/Molteno Frm's deposited – look in Trustwell!). The main water strike in this bore was recorded at 80m, but due to smudging (development of a mud cake due to low water inflow) at the drill bit, one can expect a couple if meters penetration beyond the water strike before some observations could be made at surface. In bore EC/T35/076 (collar elevation=1298mamsl), a similar pattern occurs between 32m (1266mamsl) down to 46m (1252mamsl) with the “drop-off” at 46m (second water strike at 46m with a blow yield of 0.36l/s).

It is therefore possible that this prominent contact (normally referred to as a *bedding plane contact*) between a sandstone and mudstone represents a regional aquifer system – although a bloody poor yielding one!!).

Calliper: Correlates with video logging and shows very little variation in bore diameter. Responses are typical of a massive sedimentary package with intercalated sandstone/shale horizons. The absence of so-called large “blow-outs” at the water strikes could probably relate to the possibility of “remaining” primary porosity in the sandstones (require more interpretation of the Full Wave Sonic, N≈N and BHTV logging. BHTV probe was not available due to repairs.

Full Wave Sonic: This logging parameter gives an indication of the rock mass porosity, but requires additional information which could not be logged during the October 2005 round. Unfortunately the BHTV probe was not available for the Weatherly logging and only empirical interpretations can at this stage be made.

In general, the rock mass on site consist of variable porosity characteristics, deriving from the degree of super fines (clay) and/or sand in the different depositories. The upper weathered zone in the area varies considerable (<12m to 36m). “Soft Rock” zones, indicated empirically by a poor sonic signal return, coincide with similar outstanding mudstone type horizons – for example the prominent “drop-off” at 77m in bore EC/T35/072 and at 46m in bore EC/T35/076. The FWS logging also indicates a fairly solid “basement” at roughly 1190mamsl – (dolerite sill or sandstone).

To conclude, the FWS parameter reports an overall mudstone rock with thin layers of shale and some thicker layers of sandstone. On the study area the vertical depth of weathering is in the order of 12mclose to the streambed is the thickest – some 24 to 36m below surface (reported in bores EC/T35/075&076.

Conclusions

Boreholes were probably not cleaned as required by the standard drilling specifications as the logging depths are shallower than those reported during the drilling operations.

The geological formations consist of thick mudstone with intercalated shales and sandstone layers. The sandstones may vary from fine silty (thickest beds) to course grained pure sandstone (especially those forming the lower parts of the sandstone horizons).

The groundwater occurrence in the site area is related to weathering in the upper zones (20 to 36m) and along sandstone/massive mudstone *bedding plane contacts*. Geophysical logging does not report massive sandstone layers, although it can be postulated that some of the sandstone layers may have primary porosity; thus draining groundwater from the surrounding rock mass. The permeability however is low and does not drive large regional flow systems.

Horizontal features (bedding plane contacts and a few joints) are acting as the major groundwater conduits. Vertical fracturing is not prominent.

Recharge is probably generated along the drainage systems and where drainages run over sandstone ridges (but probably only in local context). Major recharge mechanism(s) is not clear yet.

The hydraulic parameters of the rock package are probably in the lower orders. It is postulated that vertical (gravity) driven flows are minimal as some springs occurs along the major drainages (groundwater flow mainly in lateral direction in/on top of bedding plane contacts (sandstone-mudstone contacts)

Recommendations

This current borehole logging survey requires support from the BHTV and water quality parameters. As mentioned above, these two probes were not available due to repairs. Vertical differences in the groundwater quality may exist and will also help to understand the deeper flow regime, especially the deeper sandstone/mudstone bedding plane contacts (like those observed in bores EC/T35/072 and -/076.

Video logging should be repeated as the visibility of the lower sections of the boreholes is poor. The reason for this is currently unknown as the boreholes were drilled several months before the geophysical logging was done. Purging of the boreholes will also help to "clean out|" any drilling additives which might cause obscure groundwater quality results.

The groundwater flow regime is still unknown and requires a much shorter monitoring interval. The use of continuous time serie logging devices is strongly recommended. Support from a time serie and bulk rainfall logging device (at least two) is also recommended.

The Weatherley 220 Station monitoring network should be supported by DWAF as much as possible as this is the first integrated groundwater-surface water monitoring network of its kind (mountainous area). It is therefore recommended that a multi-disciplinary monitoring committee is formed to plan and implement future monitoring programmes on the study area.

Manager: Groundwater Resources Assessment & Monitoring

8-February-2006

BOREHOLES INFORMATION REPORT

DIRECTORATE: GEOHYDROLOGY

DEPARTMENT OF WATER AFFAIRS AND FORESTRY

REPUBLIC OF SOUTH AFRICA

***DATE*:** August 2004

Province : **Eastern Cape**	District Municipality: **Ukhahlamba**
Local Municipality : **Elundini**	Magisterial District **: Maclear**

Water Management Area (WMA): **12**		
Secondary Drainage Region: **T35D**		
Borehole No: EC/T35/069		
Coordinates	**Lat.: 31.10723333**	**Long.: 28.3336**
Altitude (m): ≈ **1250hasl**		
1 : 50 000 Map Number : **3128AB**		
Farm Name & Number: **Weatherly 220 Station**		

Rock Group:
Subgroup:
Formation: **Elliot / Molteno**

Lithological Description

0 –2m Reddish to Yellowish topsoil
2– 8m Yellowish white fine-grained weathered quartzitic sandstone
8–24m Greyish medium grained sandstone
24 –28m Light grayish coarse grained sandstone
28 – 35m Purple Shale
35 - 85m Dark Greyish hard sandstone

Siting criteria	***Geological*** √	*Geophysical*
Target Feature	**Sandstones**	
Site Selected By	**Geohydrologist**	
Date	**August 2004**	

Drilled by **:** **DWAF, Operation and Maintenance, Drilling Services**	
Date **:** **August 2004**	
Borehole Depth **: 85m**	
Water strike (m) **: 10 & 21**	
Blow yield (L/s) **: Seepage**	Tested Yields (l/s **) 0.2**
Water level, static (m) **16.570**	Date Measured **01/12/2004**

		Plain	Perforated
Casing, :	Length (m)	**6**	
	Diameter (mm)	**255**	
Water quality: **(samples still at laboratory**)	*Good*	*Fair*	*Poor*

BOREHOLES INFORMATION REPORT

DIRECTORATE: GEOHYDROLOGY

DEPARTMENT OF WATER AFFAIRS AND FORESTRY
REPUBLIC OF SOUTH AFRICA

***DATE*: August 2004**

Province : **Eastern Cape**	District Municipality: **Ukhahlamba**
Local Municipality : **Elundini**	Magisterial District **: Maclear**

Water Management Area (WMA): **12**		
Secondary Drainage Region: **T35D**		
Borehole No: EC/T35/075		
Coordinates	**Lat.: 31.054930**	**Long.: 28.19863**
Altitude (m): ≈ **1340hasl**		
1 : 50 000 Map Number : **3128AB**		
Farm Name & Number: **Weatherly 220 Station**		

Rock Group:
Subgroup:
Formation: **Elliot / Molteno**

Lithological Description

0 –1m Yellowish white topsoil
1– 20m Yellowish white fine-grained weathered quartzitic sandstone
20 –54m Greyish medium grained sandstone
54 – 90m Dark Greyish sandstone

Siting criteria	***Geological*** √	*Geophysical*
Target Feature	**Sandstones**	
Site Selected By	**Geohydrologist**	
Date	**August 2004**	

Drilled by **:**	**DWAF, Operation and Maintenance, Drilling Services**	
Date :	**August 2004**	
Borehole Depth : **96m**		
Water strike (m) : **18 & 25**		
Blow yield (L/s) : **0.18**		
Water level, static (m) **4.67**		Date Measured **03/12/2004**

		Plain	Perforated
Casing, :	Length (m)	**6**	
	Diameter (mm)	**255**	
Water quality: : **(still at laboratory**)	*Good*	*Fair*	*Poor*

BOREHOLES INFORMATION REPORT

DIRECTORATE: GEOHYDROLOGY

DEPARTMENT OF WATER AFFAIRS AND FORESTRY

REPUBLIC OF SOUTH AFRICA

***DATE*: August 2004**

Province : **Eastern Cape**	District Municipality: **Ukhahlamba**
Local Municipality : **Elundini**	Magisterial District **: Maclear**

Water Management Area (WMA): **12**		
Secondary Drainage Region: **T35D**		
Borehole No: EC/T35/072		
Coordinates	**Lat.: 31.054930**	**Long.: 28.19863**
Altitude (m): ≈ **1250**		
1 : 50 000 Map Number : **3128AB**		
Farm Name & Number: **Weatherly 220 Station**		

Rock Group:
Subgroup:
Formation: **Elliot / Molteno**

Lithological Description

0 –1m	Yellowish white topsoil
1– 20m	Yellowish white fine-grained weathered quartzitic sandstone
20– 54m	Greyish medium grained sandstone
54 – 120m	Dark Greyish hard sandstone

Siting criteria	***Geological*** √	*Geophysical*
Target Feature	**Sandstones**	
Site Selected By	**Geohydrologist**	
Date	**August 2004**	

Drilled by **:** **DWAF, Operation and Maintenance, Drilling Services**	
Date : **August 2004**	
Borehole Depth : **120m**	
Water strike (m) : **80**	
Blow yield (L/s) **: Seepage**	Tested Yield (L/s **) : 0.3**
Water level, static (m) **18.343**	Date Measured **02/12/2004**

		Plain	Perforated
Casing, :	Length (m)	**6**	
	Diameter (mm)	**255**	
Water quality: **(samples still at laboratory)**	*Good*	*Fair*	*Poor*

BOREHOLES INFORMATION REPORT

DIRECTORATE: GEOHYDROLOGY

DEPARTMENT OF WATER AFFAIRS AND FORESTRY

REPUBLIC OF SOUTH AFRICA

***DATE*: August 2004**

Province : **Eastern Cape**	District Municipality: **Ukhahlambha**
Local Municipality : **Elundini**	Magisterial District **: Maclear**

Water Management Area (WMA): **12**		
Secondary Drainage Region: **T35D**		
Borehole No: EC/T35/076		
Coordinates	**Lat.: 31.054930**	**Long.: 28.19863**
Altitude (m): ≈ **1250hasl**		
1 : 50 000 Map Number : **3128AB**		
Farm Name & Number: **Weatherly 220 Station**		

Rock Group:
Subgroup:
Formation: **Elliot / Molteno**

Lithological Description

0 –1m	Yellowish white topsoil
1– 20m	Yellowish white fine-grained weathered quartzitic sandstone
20–28m	Greyish medium grained sandstone
28- 60m	Light Greyish to Whitish coarse grained sandstone
60 -96m	Purple shale
96-114m	Dark Greyish hard sandstone

Siting criteria	***Geological*** √	*Geophysical*
Target Feature	**Sandstones**	
Site Selected By	**Geohydrologist**	
Date	**August 2004**	

Drilled by **:**	**DWAF, Operation and Maintenance, Drilling Services**
Date :	**August 2004**
Borehole Depth : **114m**	
Water strike (m) : **33 & 47**	
Blow yield (L/s) : **0.2**	Tested Yield (L/s **): 0.36**
Water level, static (m) **5,010**	Date Measured **07/12/2004**

		Plain	Perforated
Casing, :	Length (m)	**6**	
	Diameter (mm)	**255**	
Water quality: (**(samples still at laboratory)**	*Good*	*Fair*	*Poor*

Appendix B
Soil Water Retention Characteristics LC1-LC4

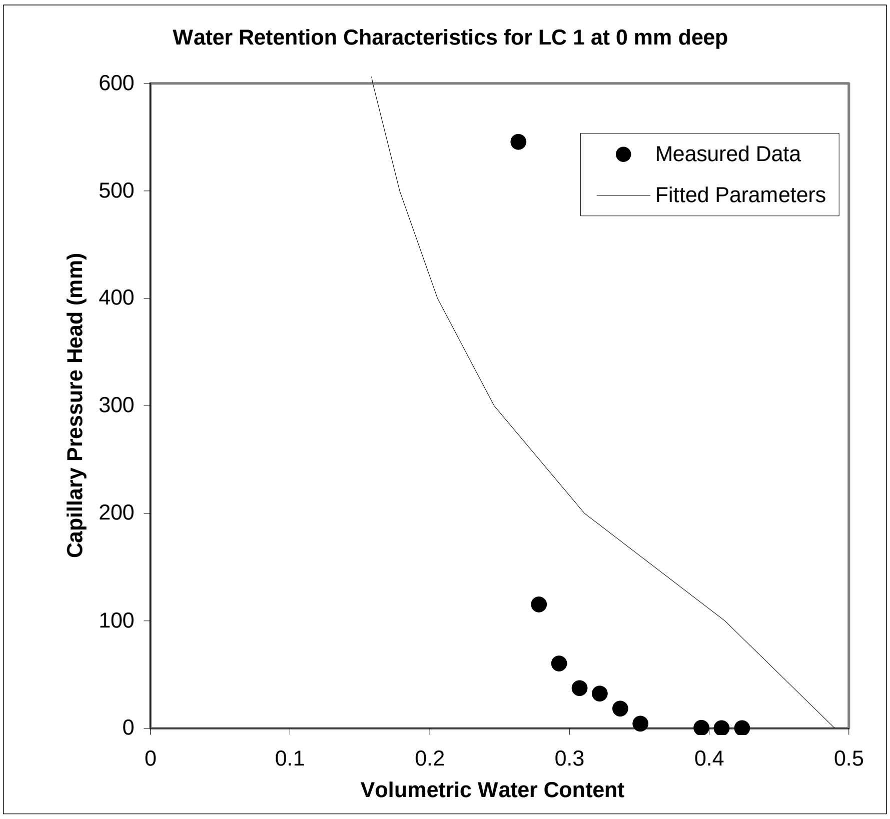

Water Retention Characteristics for LC 1 at 0 mm deep
Capillary Pressure Head (mm)
600
500
400
300
200
100
0
0
0.1
0.2
0.3
0.4
0.5
Volumetric Water Content
Measured Data
Fitted Parameters

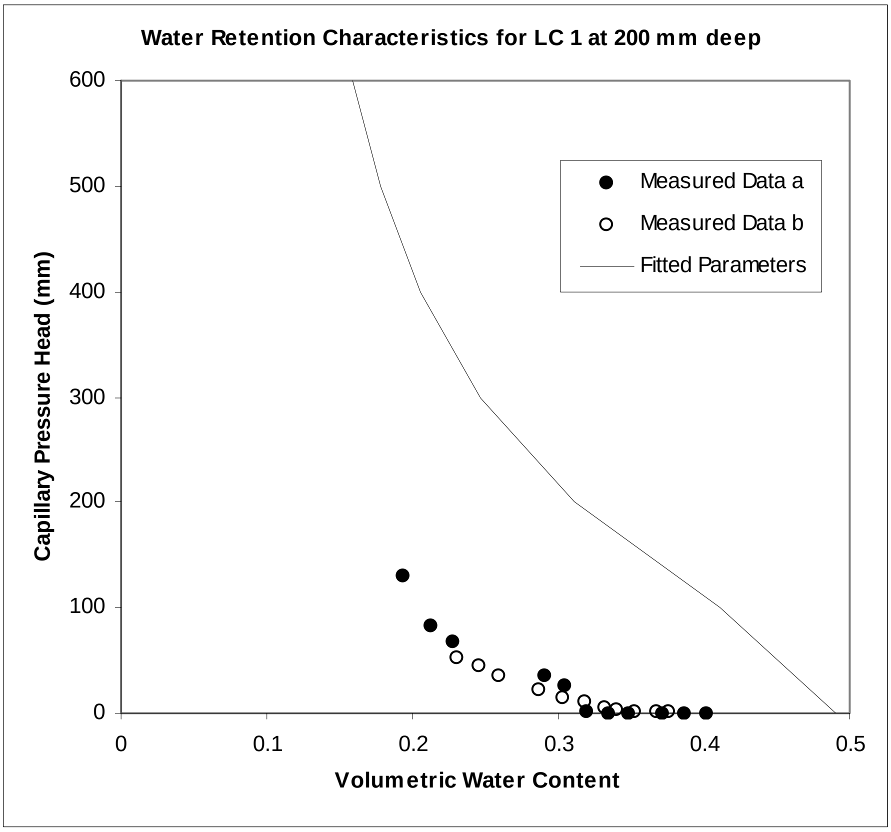

Water Retention Characteristics for LC 1 at 200 mm deep
Capillary Pressure Head (mm)
600
500
400
300
200
100
0
0
0.1
0.2
0.3
0.4
0.5
Volumetric Water Content
Measured Data a
Measured Data b
Fitted Parameters

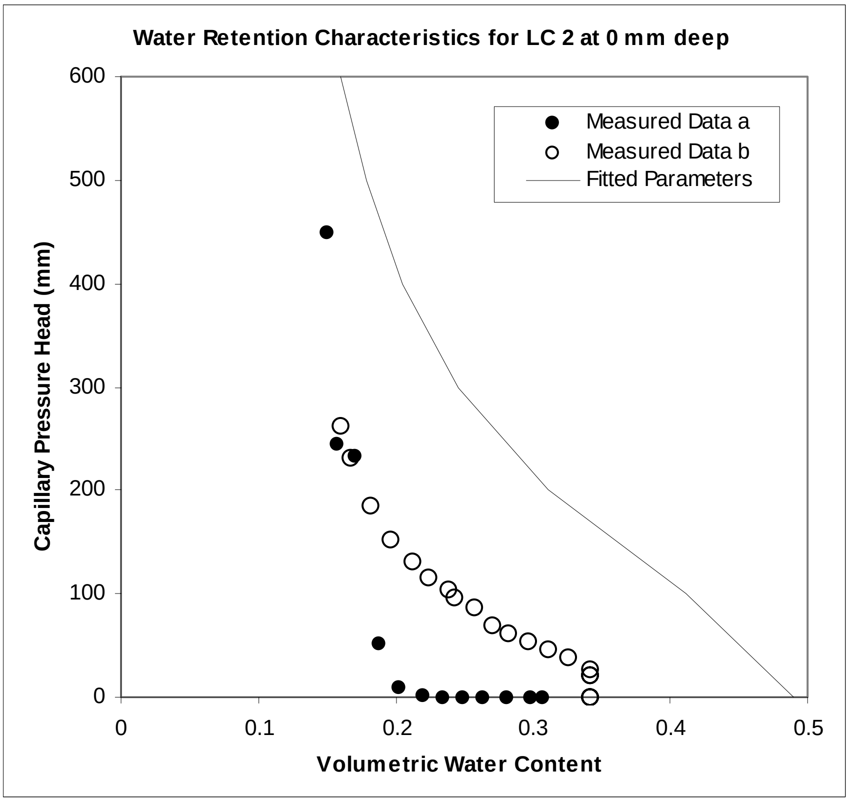
Water Retention Characteristics for LC 2 at 0 mm deep
Measured Data a
Measured Data b
Fitted Parameters
Capillary Pressure Head (mm)
Volumetric Water Content
600
500
400
300
200
100
0
0
0.1
0.2
0.3
0.4
0.5

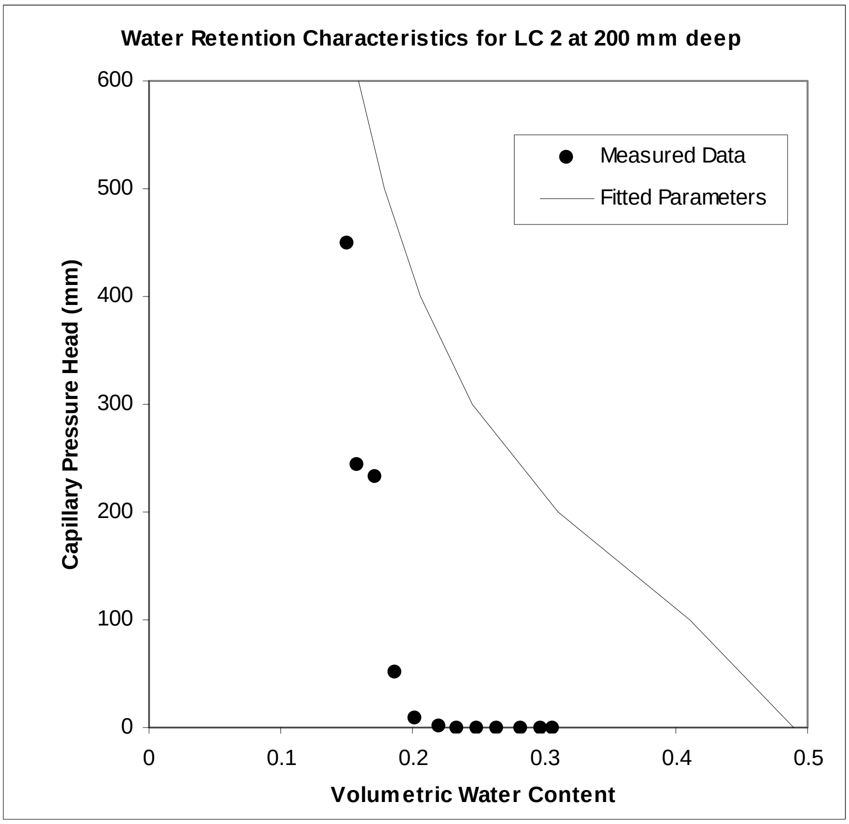
Water Retention Characteristics for LC 2 at 200 mm deep
Measured Data
Fitted Parameters
Capillary Pressure Head (mm)
Volumetric Water Content
600
500
400
300
200
100
0
0
0.1
0.2
0.3
0.4
0.5

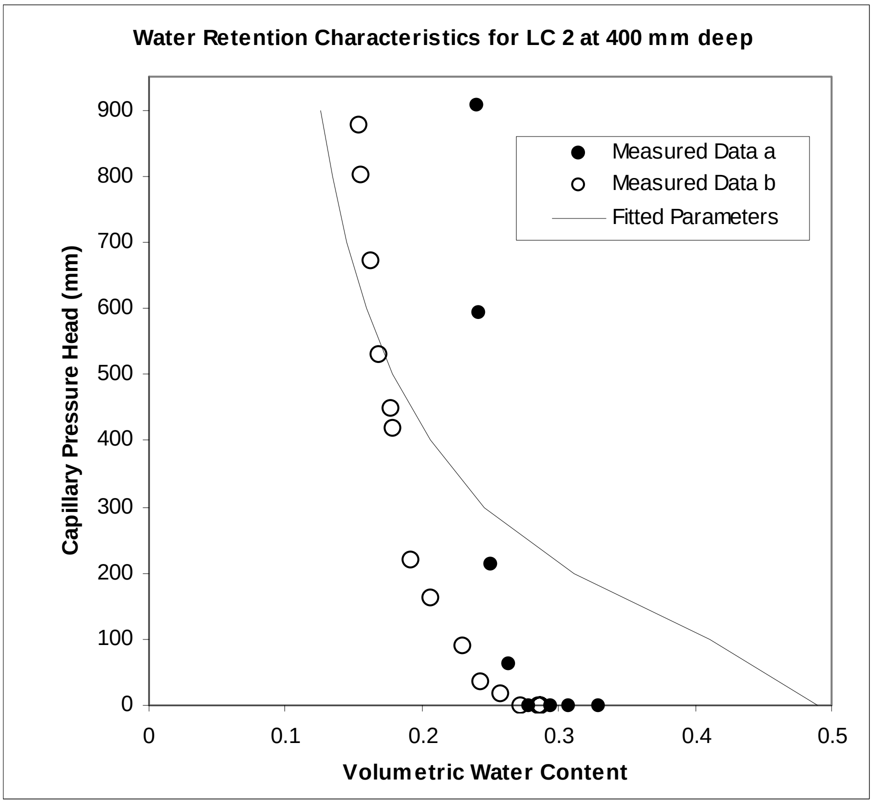
Water Retention Characteristics for LC 2 at 400 mm deep
Capillary Pressure Head (mm)
Volumetric Water Content
Measured Data a
Measured Data b
Fitted Parameters
0
100
200
300
400
500
600
700
800
900
0
0.1
0.2
0.3
0.4
0.5

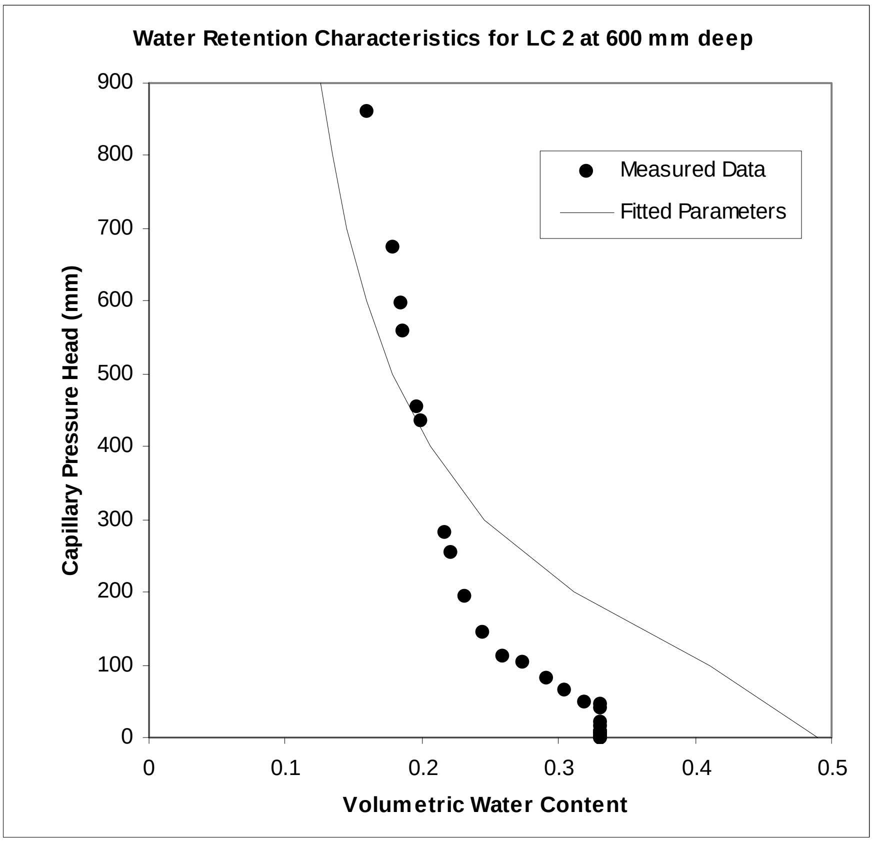
Water Retention Characteristics for LC 2 at 600 mm deep
Capillary Pressure Head (mm)
Volumetric Water Content
Measured Data
Fitted Parameters
0
100
200
300
400
500
600
700
800
900
0
0.1
0.2
0.3
0.4
0.5

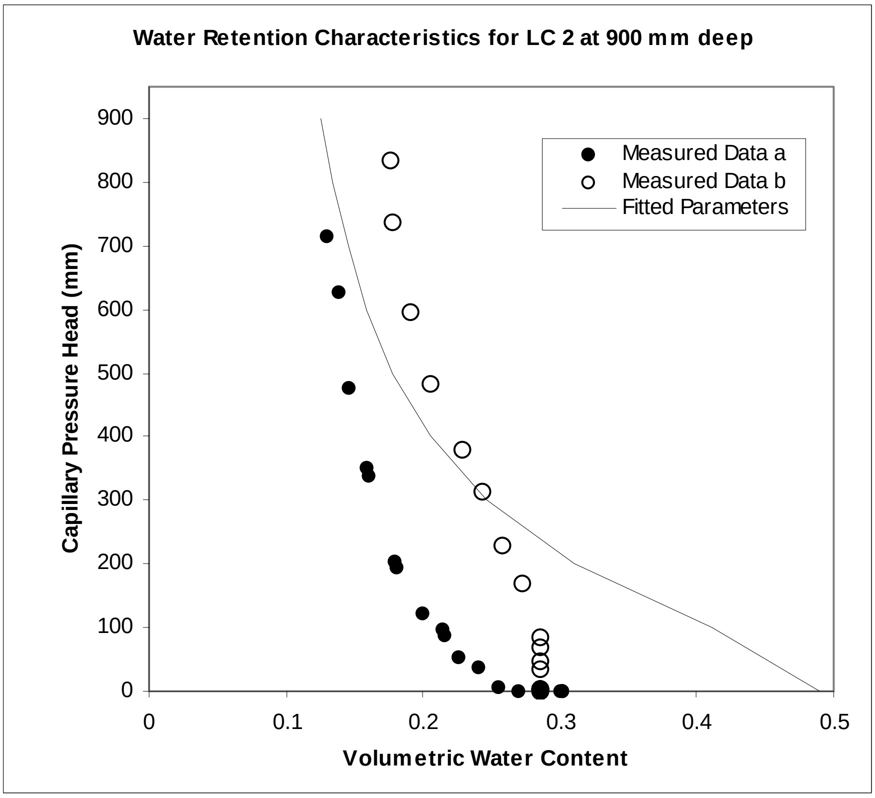
Water Retention Characteristics for LC 2 at 900 mm deep
Capillary Pressure Head (mm)
Volumetric Water Content
Measured Data a
Measured Data b
Fitted Parameters
0
100
200
300
400
500
600
700
800
900
0
0.1
0.2
0.3
0.4
0.5

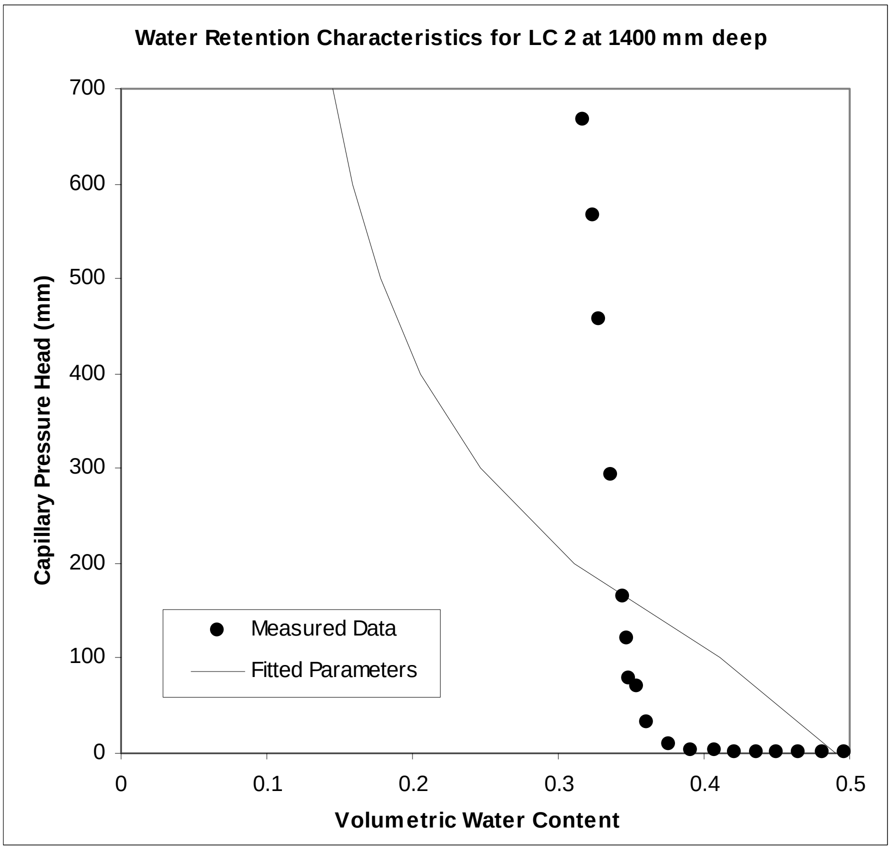
Water Retention Characteristics for LC 2 at 1400 mm deep
Capillary Pressure Head (mm)
Volumetric Water Content
Measured Data
Fitted Parameters
0
100
200
300
400
500
600
700
0
0.1
0.2
0.3
0.4
0.5

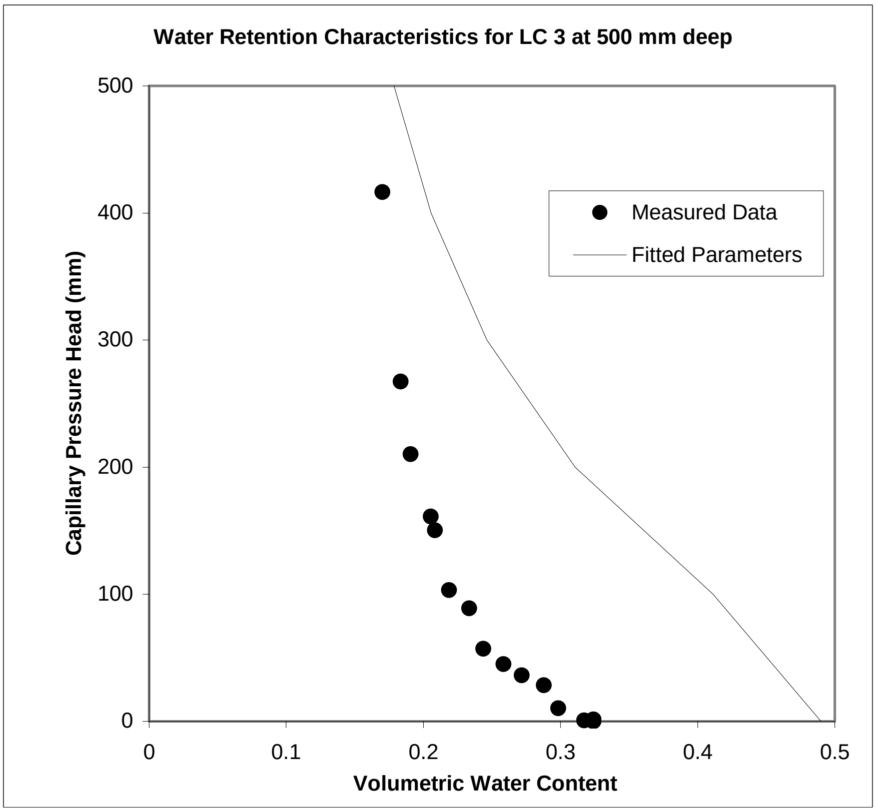
Water Retention Characteristics for LC 3 at 500 mm deep
500
400
300
200
100
0
0
0.1
0.2
0.3
0.4
0.5
Capillary Pressure Head (mm)
Volumetric Water Content
Measured Data
Fitted Parameters

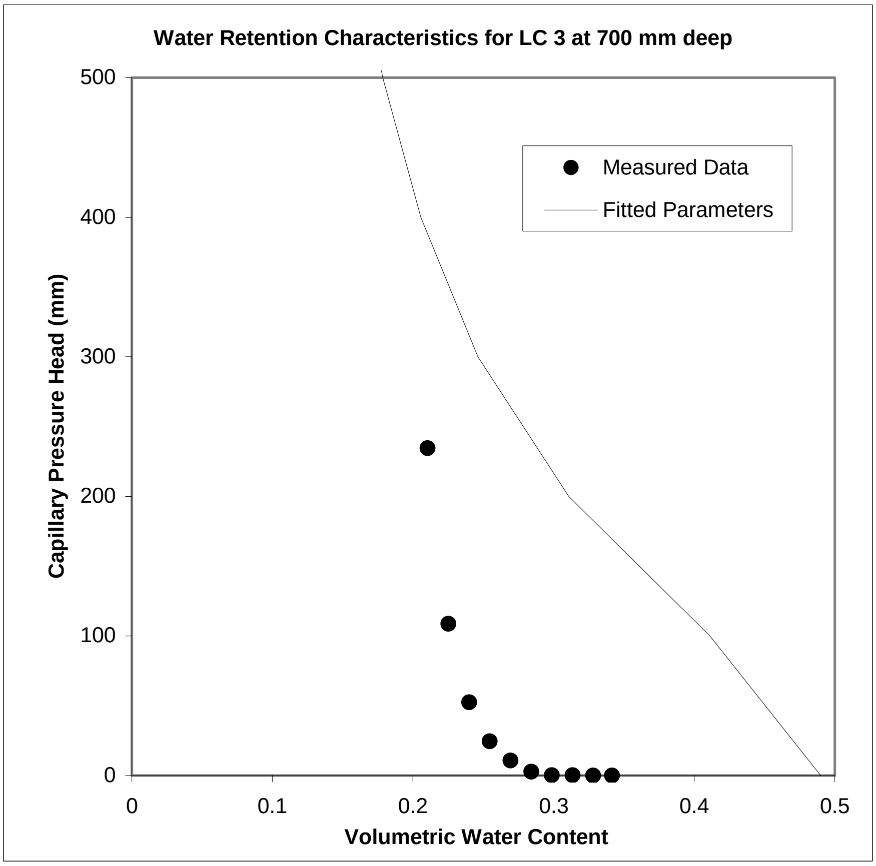
Water Retention Characteristics for LC 3 at 700 mm deep
500
400
300
200
100
0
0
0.1
0.2
0.3
0.4
0.5
Capillary Pressure Head (mm)
Volumetric Water Content
Measured Data
Fitted Parameters

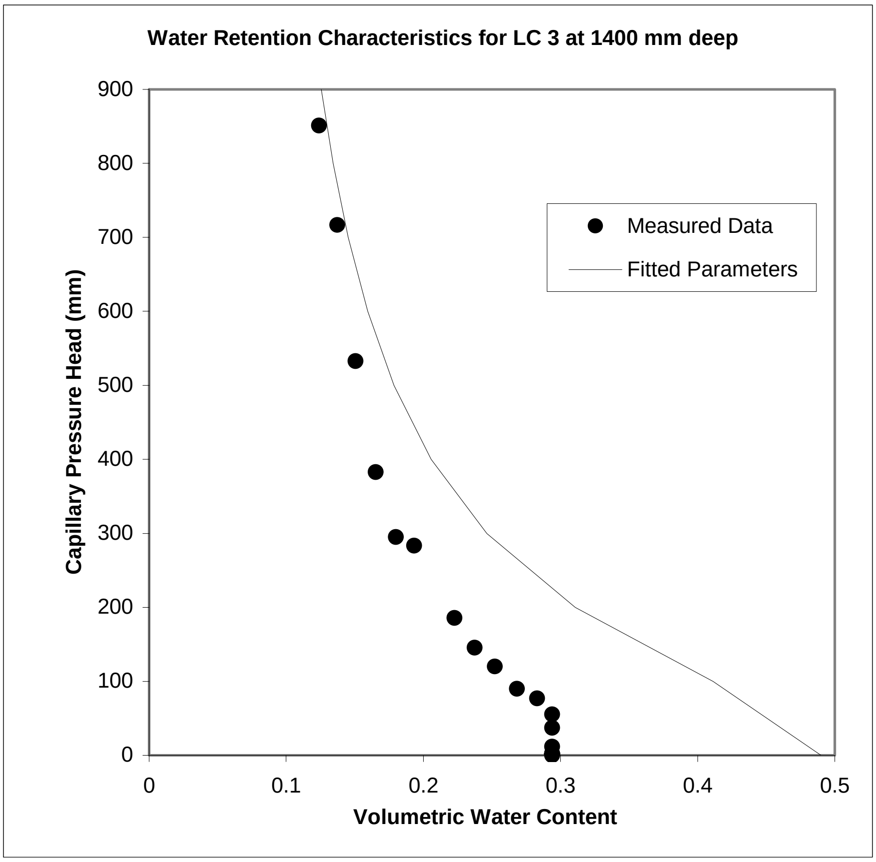
Water Retention Characteristics for LC 3 at 1400 mm deep
Measured Data
Fitted Parameters
Capillary Pressure Head (mm)
900
800
700
600
500
400
300
200
100
0
0
0.1
0.2
0.3
0.4
0.5
Volumetric Water Content

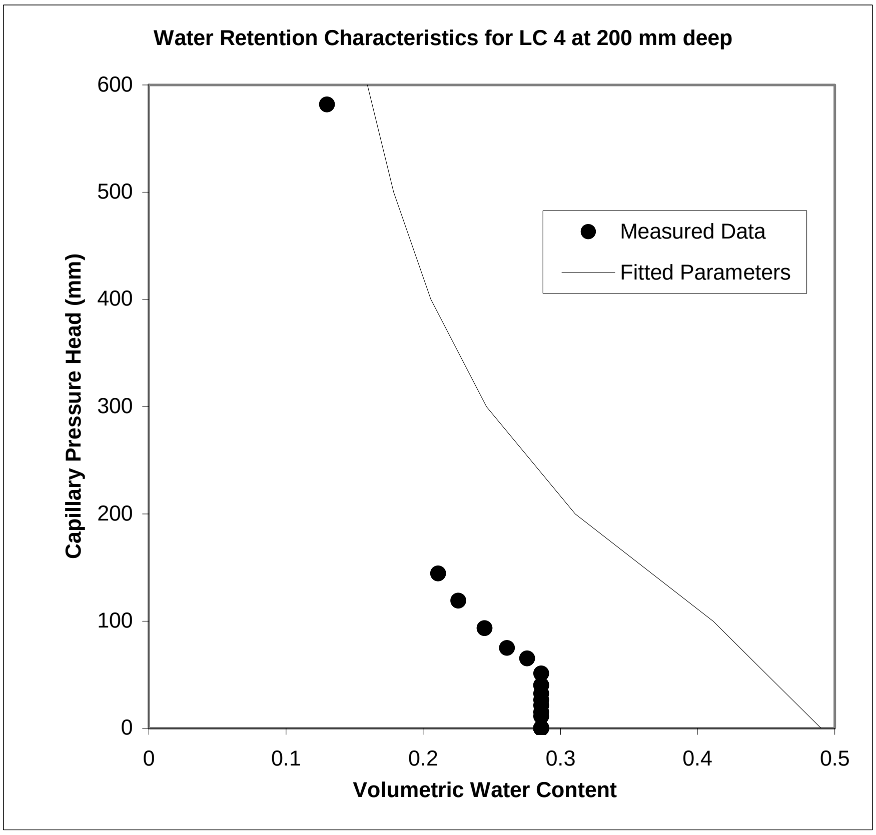
Water Retention Characteristics for LC 4 at 200 mm deep
Measured Data
Fitted Parameters
Capillary Pressure Head (mm)
600
500
400
300
200
100
0
0
0.1
0.2
0.3
0.4
0.5
Volumetric Water Content

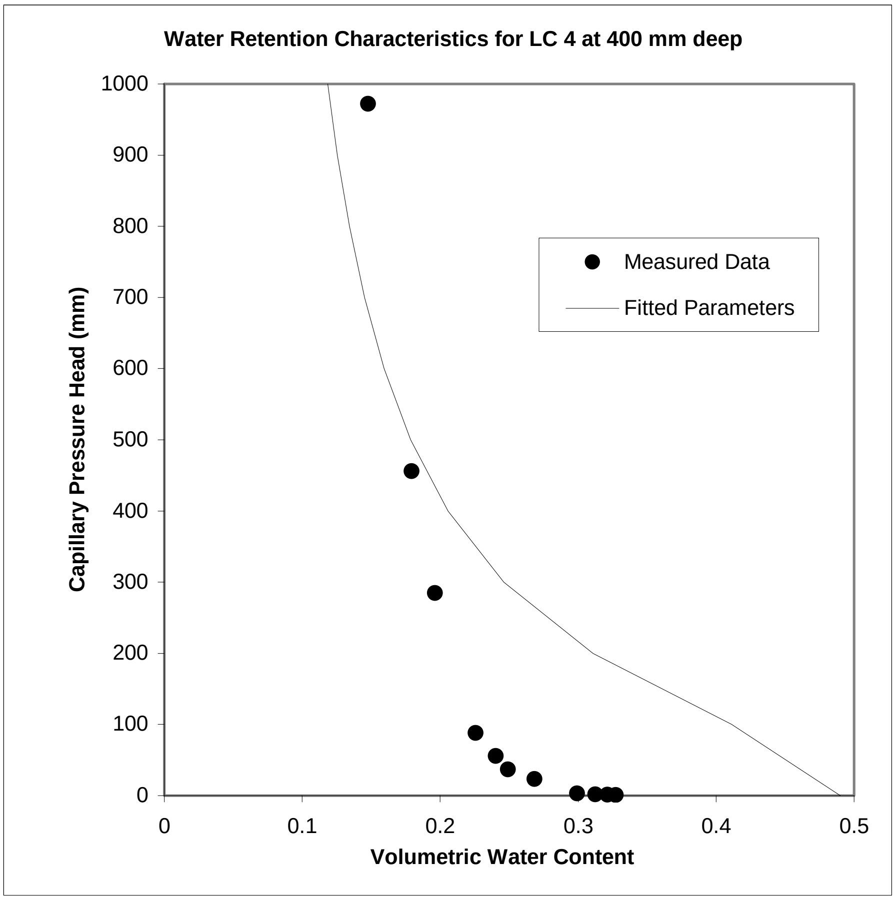
Water Retention Characteristics for LC 4 at 400 mm deep
Capillary Pressure Head (mm)
1000
900
800
700
600
500
400
300
200
100
0
0
0.1
0.2
0.3
0.4
0.5
Volumetric Water Content
Measured Data
Fitted Parameters

APPENDIX C3

HYDRUS-2D Simulations versus Observed

Nests LC8 to LC10

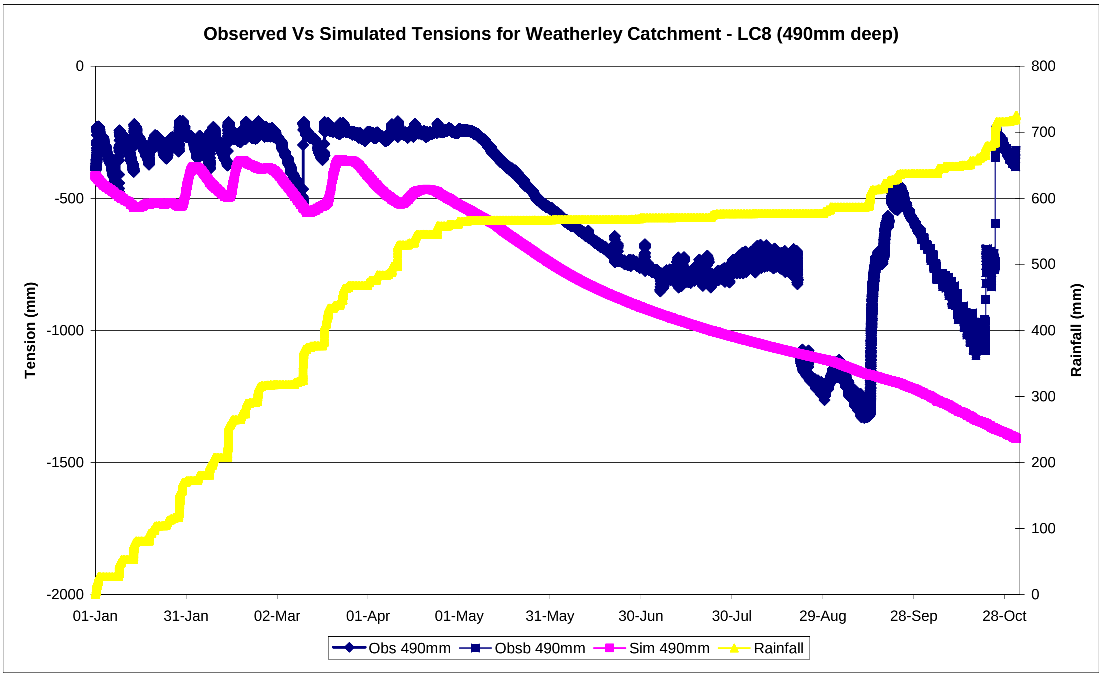
Observed Vs Simulated Tensions for Weatherley Catchment - LC8 (490mm deep)
Tension (mm)
Rainfall (mm)
0
-500
-1000
-1500
-2000
800
700
600
500
400
300
200
100
0
01-Jan
31-Jan
02-Mar
01-Apr
01-May
31-May
30-Jun
30-Jul
29-Aug
28-Sep
28-Oct
Obs 490mm
Obsb 490mm
Sim 490mm
Rainfall

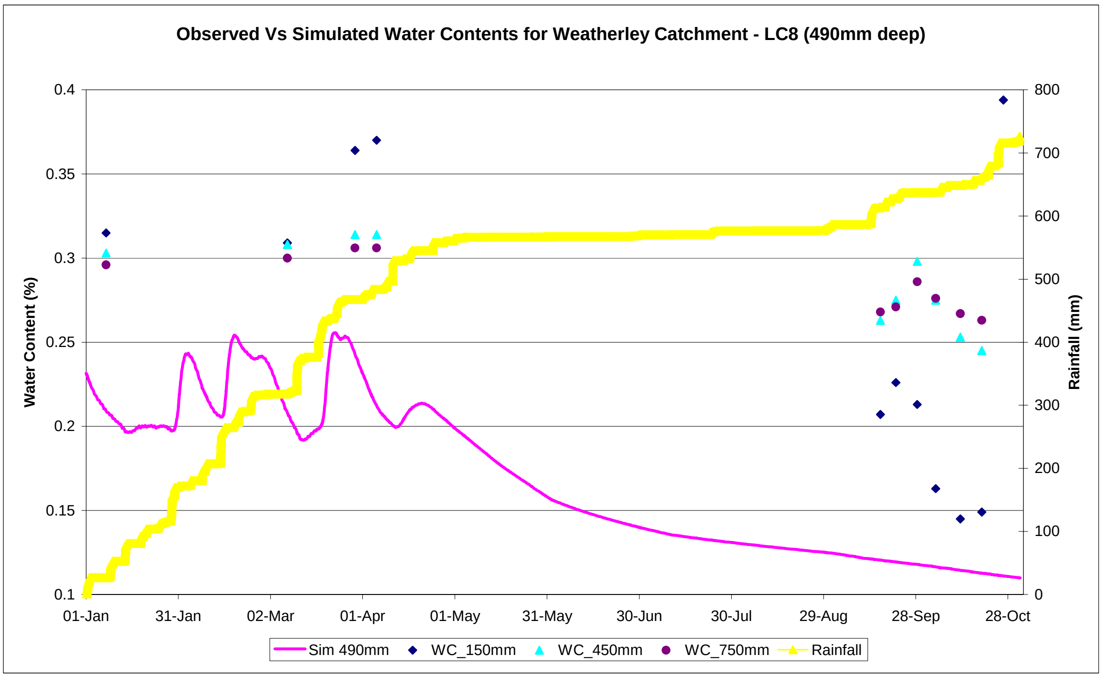
Observed Vs Simulated Water Contents for Weatherley Catchment - LC8 (490mm deep)
Water Content (%)
Rainfall (mm)
0.4
0.35
0.3
0.25
0.2
0.15
0.1
800
700
600
500
400
300
200
100
0
01-Jan
31-Jan
02-Mar
01-Apr
01-May
31-May
30-Jun
30-Jul
29-Aug
28-Sep
28-Oct
Sim 490mm
WC_150mm
WC_450mm
WC_750mm
Rainfall

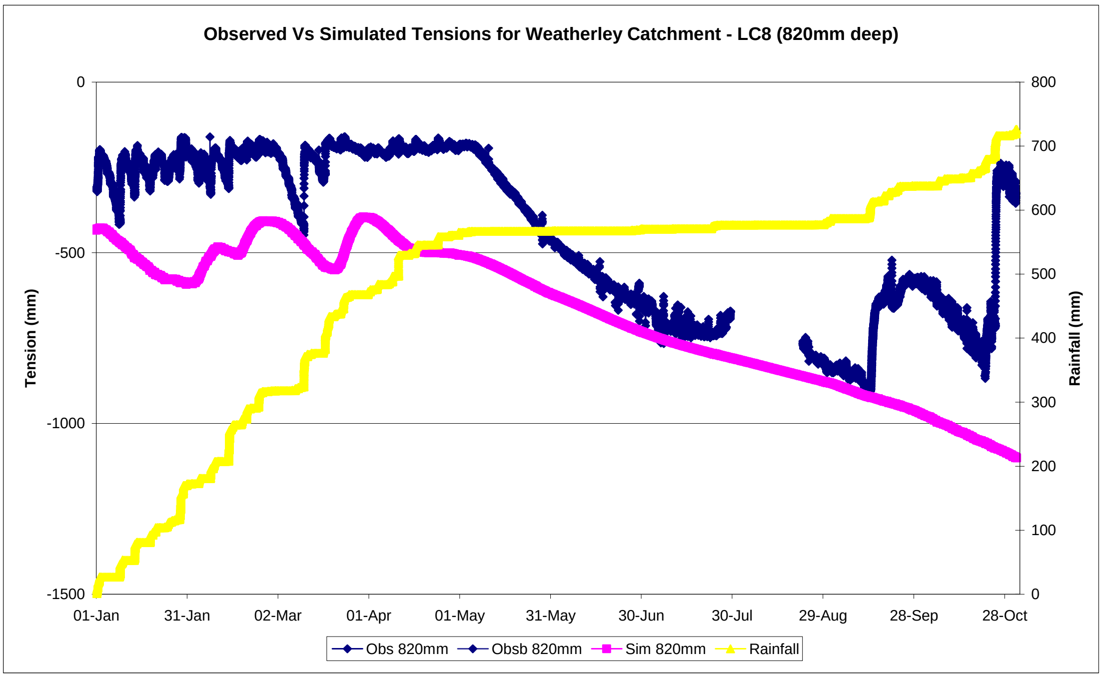
Observed Vs Simulated Tensions for Weatherley Catchment - LC8 (820mm deep)
Tension (mm)
Rainfall (mm)
0
-500
-1000
-1500
800
700
600
500
400
300
200
100
0
01-Jan
31-Jan
02-Mar
01-Apr
01-May
31-May
30-Jun
30-Jul
29-Aug
28-Sep
28-Oct
Obs 820mm
Obsb 820mm
Sim 820mm
Rainfall

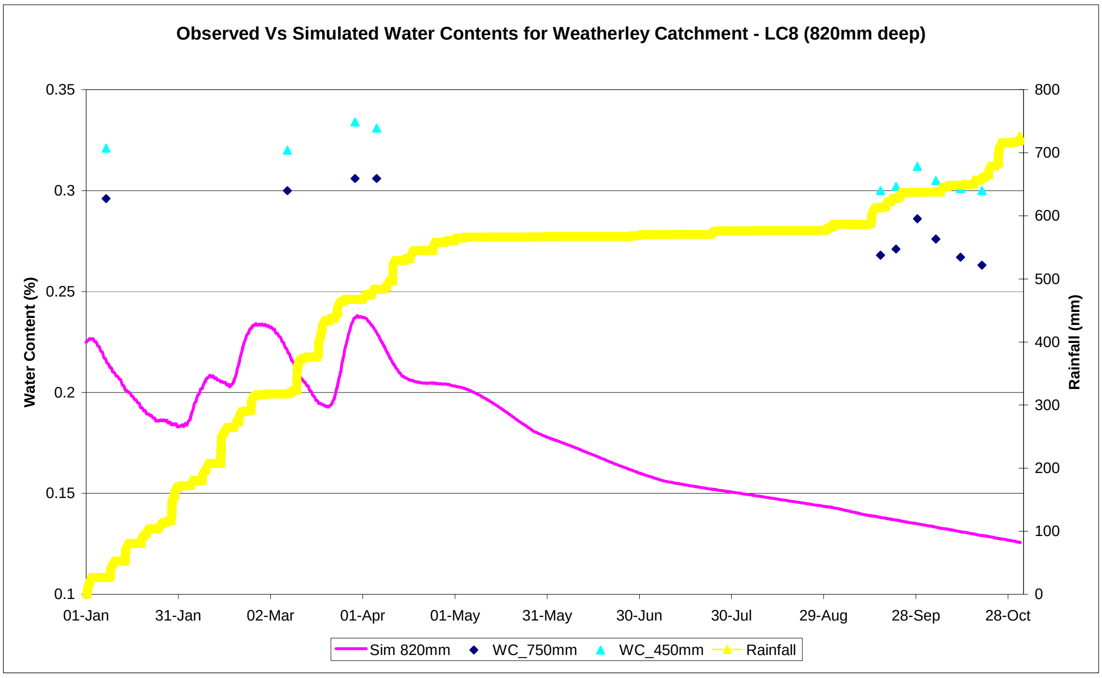
Observed Vs Simulated Water Contents for Weatherley Catchment - LC8 (820mm deep)
Water Content (%)
Rainfall (mm)
0.35
0.3
0.25
0.2
0.15
0.1
800
700
600
500
400
300
200
100
0
01-Jan
31-Jan
02-Mar
01-Apr
01-May
31-May
30-Jun
30-Jul
29-Aug
28-Sep
28-Oct
Sim 820mm
WC_750mm
WC_450mm
Rainfall

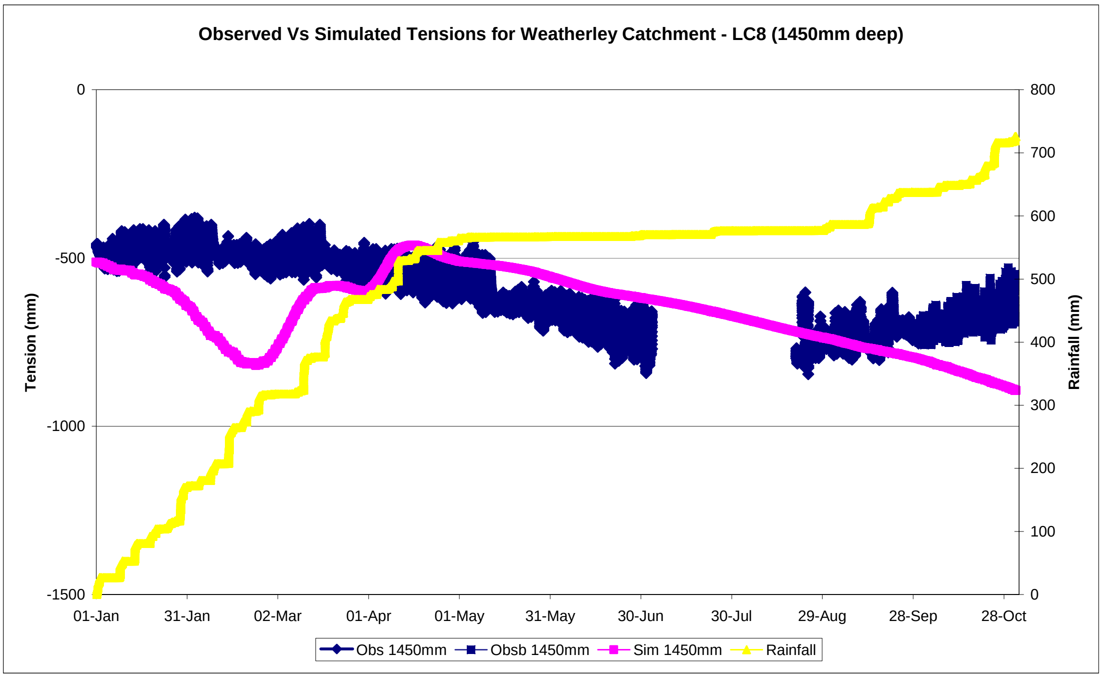
Observed Vs Simulated Tensions for Weatherley Catchment - LC8 (1450mm deep)
Tension (mm)
Rainfall (mm)
0
-500
-1000
-1500
800
700
600
500
400
300
200
100
0
01-Jan
31-Jan
02-Mar
01-Apr
01-May
31-May
30-Jun
30-Jul
29-Aug
28-Sep
28-Oct
Obs 1450mm
Obsb 1450mm
Sim 1450mm
Rainfall

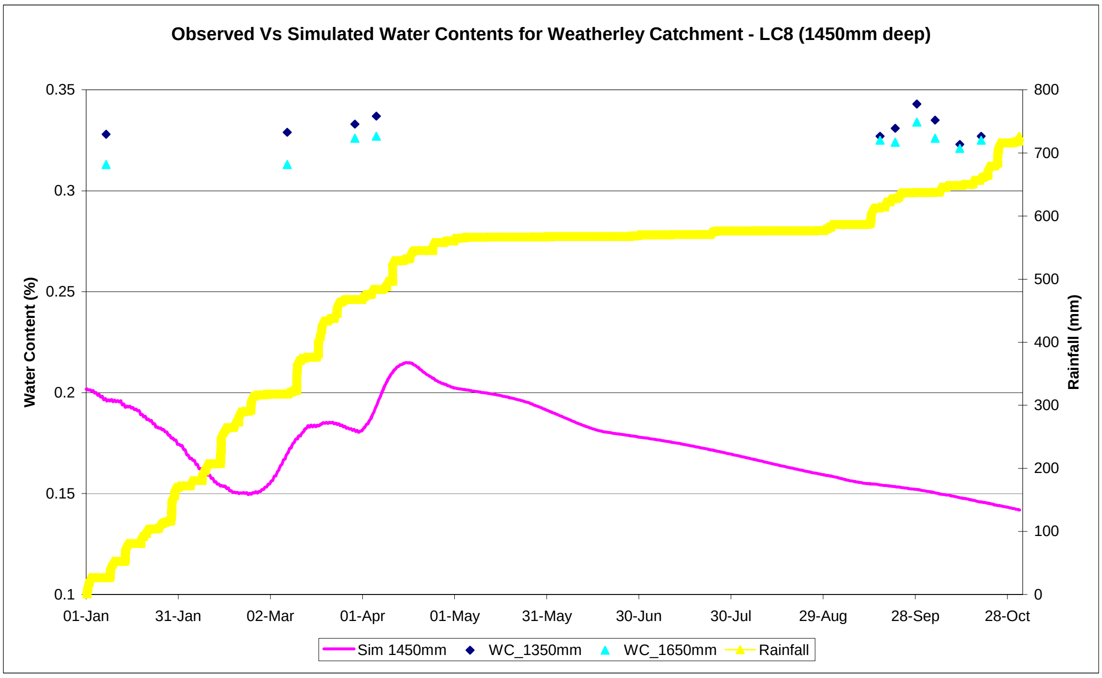
Observed Vs Simulated Water Contents for Weatherley Catchment - LC8 (1450mm deep)
Water Content (%)
Rainfall (mm)
0.35
0.3
0.25
0.2
0.15
0.1
800
700
600
500
400
300
200
100
0
01-Jan
31-Jan
02-Mar
01-Apr
01-May
31-May
30-Jun
30-Jul
29-Aug
28-Sep
28-Oct
Sim 1450mm
WC_1350mm
WC_1650mm
Rainfall

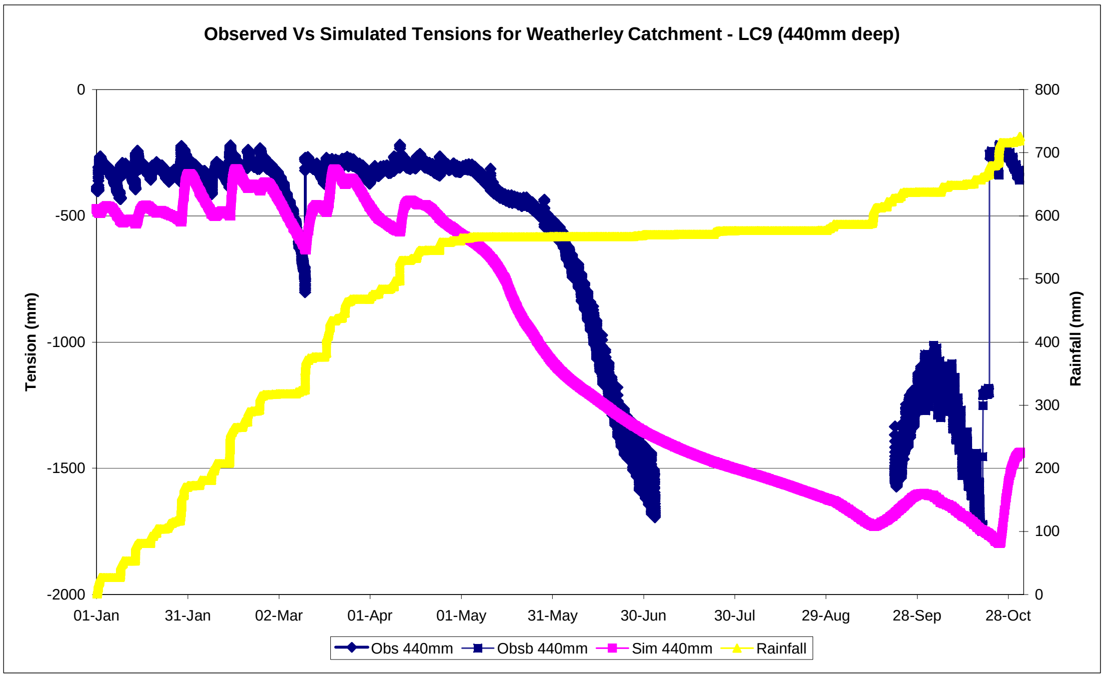

Observed Vs Simulated Tensions for Weatherley Catchment - LC9 (440mm deep)
Tension (mm)
Rainfall (mm)
0
-500
-1000
-1500
-2000
800
700
600
500
400
300
200
100
0
01-Jan
31-Jan
02-Mar
01-Apr
01-May
31-May
30-Jun
30-Jul
29-Aug
28-Sep
28-Oct
Obs 440mm
Obsb 440mm
Sim 440mm
Rainfall

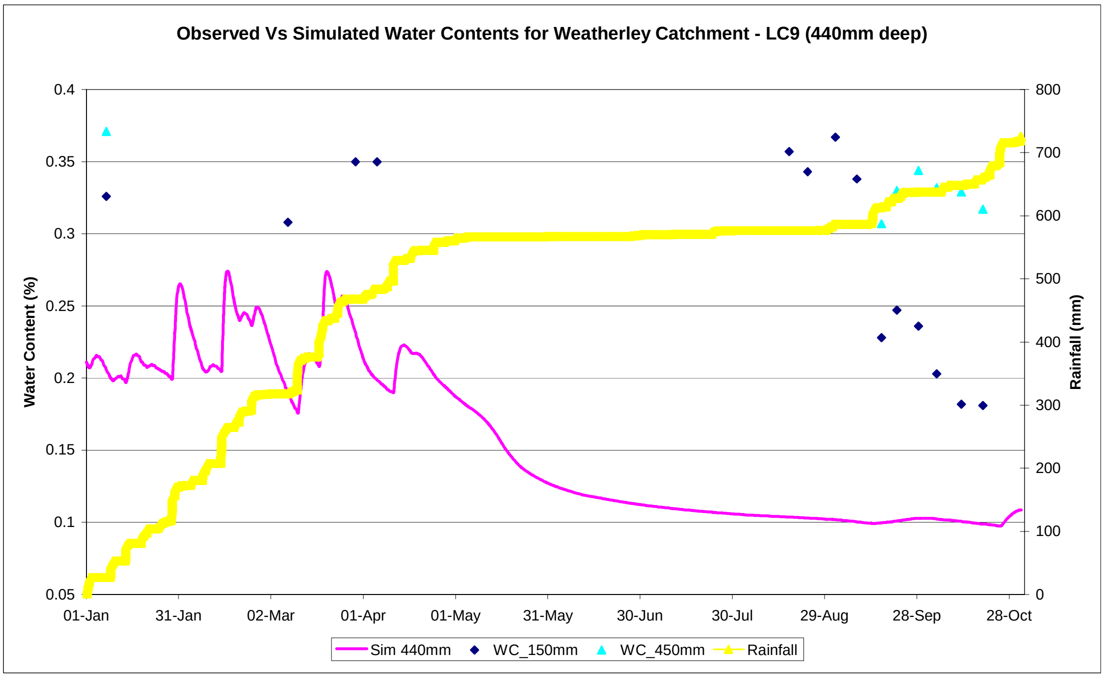

Observed Vs Simulated Water Contents for Weatherley Catchment - LC9 (440mm deep)
Water Content (%)
Rainfall (mm)
0.4
0.35
0.3
0.25
0.2
0.15
0.1
0.05
800
700
600
500
400
300
200
100
0
01-Jan
31-Jan
02-Mar
01-Apr
01-May
31-May
30-Jun
30-Jul
29-Aug
28-Sep
28-Oct
Sim 440mm
WC_150mm
WC_450mm
Rainfall

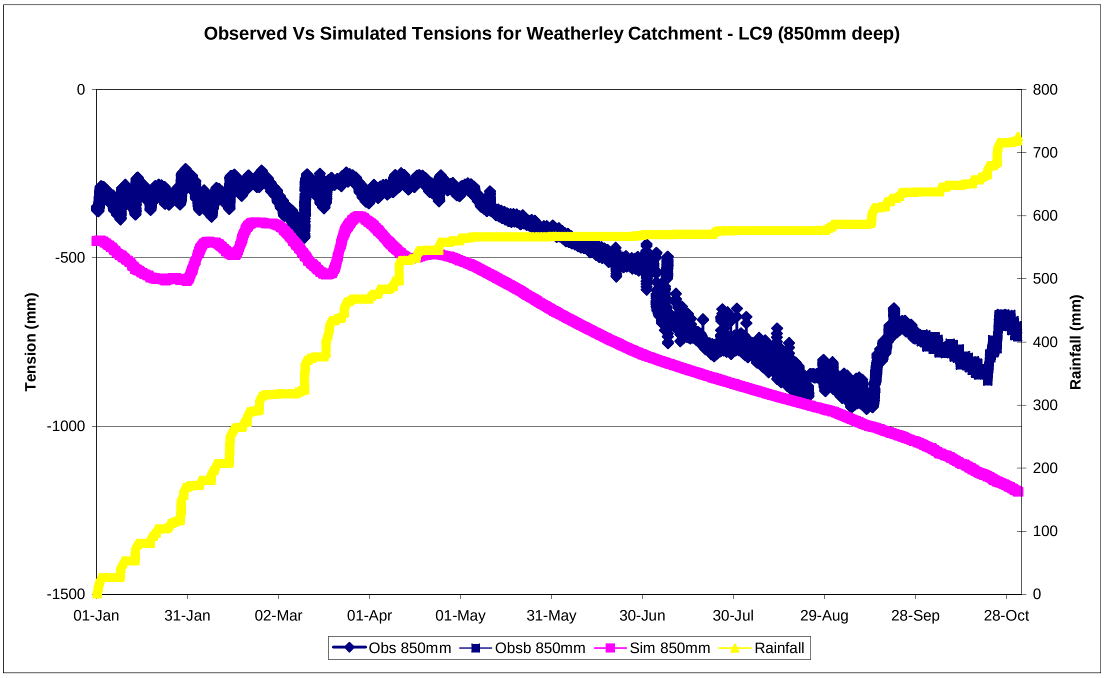
Observed Vs Simulated Tensions for Weatherley Catchment - LC9 (850mm deep)
Tension (mm)
Rainfall (mm)
0
-500
-1000
-1500
800
700
600
500
400
300
200
100
0
01-Jan
31-Jan
02-Mar
01-Apr
01-May
31-May
30-Jun
30-Jul
29-Aug
28-Sep
28-Oct
Obs 850mm
Obsb 850mm
Sim 850mm
Rainfall

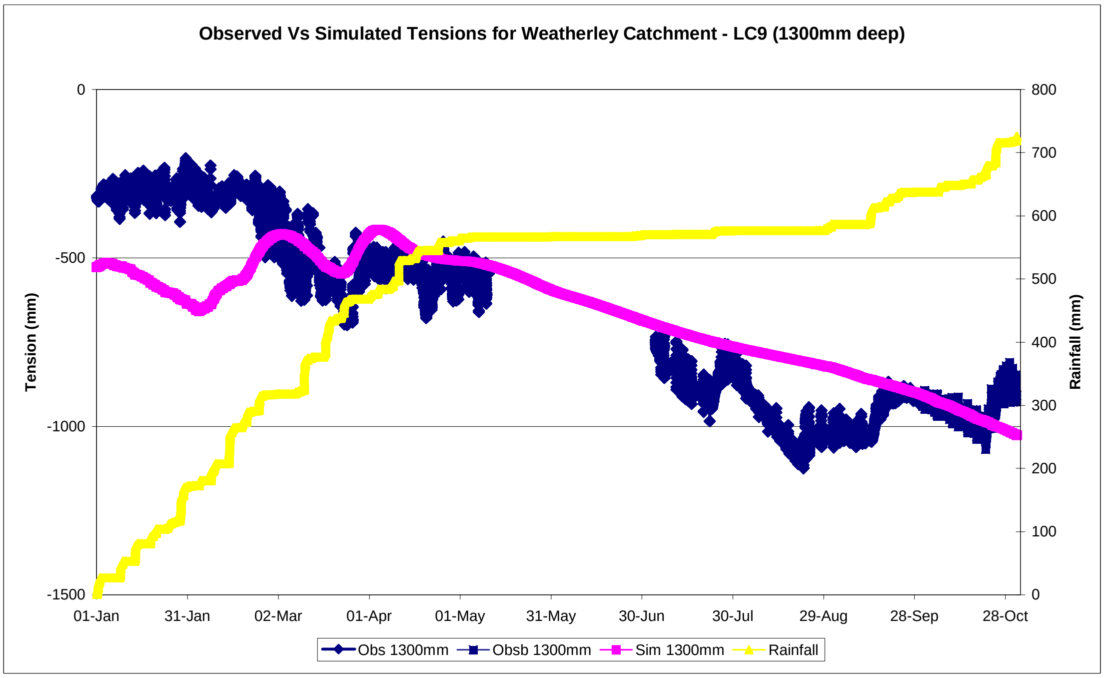
Observed Vs Simulated Tensions for Weatherley Catchment - LC9 (1300mm deep)
Tension (mm)
Rainfall (mm)
0
-500
-1000
-1500
800
700
600
500
400
300
200
100
0
01-Jan
31-Jan
02-Mar
01-Apr
01-May
31-May
30-Jun
30-Jul
29-Aug
28-Sep
28-Oct
Obs 1300mm
Obsb 1300mm
Sim 1300mm
Rainfall

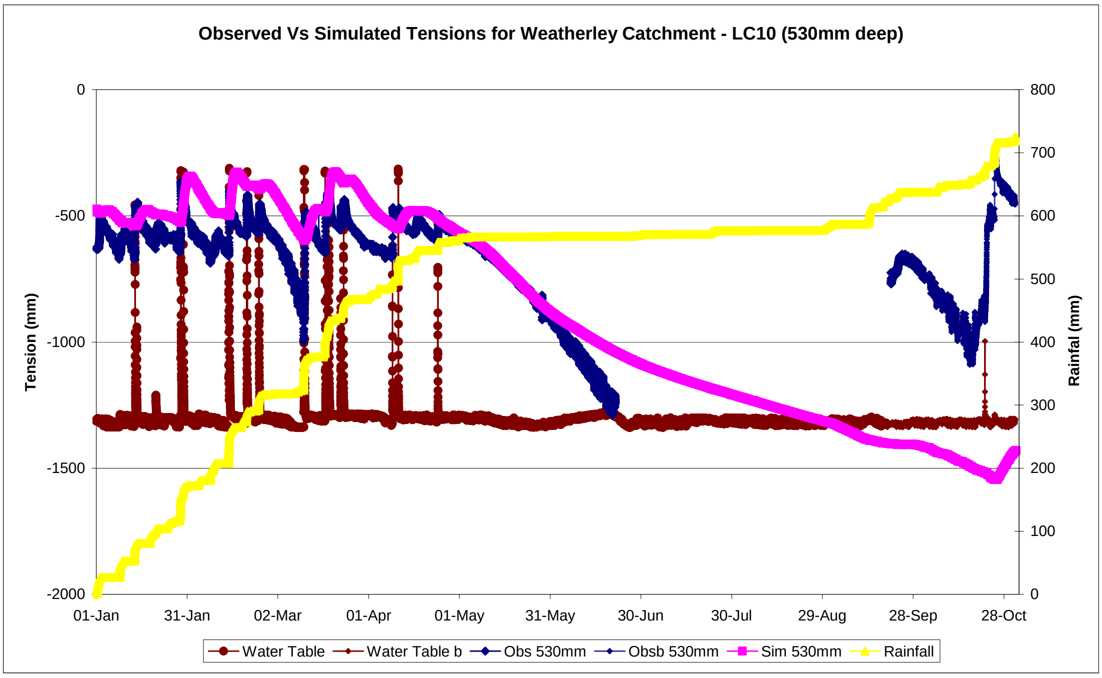
Observed Vs Simulated Tensions for Weatherley Catchment - LC10 (530mm deep)
Tension (mm)
Rainfall (mm)
0
-500
-1000
-1500
-2000
800
700
600
500
400
300
200
100
0
01-Jan
31-Jan
02-Mar
01-Apr
01-May
31-May
30-Jun
30-Jul
29-Aug
28-Sep
28-Oct
Water Table
Water Table b
Obs 530mm
Obsb 530mm
Sim 530mm
Rainfall

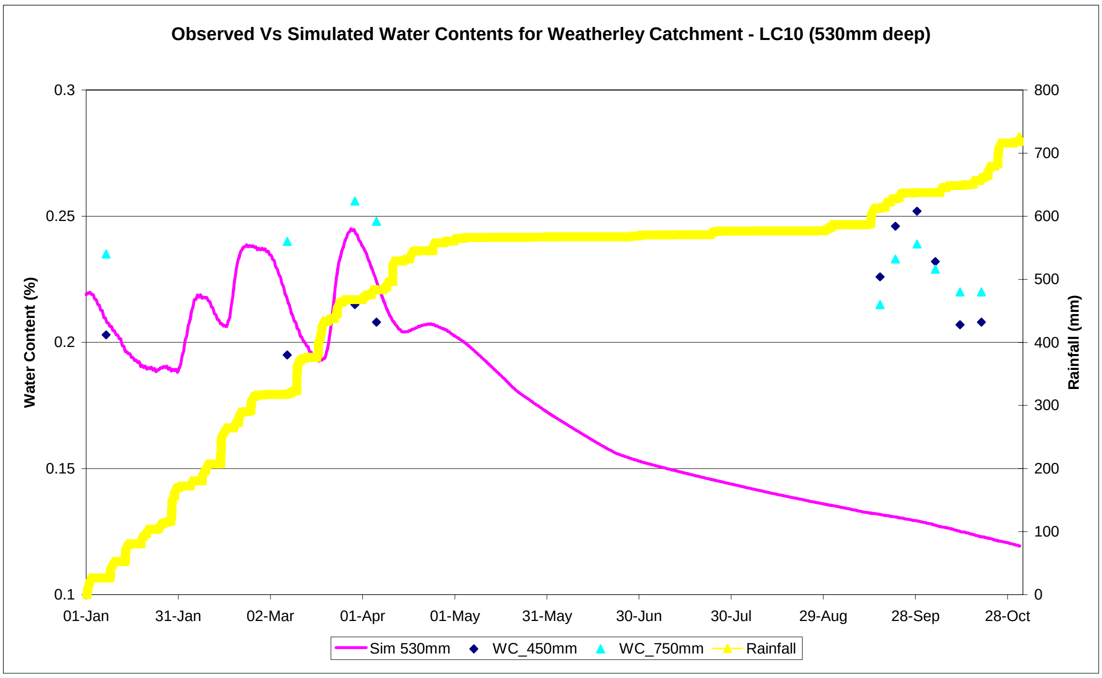
Observed Vs Simulated Water Contents for Weatherley Catchment - LC10 (530mm deep)
Water Content (%)
Rainfall (mm)
0.3
0.25
0.2
0.15
0.1
800
700
600
500
400
300
200
100
0
01-Jan
31-Jan
02-Mar
01-Apr
01-May
31-May
30-Jun
30-Jul
29-Aug
28-Sep
28-Oct
Sim 530mm
WC_450mm
WC_750mm
Rainfall

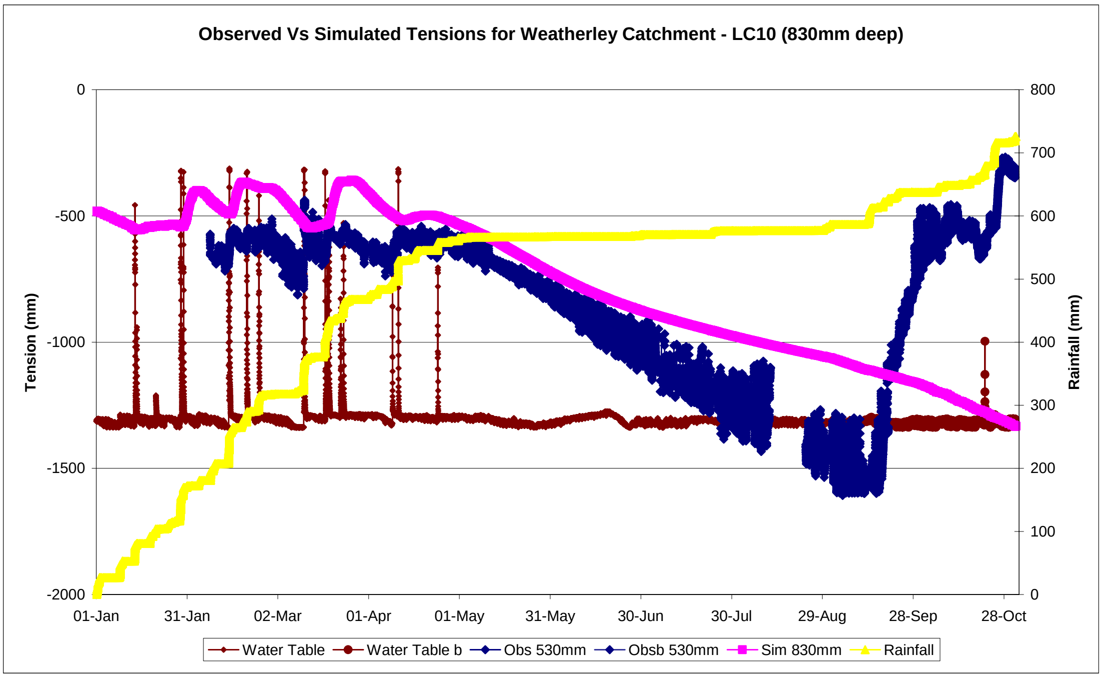

Observed Vs Simulated Tensions for Weatherley Catchment - LC10 (830mm deep)
Tension (mm)
Rainfall (mm)
0
-500
-1000
-1500
-2000
800
700
600
500
400
300
200
100
0
01-Jan
31-Jan
02-Mar
01-Apr
01-May
31-May
30-Jun
30-Jul
29-Aug
28-Sep
28-Oct
Water Table
Water Table b
Obs 530mm
Obsb 530mm
Sim 830mm
Rainfall

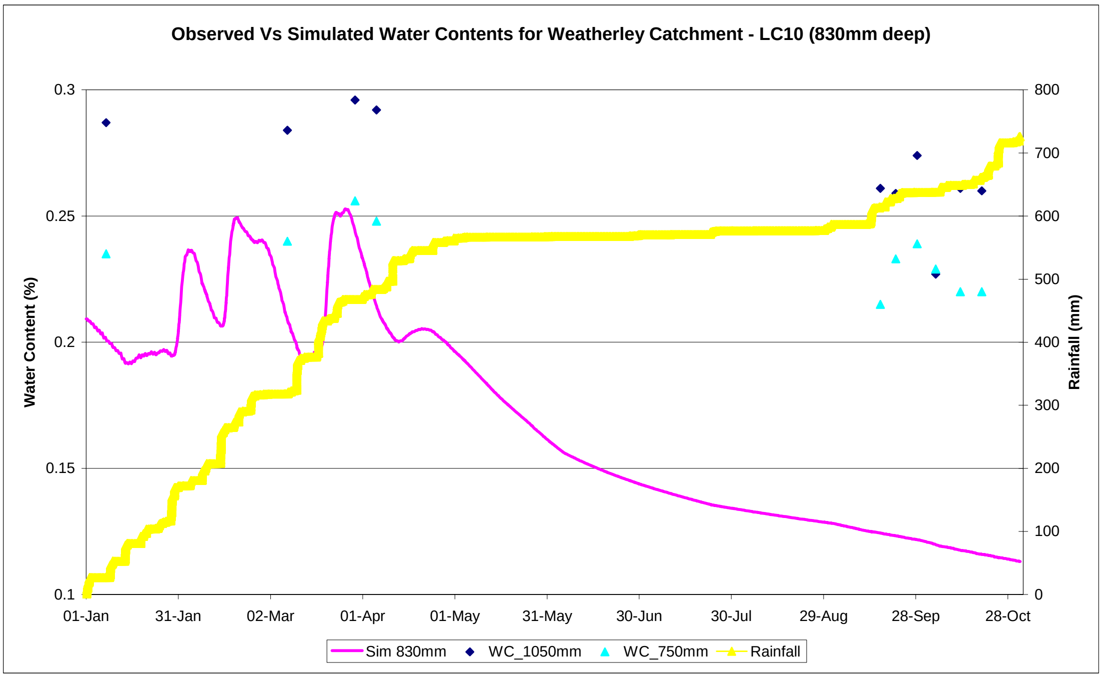

Observed Vs Simulated Water Contents for Weatherley Catchment - LC10 (830mm deep)
Water Content (%)
Rainfall (mm)
0.3
0.25
0.2
0.15
0.1
800
700
600
500
400
300
200
100
0
01-Jan
31-Jan
02-Mar
01-Apr
01-May
31-May
30-Jun
30-Jul
29-Aug
28-Sep
28-Oct
Sim 830mm
WC_1050mm
WC_750mm
Rainfall

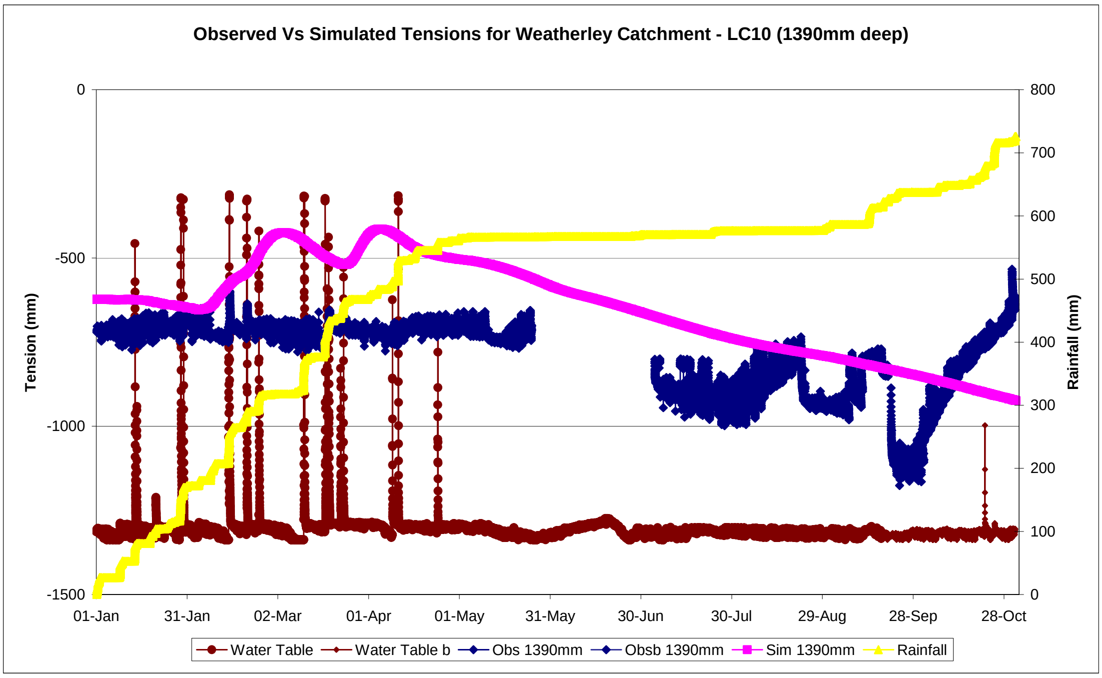
Observed Vs Simulated Tensions for Weatherley Catchment - LC10 (1390mm deep)
Tension (mm)
Rainfall (mm)
0
-500
-1000
-1500
800
700
600
500
400
300
200
100
0
01-Jan
31-Jan
02-Mar
01-Apr
01-May
31-May
30-Jun
30-Jul
29-Aug
28-Sep
28-Oct
Water Table
Water Table b
Obs 1390mm
Obsb 1390mm
Sim 1390mm
Rainfall

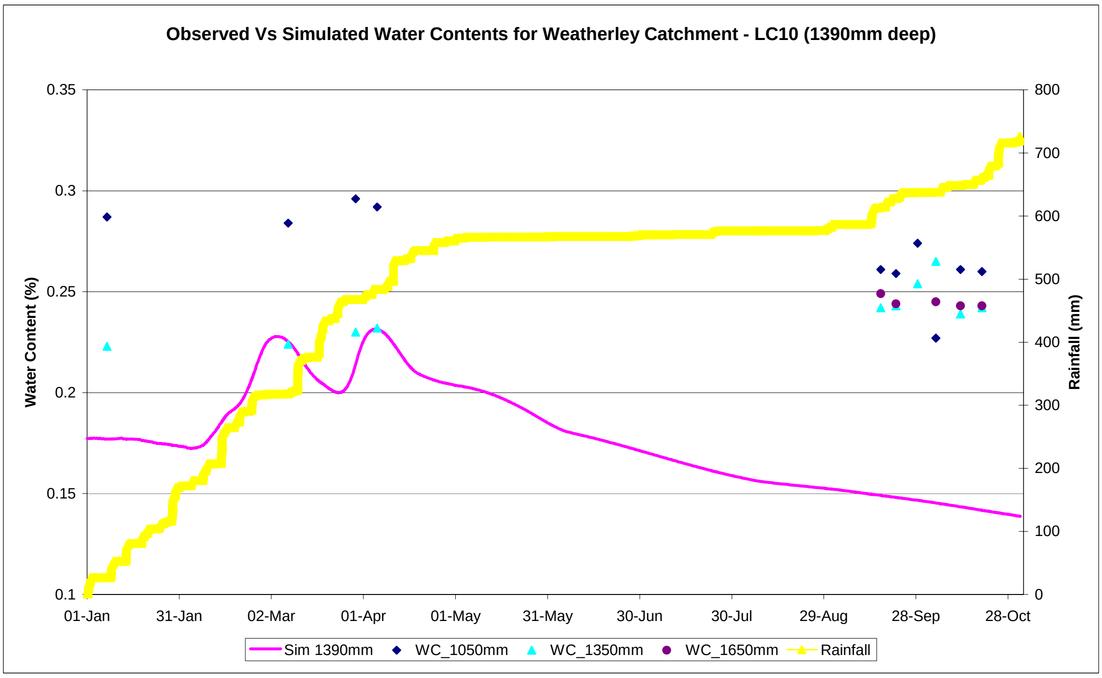
Observed Vs Simulated Water Contents for Weatherley Catchment - LC10 (1390mm deep)
Water Content (%)
Rainfall (mm)
0.35
0.3
0.25
0.2
0.15
0.1
800
700
600
500
400
300
200
100
0
01-Jan
31-Jan
02-Mar
01-Apr
01-May
31-May
30-Jun
30-Jul
29-Aug
28-Sep
28-Oct
Sim 1390mm
WC_1050mm
WC_1350mm
WC_1650mm
Rainfall

APPENDIX D
Development of *ACRU*Salinity for Coal Mining Environments

The *ACRU*Salinity module of the *ACRU* agrohydrological model has been modified to allow for processes inherent in a coal mining subcatchment. The salinity resulting from runoff from mine waste impoundments, haul areas and rehabilitated lands has been included in the updated model. In additions, interchanges between surface water and subsurface (mined out) reservoirs has also been included. The following case study, developed for Golder, Africa consultants describes the model development and testing against measured salinity responses. The case study addresses a scenario in which a virgin grassland catchment (Quaternary B11) is assumed to be mined and the resulting impacts are simulated.

DEVELOPMENT OF THE ACRUSALINITY MODULE FOR COAL MINING CATCHMENTS AND ASSESSMENT OF IMPACT OF EXTENSIVE POST MINING LAND USE IN B11C QUATERNARY CATCHMENT

By

Olufemi Idowu
Simon Lorentz

School of Bioresources Engineering and Environmental Hydrology
University of KwaZulu-Natal
Pietermaritzburg

February 2007

Executive Summary

This study is an assessment of the impact of opencast coal mining and subsequent land rehabilitation on the water resources of B11C quaternary catchment in the upper Olifants basin. Scenario simulations of the catchment in pre- and post- mining conditions using the *ACRU* agrohydrological system (in the form of *ACRU2000* and its salinity module, *ACRUSalinity*), indicate the following:

- The mean annual runoff volume and salt load from the catchment in the pre-mining condition are 40.8 x 10^6 m^3 and 5 758 metric tons respectively.
- A decrease of 18% in the mean annual runoff volume and an increase of 466% in the mean annual salt load from the entire catchment from pre- to post mining conditions; the post mining condition being 175 km^2 of rehabilitated coal mine in the 349 km^2 catchment.
- An increase in the daily average runoff salinity from the catchment from 177 mg/l to 1739 mg/l from pre- to post-mining conditions.
- An increase in the average annual percolation to groundwater from 31 mm in the pre-mining condition to 98 mm in the rehab;
- A significant increase in the groundwater salinity from 145 mg/l in the pre-mining condition to 2918 mg/l in the rehab;
- In the rehab, an average annual percolation of 98 mm/yr can be expected, with the same amount of water (17.2 x 10^6 m^3) available for pumping in a sustainable manner, thereby making the mean annual catchment yield for water supply a total of 50.6 x 10^6 m^3.

Table of Contents

List of Figures

List of Tables

1. Introduction

1.1 Brief

After extraction of coal through opencast mining and subsequent rehabilitation, increased groundwater storage in the rehab void may occur though groundwater rebound in the spoil and coal discard in the void, as well as through increased infiltration. The brief for this study is to determine the volume of groundwater that recharges to storage (and hence the groundwater availability for pumping) before and after opencast mining with subsequent rehabilitation in a part of the B11C quaternary catchment.

1.2 Study Area

The study area is located in the Mpumalanga Province, South Africa. It constitutes one of the DWAF quaternary catchments located in the Upper Olifants basin, upstream of Witbank Dam (Figure 1). The quaternary catchment is B11C and it lies between longitudes 29^0 15' and 29^0 30' E and latitudes 26^0 15' and 26^0 30' S. The catchment has a total area of 349 km^2. The main river draining the catchment is the Steenkoolspruit while the Department of Water Affairs (DWAF) gauge B1H017 records the outflow from the catchment.

1.3 Soils and Land Use

The catchment comprises clayey and clayey loam soils (Midgley, 1994). The following land use types can be found in the study area (Johnson, 1996): commercial dryland and irrigated areas, forest plantations, unimproved grassland and water bodies. The land types are listed Table 1 and their distribution is shown Figure 2.

Table1. Areas of land use types in catchment B11C

Description	Area (km^2)
Cultivated: temporary - commercial dryland	143.3
Cultivated: temporary - commercial irrigated	0.4
Forest plantations	0.2
Unimproved grassland	185.4
Water bodies (with 60 m stream width)	19.3
Urban / built up land – residential	0.007
Total	348.607

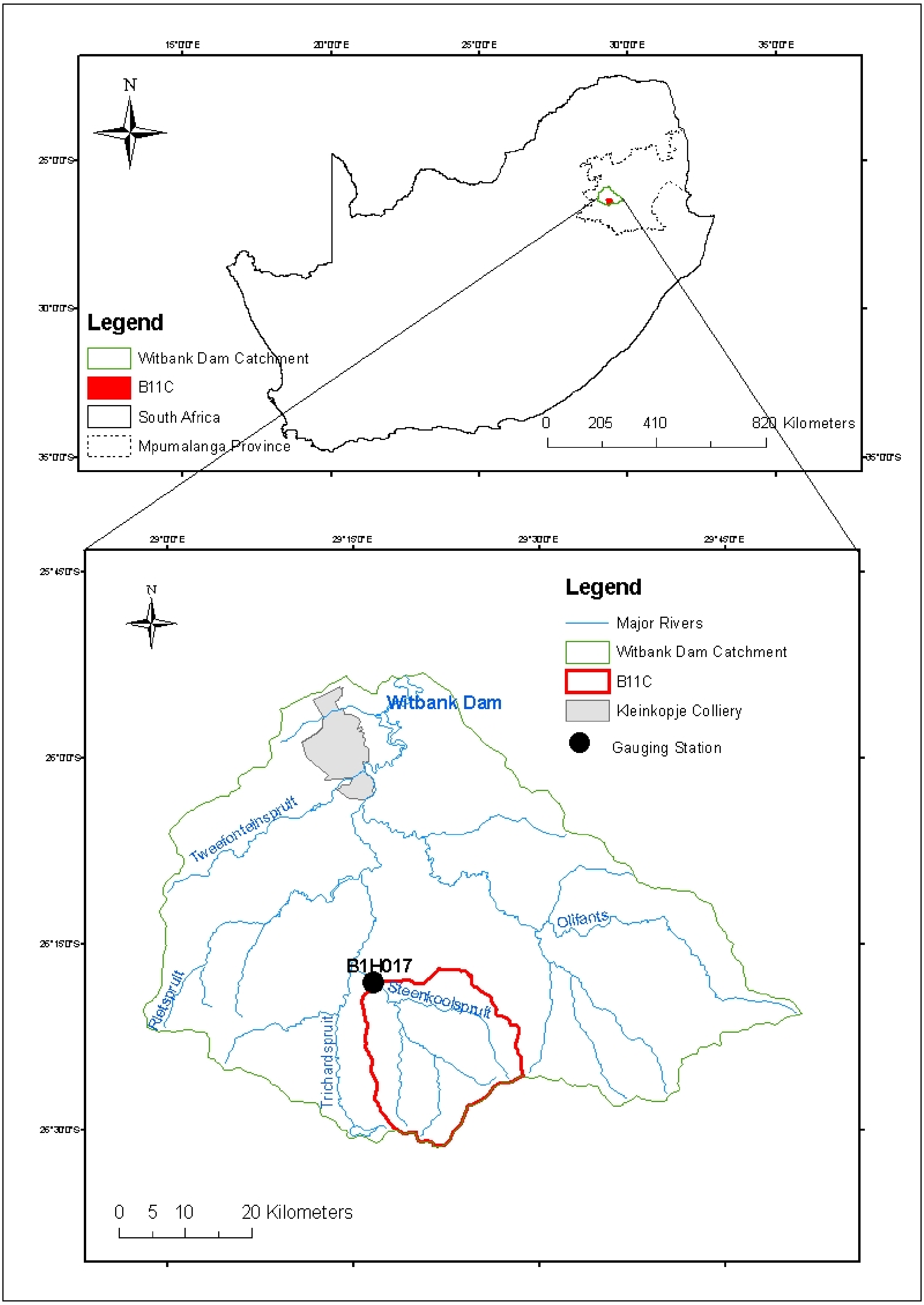

Figure 1: The study area on the Steenkoolspruit.

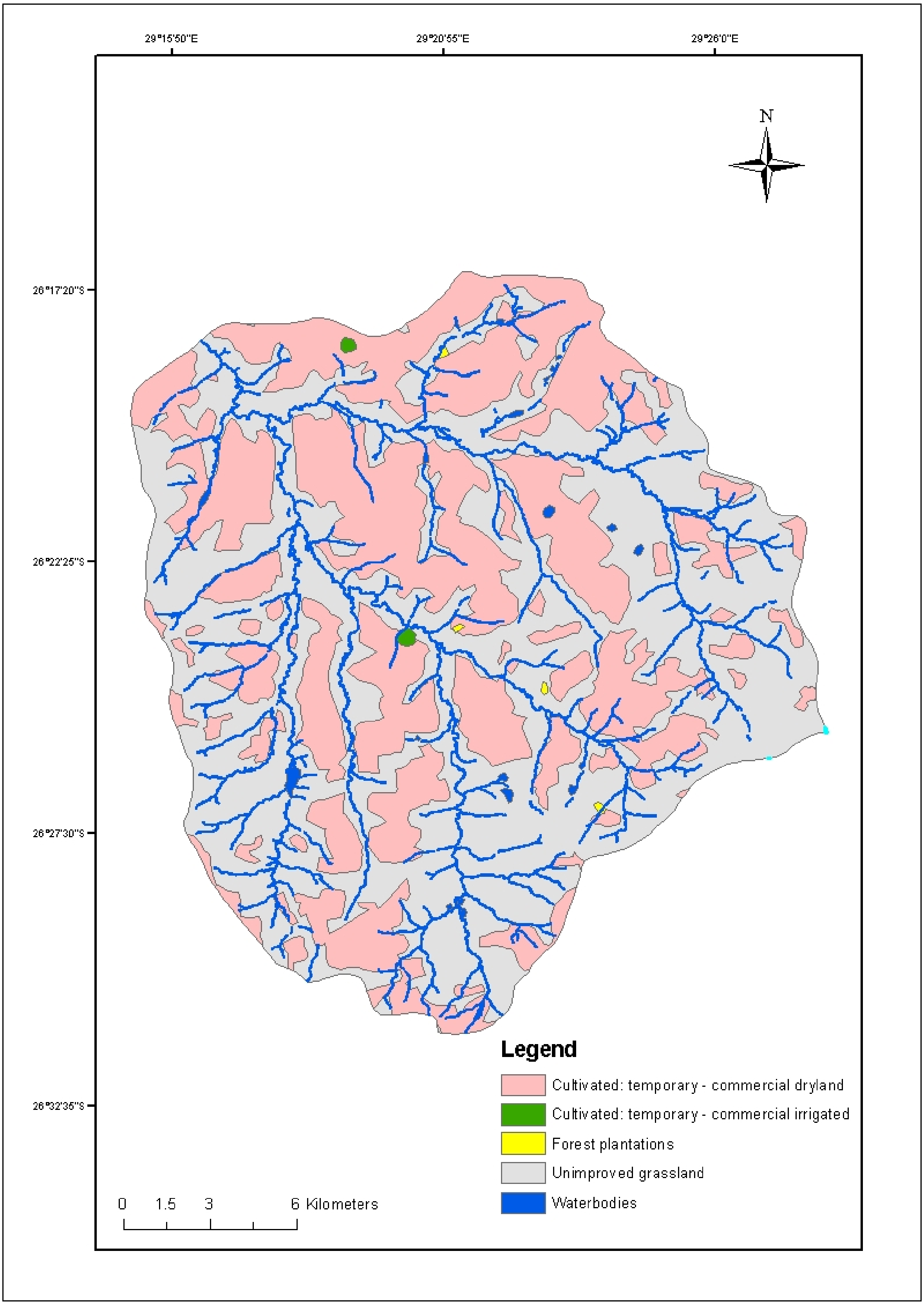

Figure 2: Land use types in the study area with the stream width assumed to include a 30 m strip on each side.

1.4 Hydrology

B11C forms part of the headwaters of the Witbank Dam catchment (Figure1). It is a summer rainfall area with a mean annual rainfall of between 600 -700 mm and a mean annual evaporation of between 1500 and 1600 mm (Midgley, 1994). The mean annual runoff of the catchment is 37 mm (DWAF, 1993). The salt concentration of the runoff from the catchment varies indirectly with the volume of runoff as a result of a dilution effect. From the observed weekly water chemistry data covering a period of 13 years (1990 – 2003), the weekly total dissolved solids (derived from the weekly electrical conductivity measurements) of the observed runoff from the catchment varies between an extreme low 89 mg/l during summer and high of 722 mg/l during the winter. However, the TDS concentrations generally vary between 100 - 300 mg/l in summer and between 400 – 500 mg/l in winter. The TDS variation with the runoff volume is shown in the Figure 3.

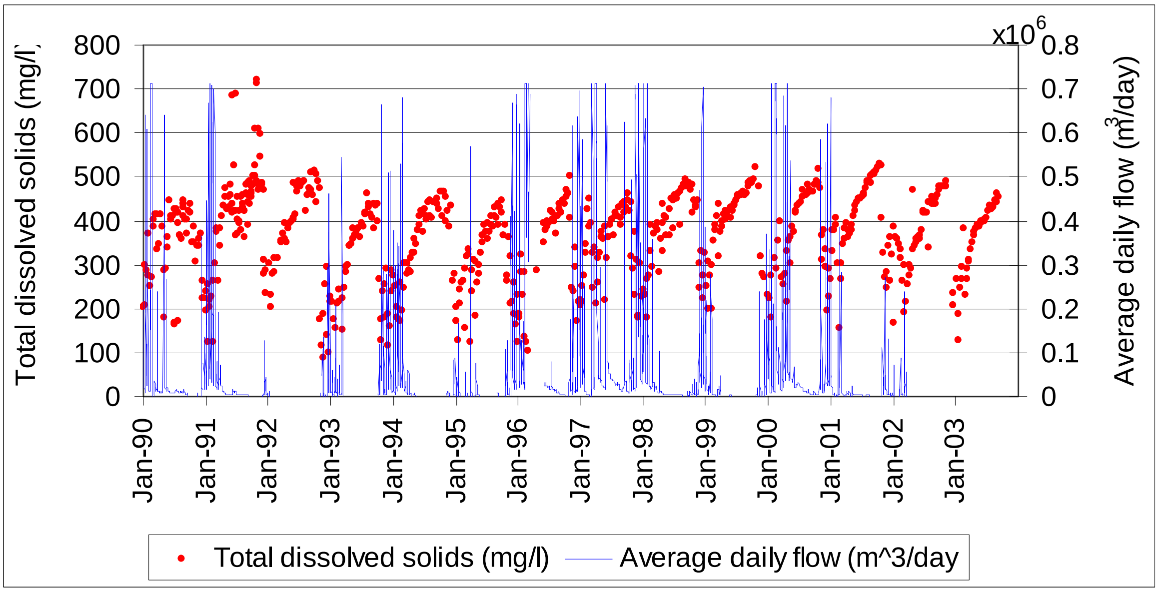

Figure 3: Observed average daily flow and weekly total dissolved solids in Steenkoolspruit.

1.5 Objectives of Study

The objective of this study is to carry out a desktop assessment of

- the runoff volume and salt load output from B11C under a condition representative of the current land use types in the catchment, and of
- the impact that the exploitation of coal in the catchment through opencast mining and the subsequent rehabilitation of the disturbed land (a rehab) will have on the runoff and groundwater in the catchment.

2. Methodology

2.1 General

Two scenarios are simulated in order to achieve the objectives. The first is the current land use (baseline) in the catchment as described by Johnson (1996). The second scenario comprises the current main land use, with a rehabilitated coal mine land (rehab) covering 50% of the entire catchment. The daily rainfall and temperature data used in the scenarios are for Bethal, on the southeastern edge of the catchment. The daily rainfall and temperature data were obtained from the South African Weather service. The rainfall quality for the catchment is assumed to have a TDS of 26 mg/l as determined by the chemical analyses of rain water in the Johannesburg city and environ by the Johannesburg City Council (Blight, 1992). Considering that air pollutants disperse quickly on the Transvaal Highveld (Blight, 1992), this value may not be significantly different from that of the study area. A 16-year record is employed for the simulation using the *ACRU2000* model and its salinity module, *ACRUSalinity*. The *ACRU2000* model and *ACRUSalinity* module have been modified to enable their application in a coal-mining environment. The relevant modifications and calibrations are summarised in the section that follows.

2.2 Scenario Description

Scenario 1

The simulated runoff from the catchment and its salt load are calibrated using the observed average daily flow and the derived total dissolved solids (TDS) of Steenkoolspruit at gauge B1H017 (Figure 1). The derived TDS concentration for a particular day is multiplied by the average daily flow for that day to obtain the average salt load. The observed average daily flow and the derived TDS data (reported on a weekly basis), between 1990 and 2003 are used. The initial soil water and groundwater salinity used for the catchment is 83 mg/l, this being the average groundwater salinity in boreholes located in the Upper Olifants basin as reported by Hodgson and Krantz (1998). Within the catchment is an irrigated area of 42 ha, which is assumed to be planted to maize, just as the dryland agricultural areas of the region. Irrigation water is assumed to be supplied directly from a stream within the catchment, with the streamflow reduced by the amount of the daily irrigation water application. Irrigation water is applied to refill the soil profile to the drained upper limit.

Scenario 2

In the second scenario, half of the catchment area, i.e. 175 km^2, is assumed to be rehabilitated coal mine land. In order to simulate the catchment with rehab as one of the land use types, the area covered by the unimproved grassland was reduced by the area of mine rehab area. The rehab is assumed to have “veld in fair condition”. The *ACRU2000* model, modified to simulate mine land hydrological processes, was validated against measured discharges and salinities in the Kleinkopje Colliery catchment by Idowu, 2007. In order to justify using the model in the B11C rehab scenario, parameter sets and validations of the Kleinkopje Colliery simulations are summarized in this study.

The soil water retention characteristics of the rehab area are assumed typical of the rehab areas in Kleinkopje colliery, derived from a monitored centre pivot on rehabilitated mined land (Idowu, 2007). The location of Kleinkopje colliery in relation to the study area is shown in Figure 1. In the monitored centre pivot (Tweefontein pivot), the soil water content and salinity, runoff quantity and quality, as well as the rainfall and irrigation water supply were observed in order to assess the water and salt balances. A summary of the verification studies in Tweefontein pivot are provided in Section 2.3. Water quality deterioration occurs in spoils because of prolonged oxidation of sulphide-bearing minerals (Hodgson and Krantz, 1998). The salt uptake rate constant in *ACRUSalinity* is used to account for the increased salt concentration in the soil water and groundwater due to salt generation from chemical weathering processes and subsequent release of solutes into solution. The calibrated salt uptake rate constant obtained for the coal discard dump in Kleinkopje Colliery (1.2×10^{-3}) is applied to the groundwater in the rehab, while in the unmined condition, the value obtained for the unmined parts of Kleinkopje Colliery (1.0×10^{-5}) is applied.

Groundwater Availability

Baseflow generation in the catchment is based on the "coefficient of baseflow response" (Smithers *et al*., 1995). The coefficient represents the fraction of the water from the groundwater store released as baseflow. The typical value of the coefficient would range from 0.01 to 0.03 (Smithers *et al*., 1995). A value of 0.02 is assumed for the baseline condition in the catchment i.e. prior to opencast mining. In the rehab, the calibrated coefficient of baseflow response (0.0002), obtained for the monitored rehab area in a centre pivot in the Kleinkopje Colliery, is used. The lower value of the coefficient in the rehab is a result of the higher permeability in the spoil (than the unmined sediments) underlying the rehabilitated area causing percolating water to move more quickly through the spoil and accumulate at the bottom of the spoil, in comparison to the pre-mining condition. Opencast mining leads to dewatering of aquifers and the lowering of the water table, which may form a depression cone not usually extending laterally more than 40 m in the Upper Olifants (Hodgson and Krantz, 1998). In the rehab void, water level recovery may occur, with the water level rising to the lowest rehabilitated surface elevation and then decanting, thereby establishing a new equilibrium. Prior to the re-establishment of the new equilibrium however, percolating water will gradually accumulate in depressions at the bottom of the rehab area, with the water table gradually rising until the decanting level is reached. Consequently, contribution of baseflow to runoff would be insignificant during the period of groundwater rebound, but may well continue to contribute to runoff after the establishment of the new equilibrium when groundwater will flow in the direction of the hydraulic gradient. However, this will not detract from the water available for pumping from the groundwater store, as this is dependent in the average recharge rate.

2.3 Summary of Relevant Modifications to and Application of *ACRU2000* and *ACRUSalinity*

2.3.1 Modifications to *ACRU*

ACRU2000 and *ACRUSalinity* have been modified to enable their application to a coal-mining environment. A summary of the modifications is presented below, followed by demonstration of calibrations relevant to this study.

- The addition of a soil surface layer to model the process of overland flow taking into solution, salts accumulated near the surface due to evaporation;
- The addition of a new hydrologic component, an underground reservoir, to represent the occurrence of water in underground mined-out areas. Leakages into and seepages from the reservoir are taken into consideration. Parameters driving fluxes from these sources are based on knowledge of these processes;
- The possibility of multiple transfer of water of different salinities from at least six different sources into a surface reservoir;
- The addition of a special kind of surface reservoir, a mine-pit reservoir, to represent water that accumulates in opencast pits (Figure . Relevant fluxes of rainfall and seepage are taken into consideration;
- Inclusion of controlled releases from reservoirs in coal mines, which can be permitted during periods of high flow (Coleman *et al.*, 2003) in the reservoir water and salt budgeting; and
- In the surface reservoir yield analysis, seepage has been modified to be dependent on the volume of water in storage and reflect the dynamics with which the surface reservoir interacts with groundwater.

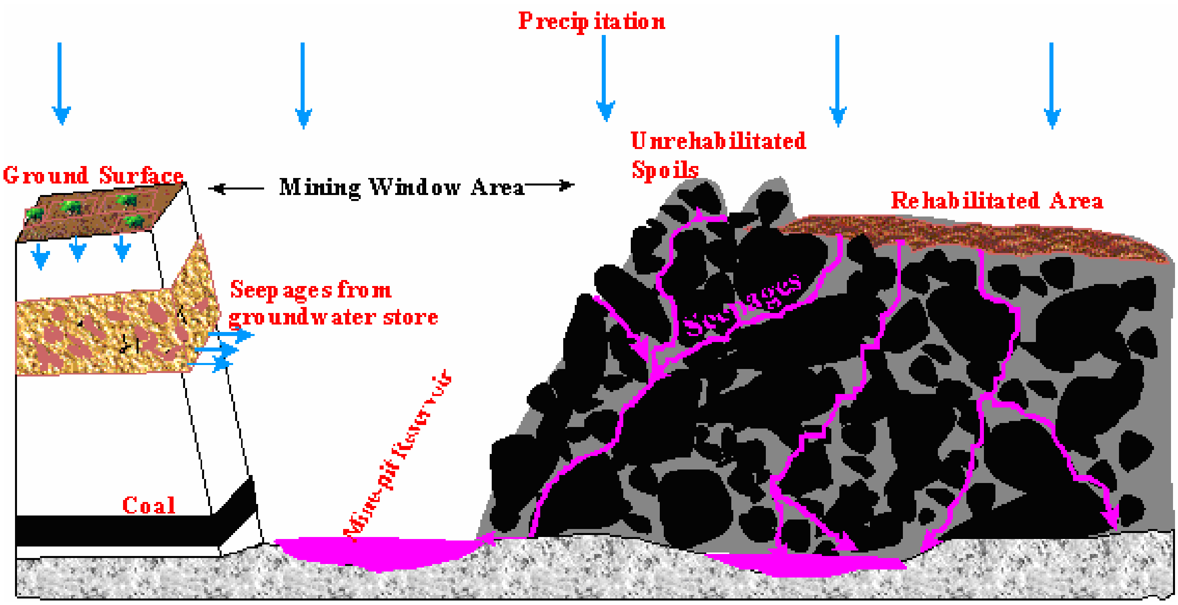

Figure 4. Schematic of open pit coal mine water sources.

2.3.2 Verification of Routines and Parameter Sets at Kleinkopje Colliery

The modified *ACRU2000* model and *ACRUSalinity* module have been applied to a centre pivot on rehabilitated land and to a catchment to demonstrate their applicability in a coal mining environment (Idowu, 2007).

2.3.2.1 Tweefontein Pivot

The Tweefontein pivot is on rehabilitated mine land. The results of the verification study, using the volume and salinity of the runoff from the centre pivot, are presented in Figures 4 and 5. The results show that the runoff volume and salinity are adequately simulated.

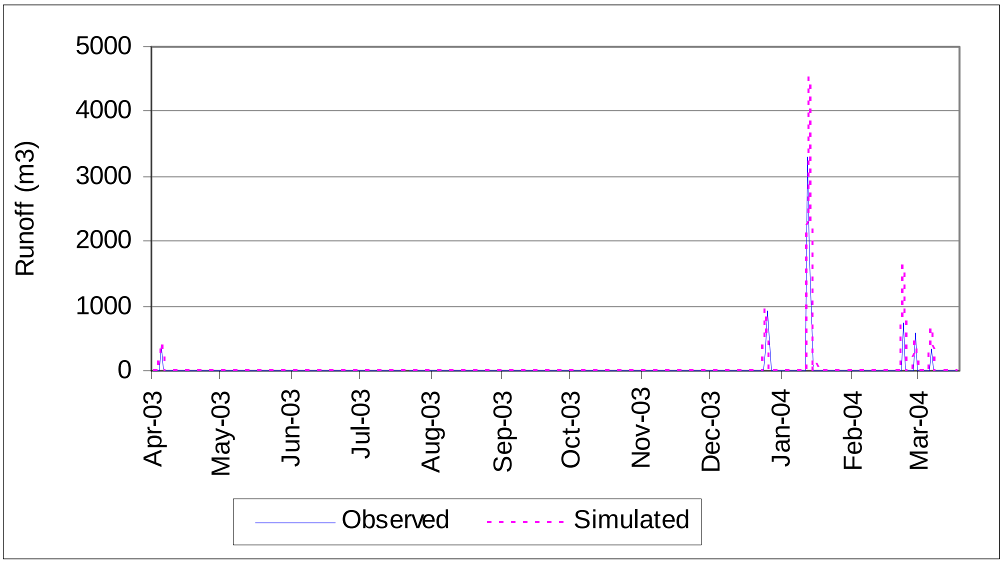

Figure 5a: Observed and simulated daily runoff from pivot Tweefontein.

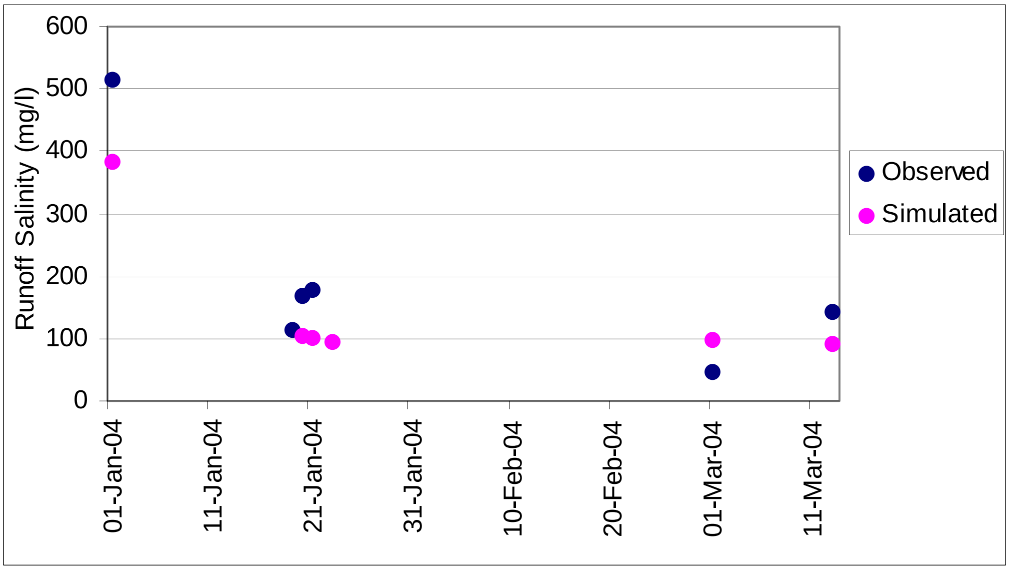

Figure 5b: Daily salinities of sampled and simulated runoff from pivot Tweefontein.

2.3.2.2 Tweefontein Catchment

The Tweefontein Pan catchment is unmined but lies almost entirely within the Kleinkopje Colliery. Successful simulations of the catchment proved that the revised model yields realistic results in this environment. The Tweefontein Pan catchment has the following characteristics:

- An area of 4.7 km^2
- An internally draining surface reservoir (Tweefontein Pan) containing mine wastewater and with a capacity and surface area (at full capacity) of 4 000 Ml and 1. 5 km^2 respectively,
- A centre pivot of 30 ha (pivot Fourth) irrigating agricultural crops with water from the Tweefontein Pan,
- The non-irrigated area in the catchment has grasses and the vegetation is assumed to “Veld in poor conditions” and
- An underground reservoir with estimated capacity of 2 x 10^9 Ml.

Three illustrative scenarios are presented in the following section, viz,

Scenario 1: Baseline simulation against recorded data representing the current condition in the catchment,

Scenario 2: Assumed widespread irrigation on unmined soils in the catchment and

Scenario 3: Assumed widespread irrigation on rehabilitated mine land in the catchment .

The following were taken into consideration in simulating the catchment:

- volume of water pumped in and out of the Tweefontein Pan,
- return flow from the irrigated area, as well as the
- leakages into the underground reservoir

Scenario 1

The volume and salinity of water in storage in the Tweefontein Pan over a period of 5 years (1999 – 2004), as well as the salinity of the soil water in the irrigated pivot are used for verification. The results of the verification are presented in Figures 6 - 7. With correlation coefficients of 0.96 and 0.76 respectively, the volume and salinity of water in the Tweefontein Pan are simulated satisfactorily. Limited observed data was available on the soil water quality in pivot Fourth due to difficulties encountered in extracting soil water with the ceramic soil water samplers, particularly under dry conditions (Figure 8). The observed and simulated salinity in the underground reservoir is shown in Figure 9.

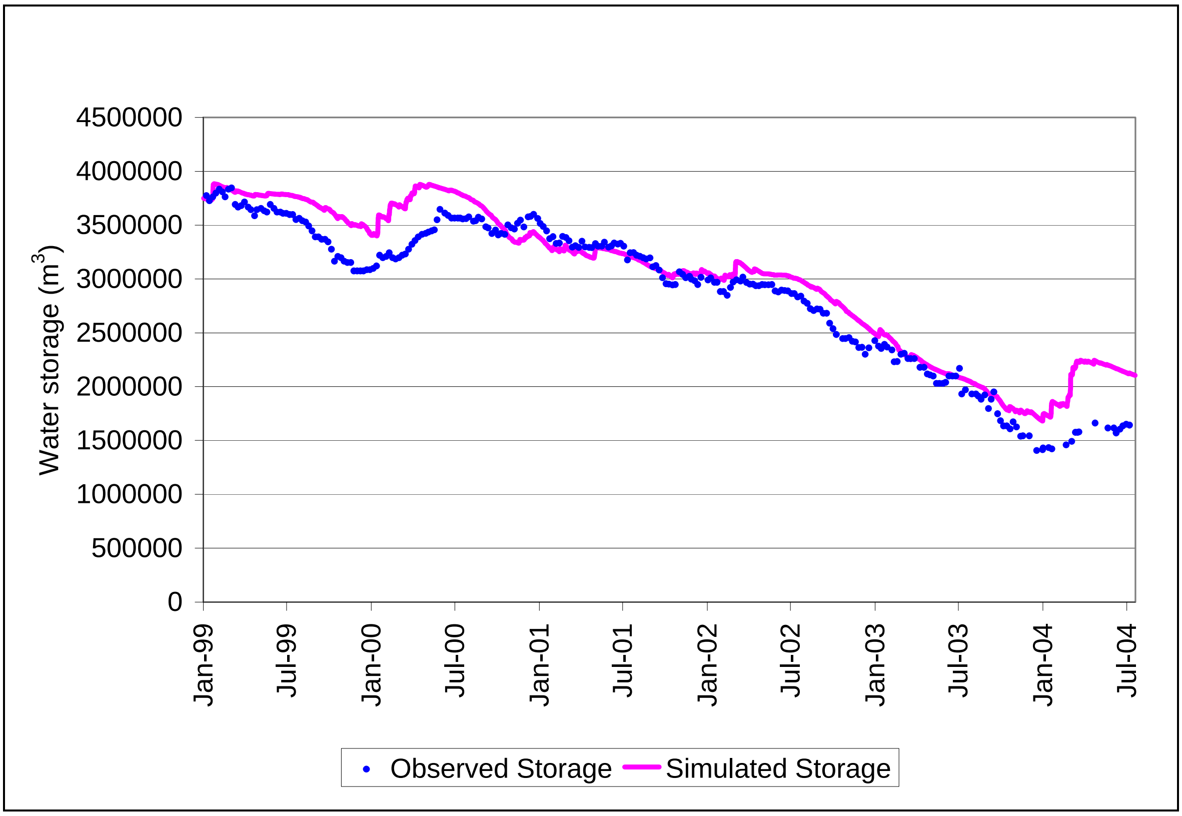

Figure 6: Simulated and observed daily water storage in the Tweefontein Pan.

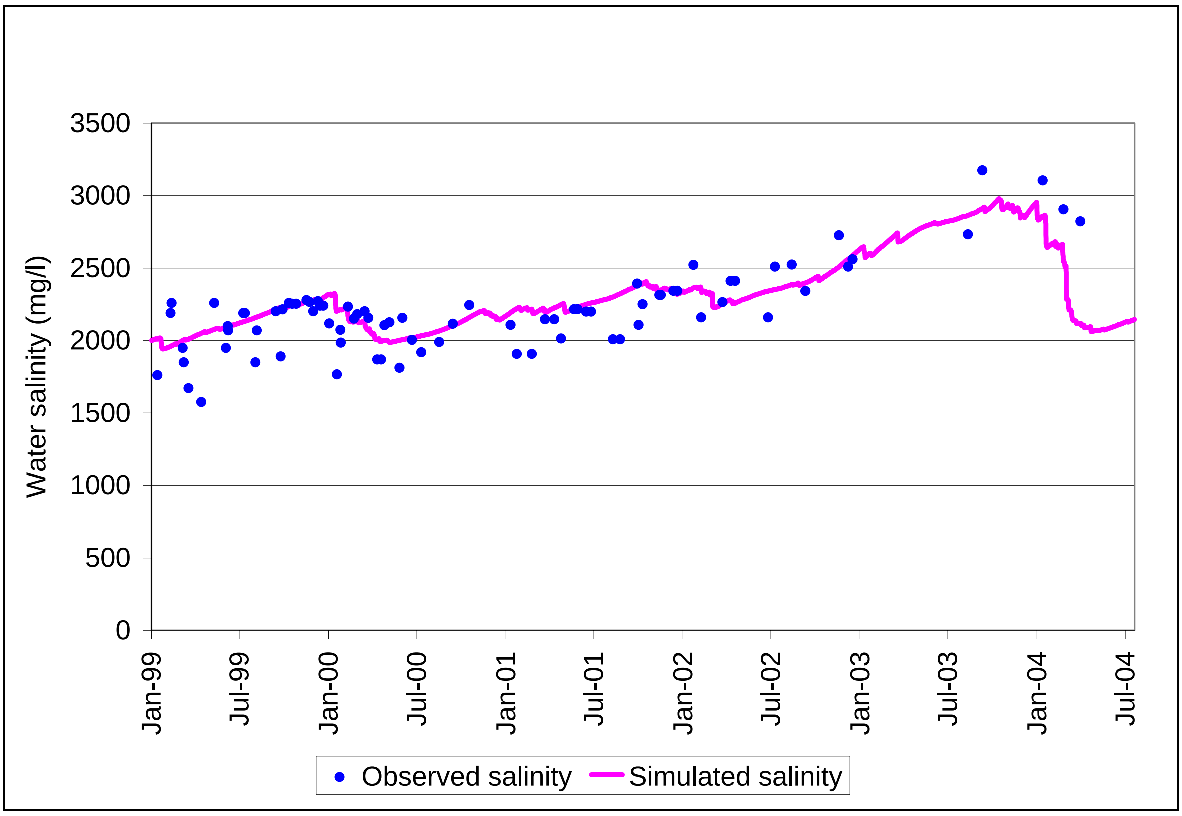

Figure 7: Observed and simulated quality of water in storage in the Tweefontein Pan.

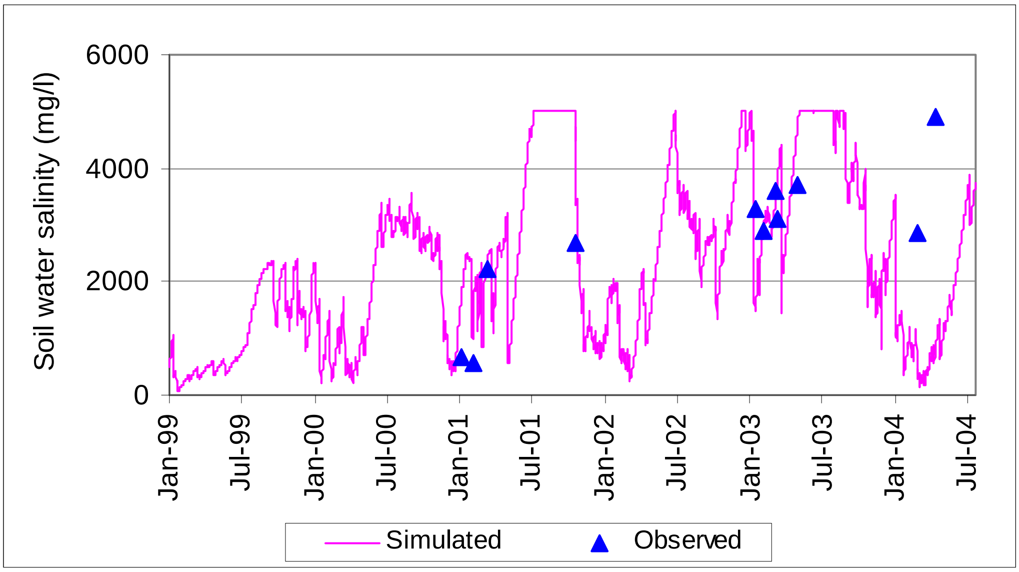

Figure 8: Observed and simulated daily salinities of soil water at 100 cm in the irrigated area of pivot Fourth.

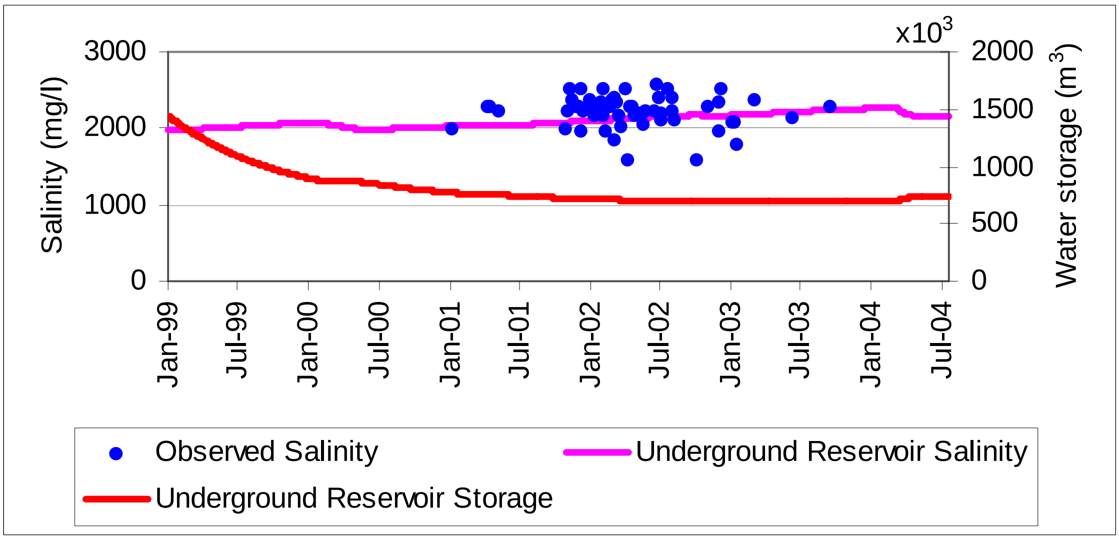

Figure 9: Observed salinity and simulated daily water storage and salinity in the underground reservoir.

Scenario 2

The impact of widespread irrigation, using the mine water in the Tweefontein Pan, is assessed by increasing the irrigated area in the catchment. The irrigated area is assumed to be similar to pivot Fourth located in the catchment. The assessment shows that in addition to the irrigation of a rehabilitated area of 20 ha at pivot Tweefontein (located outside the catchment) with the water from Tweefontein Pan, a virgin area of 160 ha, representing an additional 8 centre pivots of 20 ha each, could still be sustained with irrigation water from Tweefontein Pan over the simulation period. The impact of widespread irrigation in the catchment is compared with the baseline scenario in Figures 10 and 11. What is demonstrated with the results is that, in making decisions on widespread irrigation with mine water, it is very important that sustainability, in terms of the availability of adequate mine water for widespread application, be assessed.

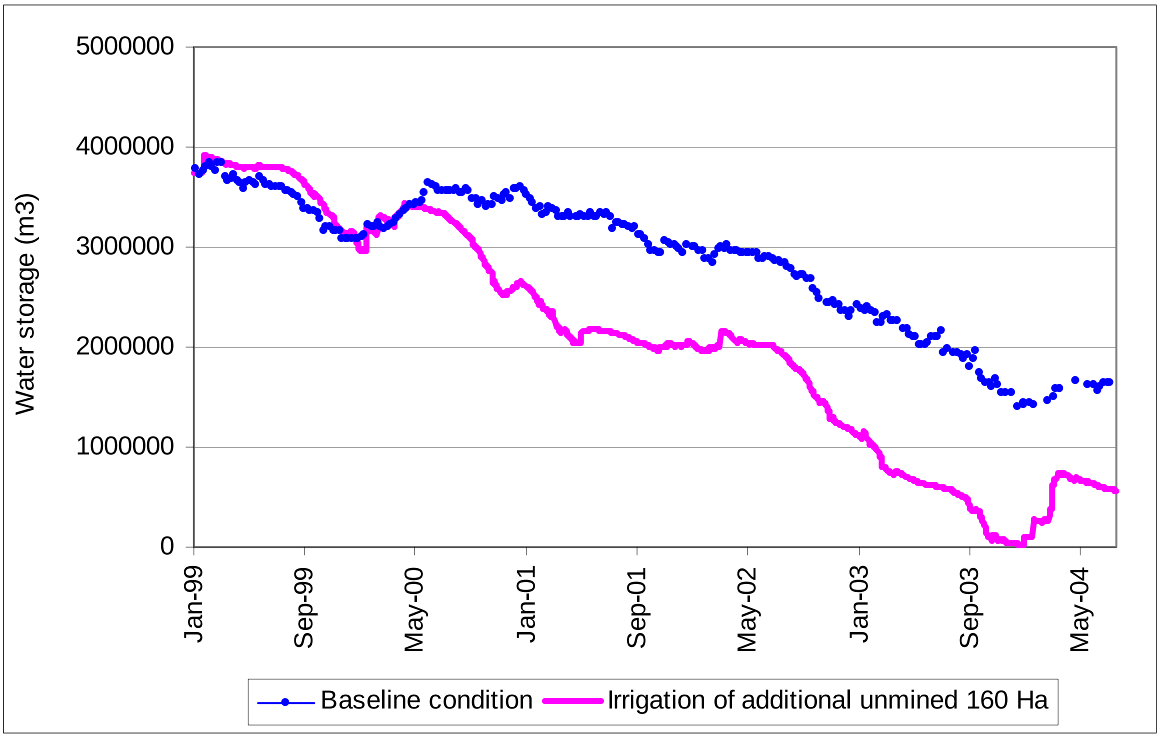

Figure 10: Effect of widespread irrigation of 160 ha in the Tweefontein Pan catchment on the water storage in the Tweefontein Pan.

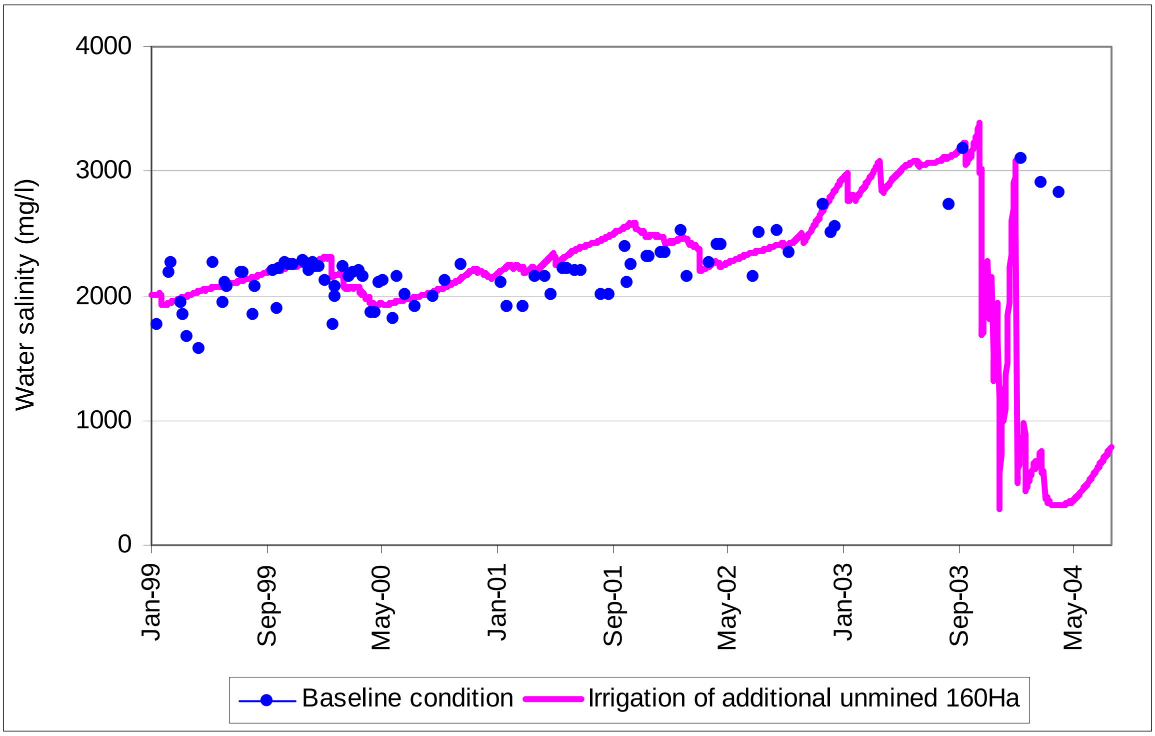

Figure 11: Effect of widespread irrigation of 160 ha in the Tweefontein Pan catchment on the water quality in the Tweefontein Pan.

Scenario 3

In a rehab void, prior to the re-establishment of the new ground water equilibrium as explained in Section 2.1, percolating water will gradually accumulate in depressions at the bottom of the rehab area, with the water table gradually rising until the decanting level is reached. Consequently, contribution of baseflow to runoff may be insignificant, unlike after the establishment of the new equilibrium when groundwater will flow in the direction of the hydraulic gradient and make more contribution to the runoff. Taking these into consideration, during the simulation of rehabilitated areas representing post-water table re-establishment, the default value of the baseflow response fraction is taken as 0.02. Prior to the re-establishment of the water table however, the baseflow response parameter is set at 0.0002, which is the calibrated value used for the centre pivot located on an irrigated rehabilitated mine land in Kleinkopje Colliery. If Tweefontein Pan catchment is mined-out, rehabilitated and the water table has not been re-established, only a maximum of 120 ha can be adequately irrigated with mine water from the pan, indicating that the area that can be sustained by irrigation with water from the Tweefontein Pan will be less than if the catchment were unmined.

A comparison of the impact of this scenario on the volume and salinity of water in Tweefontein Pan with the two other scenarios of irrigating an unmined area and a rehabilitated area, post water table re-establishment, are presented in Figures 12 and 13. Irrigating a rehabilitated area of 120 ha in Tweefontein Pan catchment (either pre- or post- water table re-establishment) will deplete the water in the pan more rapidly than irrigating a virgin area of 120 ha (Figure 10). This would be because, the runoff (and runoff salt load) from the rehabilitated area would be lower and the volume of water and salt that would go into groundwater storage would be more when the irrigated area is rehabilitated than when it is unmined. Hence, less water reaches the Tweefontein Pan in the rehab scenario than in the baseline case.

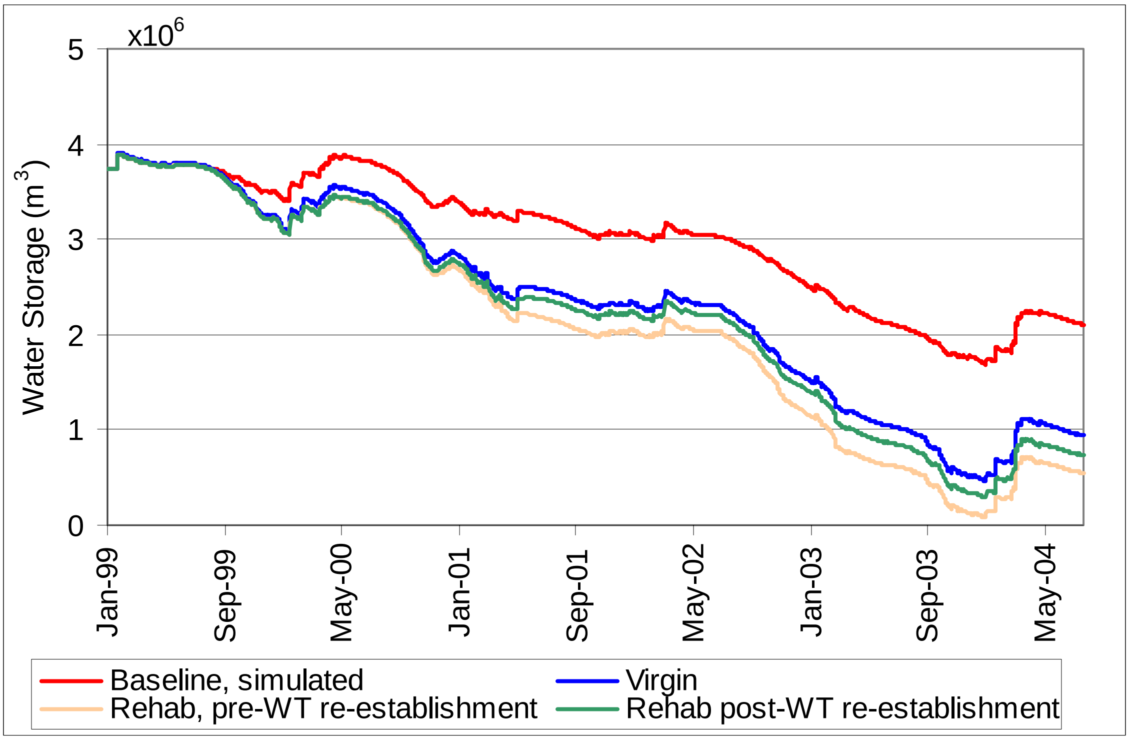

Figure 12: Comparison of the effect of widespread irrigation on the Tweefontein Pan water storage for irrigation on unmined and rehabilitated land.

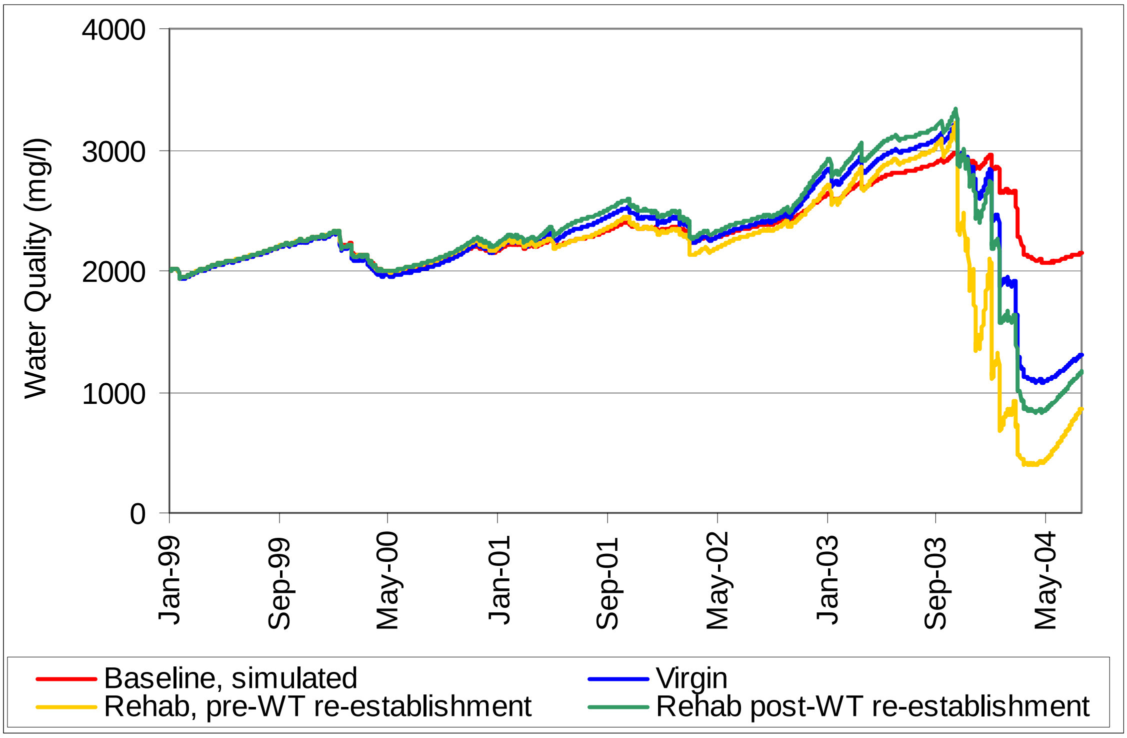

Figure 13: Comparison of the effect of widespread irrigation on the Tweefontein Pan water quality for irrigation on unmined or rehabilitated land.

3. Results of Scenario Simulations for B11C Quaternary

A comparison of the observed average daily runoff and the simulated total daily runoff at gauge B1H017 is presented in Figure 14. The over topping of the rating limit during high flows (as recorded by DWAF) meant that such flows could not be accurately recorded. The calculated daily salt loads are compared with the simulated daily salt load in Figure 15. The simulations are realistic, despite the extreme values exceeding the gauge capacity.

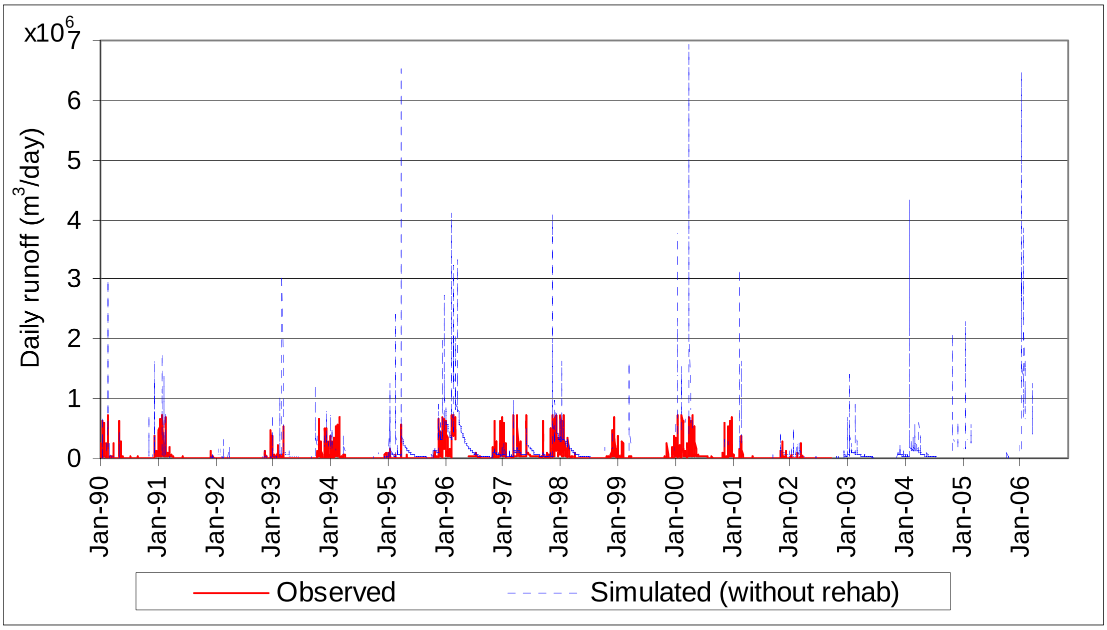

Figure 14: The observed and simulated daily runoff of B11C.

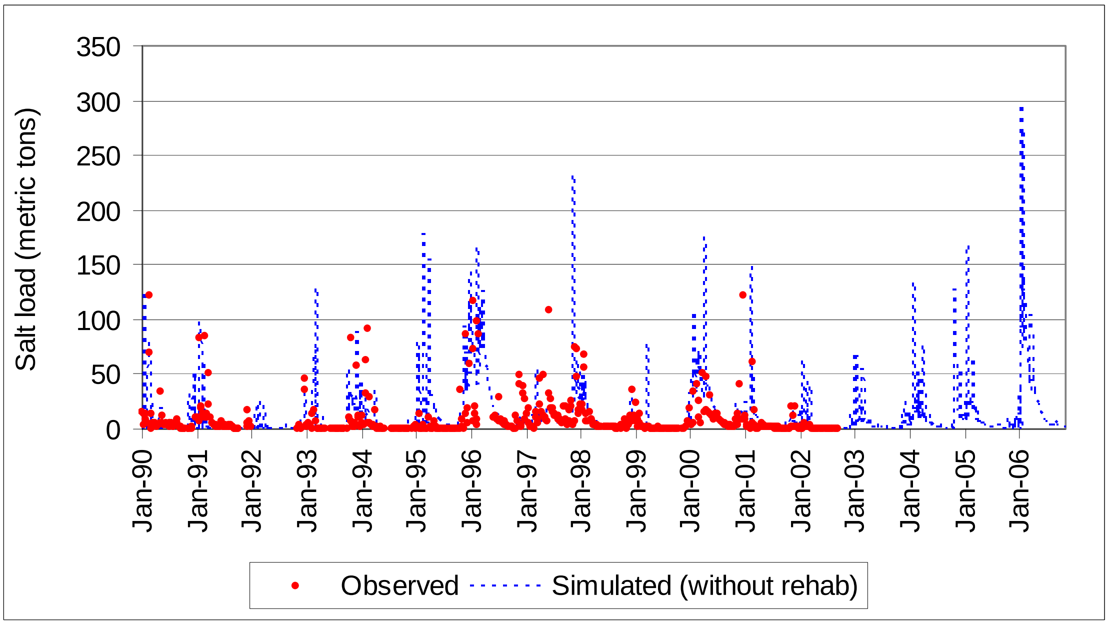

Figure 15: The observed and simulated daily salt load from B11C.

In the baseline condition, the simulated mean annual runoff volume and salt load from the catchment are 40.8 x 10^6 m^3 and 5758 metric tons respectively (Table 2).

Table 2: Results of simulations in catchment B11C

Runoff	**Catchment under baseline condition**	**Catchment with 175 km^2 rehab**	**Difference %**
Mean annual runoff (m^3)	40.8 x 10^6	33.5 x 10^6	-18
Mean annual salt load (metric tons)	5758	32612	466
Average daily runoff salinity (mg/l)	177	1739	882
Groundwater and Runoff	**Unimproved grassland**	**Rehab**	**Difference %**
Average annual percolation (mm)	31	98	216
Percolation as % of rainfall	4	13.3	232
Average groundwater salinity (mg/l)	145	2918	1912
Mean annual runoff (mm)	114	72	-37
Average runoff salinity (mg/l)	152	2794	1738

A decrease in the mean annual runoff volume of 18% from the catchment was obtained with the existence of a rehab of 175 km^2, which is half the area of the catchment (Figure 16, Table 2), whereas a significant increase of 466% was obtained in the mean annual runoff salt load. The daily average runoff salinity increased from 177 mg/l to 1 739 mg/l. A comparison of the daily runoff and its salinity, with the catchment simulated under baseline conditions and with a rehab of 175 km^2, are presented in Figures 16 and 17 respectively.

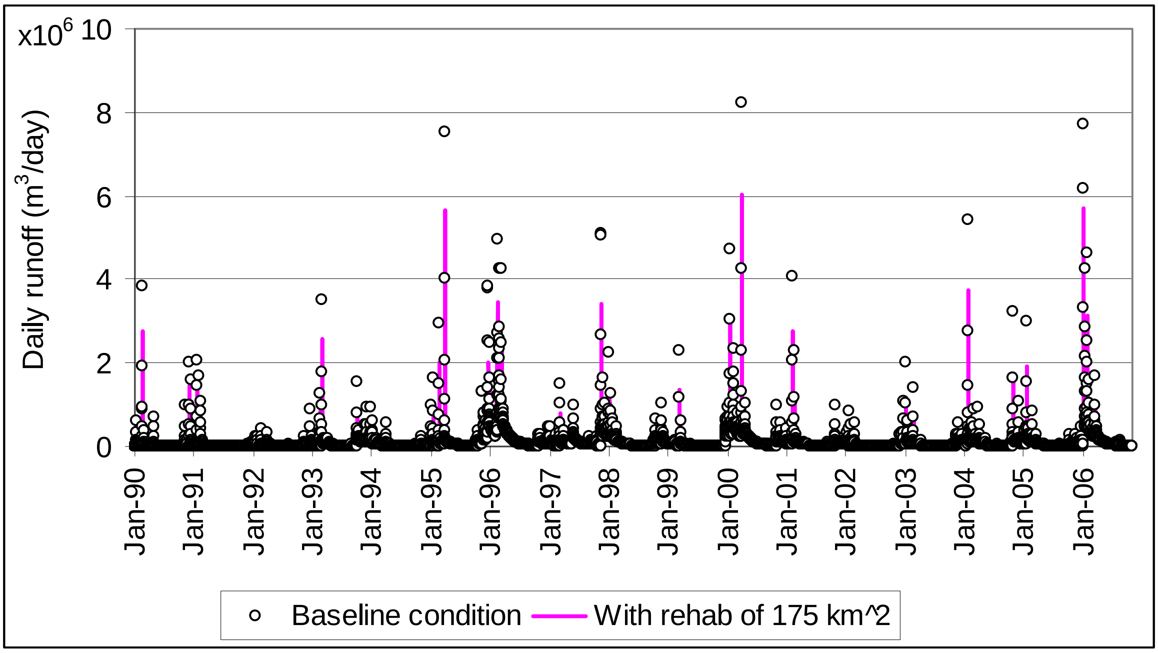

Figure 16: Comparison of the simulated daily runoff volume under baseline conditions and with a rehab of 175 km^2.

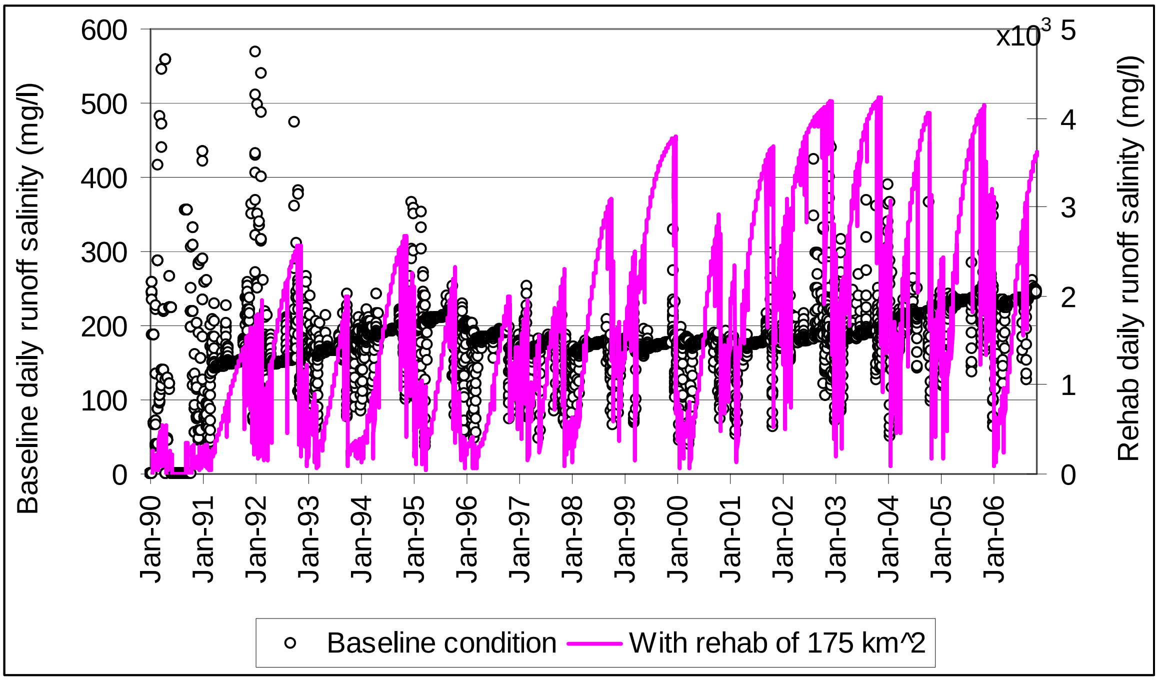

Figure 17: Comparison of the simulated daily runoff salt load under baseline condition and with a rehab of 175 km^2.

Significant differences were obtained in the characteristics of the groundwater in the baseline condition and in the corresponding rehab area covered by the unimproved grassland. An increase from 31 mm to 98 mm in the average annual amount of percolation to groundwater will occur in the rehab over that in the original unimproved grassland (Table 2). The average annual amount of water that can be utilised for pumping in a sustainable manner in the rehab is therefore 98 mm, amounting to $17.2x10^6$ m^3 per annum from the 175 km^2 rehab. However, the average annual volume of groundwater in storage resulting from recharge through the spoil is 512 mm. It should be noted that this amount represents the accumulated volume of water that goes into storage from percolation and contributes to the water level recovery in the rehab. If a new equilibrium has been re-established as a result of the water level rising to a decanting level, the amount of groundwater in storage may be less. However recharge will not change and pumping capacities would be sustainable. Therefore, careful monitoring of groundwater is necessary to ascertain the nature of water level recovery in a rehabilitated mine land.

In the simulated pre-mining condition, the average annual volume of groundwater store is much less (4.6 mm) than in the rehab scenario. The average groundwater salinity will increase to 2 918 mg/l in the rehab from 145 mg/l in the pre-mining condition in the unimproved grassland, while the runoff from the rehab will be less by 37% from the runoff from the unimproved grassland (Table 2, Figure 18). The mean annual runoff from the rehab and baseline are 68 mm and 100 mm respectively (Table 2). An increase in runoff salinity manifests in the rehab compared to the pre-mining condition. The decrease in the total runoff from the whole catchment when it contains a rehab area of 175 km^2 compared to the baseline condition can be attributed to the decrease in the runoff from the rehabilitated area, caused by the increase in infiltration and percolation into the spoil.

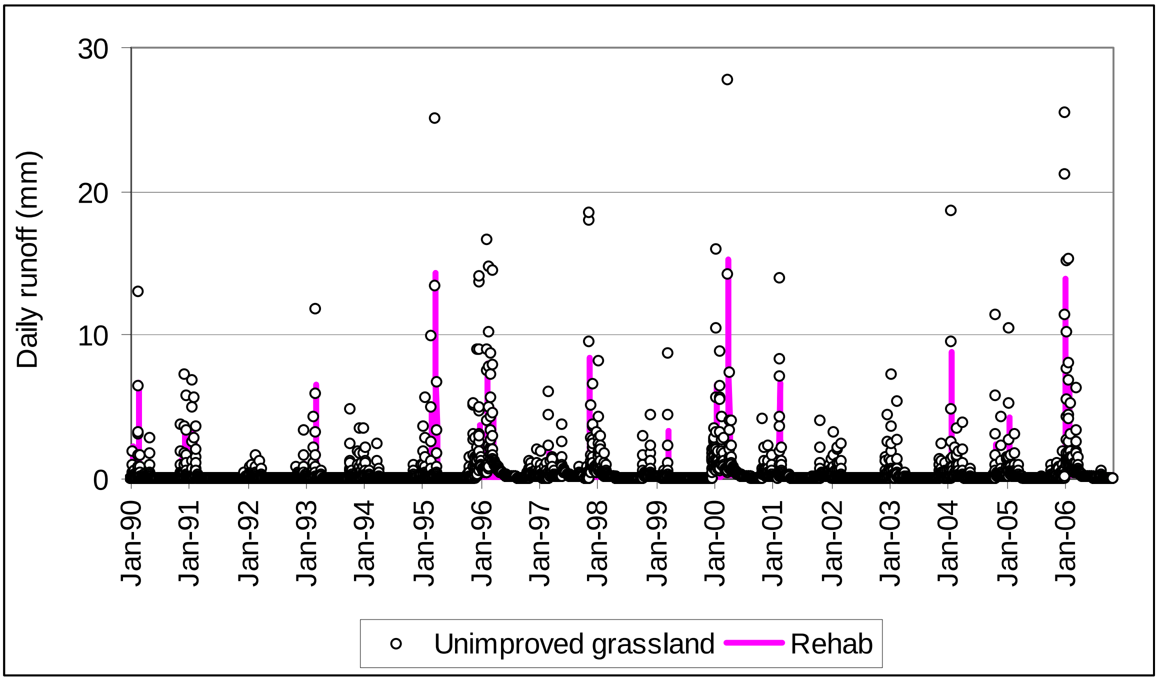

Figure 18: Comparison of runoff from the unimproved grassland and rehab B11C catchment scenarios.

\

4. Conclusions

With the mining-out and rehabilitation of half of B11C, a decrease in the total runoff volume from the catchment can be expected. However, a significant increase in the salt load and the salinity of the runoff will occur. The runoff from the rehab area can be expected to decrease compared to that from the same area under pre-mining condition, while the quality of groundwater can be expected to deteriorate in the rehab compared to the pre-mining condition. In the rehab, an average annual percolation of 98 mm/yr can be expected, with the same amount of water (17.2 x 10^6 m^3) available for pumping in a sustainable manner, thereby making the mean annual catchment yield for water supply a total of 50.6 x 10^6 m^3.

The average total storage in the rehab over the simulation period is 512 mm, which would be adequate for continuous groundwater extraction. However, because of the varied nature of spoils and methods of their rehabilitation, a careful monitoring of the groundwater in the rehab is recommended to determine the nature of water level recovery and the effects of possible high permeability in the spoil affecting yield.

5. References

Blight, J. J. 1992. The influence of landfill covers on the generation of leachate. Unpubl. M.Sc. Dissertation, Univ. of Witwatersrand, RSA.

Coleman, T. J., Rossouw, J. N. and Bath, A. 2003. A decision support system for the controlled release of saline mine water during flood conditions in the Witbank Dam Catchment. Water Research Commission Report No 900/1/03, Pretoria, South Africa.

DWAF. 1993. Witbank Dam Catchment Quality Management Plan. Department of Water Affairs and Forestry. Pretoria.

Hodgson, F. D. I. and Krantz, R. M. 1998. Groundwater quality deterioration in the Olifants River catchment above the Loskop Dam with specialised investigations in the Witbank Dam sub-catchment. Water Research Commission Report No 291/1/98. Pretoria.

Idowu, O. A. 2007. Impact of irrigation with gypsiferous mine water on water resources at and around Kleinkopje Colliery. Unpubl. PhD Thesis, Univ. of KwaZulu-Natal, Pietermaritzburg

Smithers, J. C., Schulze, R. E., Lecler, N. L., Kienzle, S. W., Lorentz, S. A and Kunz, R. P. 1995. User guidelines for setting up information. *In*: Smithers, J. C. and Schulze, R. E. *ACRU Agrohydrological Modelling System: User Manual Version 3.00.* Water Research Commission, Pretoria, RSA. Report TT70/95.

Thompson, M. 1996. A standard land-cover classification scheme for remote-sensing applications in South Africa. *South African Journal of Science.* 92: 34-42.

APPENDIX E
CAPACITY BUILDING AND TECHNOLOGY TRANSFER REPORT

E1. CAPACITY BUILDING

The following table summarises the individuals and institution involved in capacity building activities.

Individual	Institution	Activity
Phakade Goba*	SBEEH	Manager of the soils and water laboratory for SBEEH Training in porous media hydraulic property determination. Managing equipment for field trips. Safety officer training.
Brenton Mabuza* Mfundo Jili* Patrick Phaladi* Matt Langton	BEEH SBEEH SBEEH SBEEH	Training in hydrometry, data analysis and soil physics laboratory and field measurements. (Completed undergraduate studies during the course of the project)
Gary Morgan*	SBEEH	MSc candidate (AECI slimes dam vegetative cap study. Completed MSc during the project)
Kevin Bursey	SBEEH	MSc candidate (Weatherley hillslope and catchment processes. Completed MSc during the course of the project)
Olufemi Idowu	SBEEH	PhD candidate (Upper Olifants: Surface-groundwater interactions and salinity modelling. Completed PhD during the course of the project)
John Ngeleka	SBEEH	(BSC geology, DRC Congo) Field technical assistant
Dumisani Gqiba*	Council for Geosciences	MSc candidate: Training in hydrometry and natural isotope sampling and anlysis in collaboration with the Schonland research Institute (Prof Balt Verhagen)
Washington Tunha	DWAF	PhD candidate: (Letaba or Steelpoort: Surface-groundwater interactions)
Stefan Uhlenbrook	University of Freiburg	Advising SBEEH on tracer studies
Albert van Zyl	ISCW	Training in hydrometry, hydrology and sediment yield modelling
Hdyrology 300 class*	SBEEH	Training in the use of field monitoring and measurement instrumentation

* from previously disadvantaged backgrounds (South Africa)

E2. TECHNOLOGY TRANSFER

The following papers were presented and journal articles submitted during the course of this project:

Lorentz, S., Gqiba D. and Verhagen, B. 2003a. Combining hydrometry observations with 2H and 18O tracers in Molteno formations, South Africa. EGS-AGU-EUG Joint Assembly, Nice, France. 6-12 April 2003.

Lorentz, S.A. 2003. Automated soil water potential monitoring in irrigation. South African Irrigation: Aug/Sept. 2003:20-21.

Lorentz, S., Bursey, K. and Gqiba, D. 2003b. Surface Water-Ground Water interaction at small scales: implications for low flow estimates. *SANCIAHS 2003 SW-GW Interactions Workshop*. Grahamstown, September 2003.

Lorentz,S.A., Hughes, G.O. and Schulze, R.E. 2003c. Techniques for estimating groundwater recharge at different scales in Southern Africa. In: Xu, Y. and Beckman, H.E. (Eds) Groundwater Recharge Estimation in Southern Africa. UNESCO IHP Series No 64, UNESCO, Paris, France. ISBN 92-9220-000-3. Chapter 11, 149-164.

Uhlenbrook, S., Wenninger, J., Didszun, J. and Lorentz, S. 2004 Combined tracer, geophysical and modeling studies to explore hydrological processes at the catchment scale. International Instrumented Watershed Symposium, Edmonton, Canada, June 2004.

Schulze, R.E., Lorentz, S.A., Kienzle, S.W. and Perks, L.A. 2004. Case Study 3: Modelling the impacts of land-use and climate change on hydrological responses in the mixed underdeveloped/developed Mgeni catchment, South Africa. *In:*Kabat, P., Claussen, M., Dirmeyer, P.A., Gash, J.H.C., Bravo de Guenni, L., Meybeck, M., Pielke, R.A. Snr., Vörösmarty, C.J., hutjes, R.W.A. and Lütkemeier, S. (Eds) *Vegetation, Water Humans and the Climate. A New Perspective on an Interactive System.* Springer-Verlag, Heidelberg, Germany. Chapter D7, 441-453.

Lorentz S. and Talma A.S. 2005a. Isotope Compositions of Runoff in Large Catchments in southern Africa, VIIth Scientific Assembly IAHS, 3-9 April 2005, Foz do Iguaçu, Brazil

Lorentz SA and Talma A.S. 2005b. Isotope composition of runoff in large catchments in southern Africa, Proceedings 12th SANCIAHS Symposium, Midrand, South Africa. 5-7 September 2005.

Lorentz, S., Bursey, K., Verhagen, B. and Butler, M. 2005. Combining environmental isotope and process dynamics observations for low-flow quantification in an afforested catchment in South Africa. Workshop: W8: Isotope Tracers and Remote Sensing Techniques for Assessing Water Cycle Variability. VII IAHS Scientific Assembly, April 2005, Foz do Iguaçu, Brazil.

Uhlenbrook, S., Wenninger, J. and Lorentz, S. 2005. What happens after the catchment caught the storm? Hydrological processes at the small, semi-arid Weatherley catchment, South Africa. EGU, Advances in Goesciences, 2:237-241.

Helmschrot, J., Lorentz, S., and Flügel, W.-A. 2005. Integrated wetland and landscape modeling. A case study from the Eastern Cape Province, South Africa. In Zerger, A. and Argent, R.M. (eds) MODSIM 2005 International Congress on Modelling and Simulation. Modelling and Simulation Society of Australia and New Zealand, December 2005, pp. 1382-1388. ISBN: 0-9758400-2-9.

Wenninger, J., Uhlenbrook, S. and Lorentz, S. 2007. Identification of runoff generation processes using combined hydrometric, tracer and geophysical methods in a headwater catchment in South Africa. J of Hydrology. (In Press).